Fakultät für Medizin
Institut für Virologie

Characterization of Early Events in Hepatitis B Virus Infection

Anindita Chakraborty

Vollständiger Abdruck der von der Fakultät für Medizin der Technischen Universität München zur Erlangung des akademischen Grades eines

Doktors der Naturwissenschaften (Dr. rer. nat.)

genehmigten Dissertation.

Vorsitzende/-r: Prof. Dr. Jürgen Ruland

Prüfende der Dissertation:

1. Prof. Dr. Ulrike Protzer
2. Prof. Dr. Benjamin Schusser

Die Dissertation wurde am 09.03.2020 bei der Technischen Universität München eingereicht und durch die Fakultät für Medizin am 11.08.2020 angenommen.

Table of content

Abbreviations

A	
ATR	Ataxia telangiectasia and Rad3-related protein
C	
Cav-1	Caveolin-1
cccDNA	Covalently closed circular DNA
D	
DHBV	Duck hepatitis B
DMSO	Dimethyl sulfoxide
DNase	Deoxyribonuclease
dpi	Days post infection
DR1	Direct repeats 1
DR2	Direct repeats 2
DslDNA	Double stranded linear DNA
E	
EdC	Ethynyl-2'-deoxycytidine
EGF	Epidermal growth factor
EGFR	Epidermal growth factor receptor
F	
FBS	Fetal bovine serum
FCS	Fetal calf serum
G	
GAPDH	Glyceraldehyde 3-phosphate dehydrogenase
GFP	Green fluorescent protein
GLuc	Gaussia Luciferase
H	
HBeAg	HBV e antigen
HBs	HBV surface protein
HBsAg	HBV surface antigen
HBV	Hepatitis B virus
HBx	HBV X protein
HCC	Hepatocellular carcinoma
HCV	Hepatitis C virus
HDV	Hepatitis D virus
HIV-1	Human immunodeficiency virus - 1
HSPG	Heparan sulfate proteoglycan
I	
IU	International Units
L	
Lig	Ligase
L-protein, LHBs	Large HBV surface protein
M	

M-protein, MHBs	Middle HBV surface protein
MOI	Multiplicity of infection
mRNA	Messenger RNA
N	
n.d.	Not detected
NPC	Nuclear pore complex
NLS	Nuclear localisation signal
ns	Not significant
NTCP	Na^+-taurocholate cotransporting polypeptide
P	
P-protein	Polymerase of HBV
PBS	Phosphate-buffered saline
PBS-T	Phosphate-buffered saline-Tween 20
PCR	Polymerase chain reaction
PDH	Primary duck hepatocyte
pgRNA	Pregenomic RNA
PHH	Primary human hepatocyte
p.i.	Post infection
PKC-a	Protein kinase C alpha
PRNP	Prion protein gene
PVDF	Polyvinylidene difluoride
Q	
qPCR	Quantitative polymerase chain reaction
R	
rcDNA	Relaxed circular DNA
RNase	Ribonuclease
S	
S-protein, SHBs	Small HBV surface protein
SDS	Sodium dodecyl sulfate
SDS-PAGE	Sodium dodecyl sulfate polyacrylamide gel electrophoresis
T	
TBS-T	Tris-buffered saline- Tween20
TC	Tetracystein
Tdp2	Tyrosyl-DNA phosphodiesterase 2
TEMED	Tetramethylethylenediamine
U	
U	Unit
W	
WHV	Woodchuck hepatitis virus
WT	Wildtype

Abstract

Despite accumulating knowledge of the HBV life cycle, early stages of HBV infection including particle entry dynamics, cytoplasmic transport and cccDNA formation still remain poorly understood.

The discovery of NTCP as the viral receptor enabled us to generate permissive cell lines and to study synchronised particle internalisation, nuclear transport and cccDNA formation.

We established a PCR-based assay to quantify the kinetics of HBV particle attachment and internalisation into permissive hepatocyte-derived cells. Virus attachment at 4 °C was NTCP independent, whereas subsequent particle internalisation at 37 °C required NTCP, demonstrating a role for NTCP in HBV internalisation. HBV uptake was clathrin- and dynamin dependent with actin and tubulin playing an essential role within the first 6 hours, consistent with particle transport to the nucleus within this time frame. We noted a dose and time-dependent internalisation of particles into NTCP expressing hepatoma cells that associated with antigen expression, suggesting that HBV entry into cells is a rate-limiting step in establishing productive infection. HBV internalisation was determined by measuring intracellular core or envelope glycoproteins and HBV DNA that peaked after 8 and 12 hours, respectively, highlighting a slow and inefficient process. The majority (83 %) of cell bound virus internalized in HepG2-NTCP cells, however, approximately 0.6 % of attached viral genomes resulted in cccDNA formation.

To investigate this further we studied the dynamics of HBV particles accessing the nucleus and demonstrated this process took 3-6 hours. Moreover, we only detected cccDNA after 24 hours increasing over the following 48 hours. These studies show that HBV infection is a slow process, and provide evidence that conversion of rcDNA into cccDNA in the nucleus is the rate-limiting step *in vitro*.

Investigations on the role for NTCP in HBV entry showed that single N-glycosylation of NTCP was required for membrane localization, bile acid uptake and HBV infection. Dose dependent transfection of NTCP mRNA into parental hepatoma cells showed that NTCP expression levels at the cell surface associated with HBV internalisation.

Non-hepatoma cell lines transiently expressing NTCP were able to promote physiological function and transport bile acids but failed to confer HBV uptake and infection. This demonstrates that additional hepatocytes specific factors are required for NTCP dependent HBV infection.

This study contributes to a better understanding of a spatio-temporal resolution of virus –host interactions at its earliest time points. This is a relevant basis for investigating host factors involved in HBV entry facilitating the development of antiviral strategies.

Zusammenfassung

Trotz intensiver Forschung des Lebenszykluses des Hepatitis B Virus (HBV), sind die ersten Schritte der Infektion einschließlich der Virusaufnahme bis hin zur cccDNA Formation noch nicht vollständig erforscht. Die Entdeckung von NTCP als viraler Rezeptor ermöglicht uns die Etablierung einer permissiven Zelllinie, um eine synchronisierte Partikelinternalisierung, den Transport in den Nukleus und cccDNA Formation zu analysieren.

Wir haben eine PCR-basierte Methode entwickelt, welche die Kinetik von HBV Bindung und Aufnahme in permissiven, Hepatozyten-ähnlichen Zellen quantifiziert. Die Virusbindung an die Zelloberfläche war NTCP unabhängig, während eine subsequente Partikelaufnahme NTCP benötigte. Die HBV Aufnahme war abhängig von Clathrin und Dynamin, wobei Aktin und Tubulin eine entscheidende Rolle in den ersten sechs Stunden der Aufnahme gespielt haben. Diese Dauer entspricht dem Zeitrahmen des Partikeltransportes zum Nukleus. Wir beobachteten eine konzentrations- und zeitabhängige Partikelaufnahme in NTCP exprimierenden Hepatomazellen, welche mit der Antigen Expression korrelierte. Dies suggeriert, dass die HBV Aufnahme der limitierende Schritt in einer produktiven Infektion ist. Die quantitative Analyse der HBV Aufnahme durch Messung von Viruskapsid, Glykoproteinen der Virushülle und HBV DNA erreichte zwischen 8 und 12 h ihren Höhepunkt, was auf einen langsamen und ineffizienten Prozess hindeutet. Circa 83 % des an der Oberfläche gebundenen Virus konnte in HepG2-NTCP Zellen aufgenommen werden, aber nur etwa 0,6 % des gebundenen Virus resultierte in einer cccDNA Formation. Eine weitere Untersuchung ergab, dass die HBV Aufnahme in den Nukleus 3-6 h dauerte. Darüber hinaus wurde cccDNA erstmals 24 h nach Aufnahme detektiert und stieg innerhalb von 48 h weiter an. Diese Ergebnisse zeigen, dass die HBV Infektion ein langsamer Prozess ist, wobei die rcDNA zur cccDNA Konversion den limitierenden Schritt *in vitro* darstellt.

Anschließend wurde die Rolle der N-glykosylierung von NTCP im Zusammenhang mit HBV untersucht. Eine einzelne N-glykosylierung ist ausreichend für die korrekte Membranlokalisierung von NTCP, eine physiologische Gallensäureaufnahme und ermöglicht eine Infektion mit HBV. Die konzentrationsabhängige Transfektion von NTCP mRNA in parentale Hepatomazellen zeigte, dass die NTCP Expression an der Zelloberfläche mit der HBV Aufnahme korreliert. Nicht Hepatomazellen, welche transient NTCP exprimieren, erlauben eine physiologische Funktion und transportierten Gallensäure. Trotz dessen war eine HBV Aufnahme und Infektion in diesen Zellen nicht

möglich. Dies weist darauf hin, dass zusätzliche hepatozyten-spezifische Faktoren notwendig für eine NTCP abhängige HBV Infektion sind.
Diese Ergebnisse führen zu einem besseren Verständnis der räumlichen und zeitlichen Lokalisation von Virus-Wirt Interaktionen in den frühen Schritten des Lebenszykluses. Dies ist relevant für weitere Untersuchungen von Wirtsfaktoren im Zusammenhang mit der HBV Aufnahme und ermöglicht die Entwicklung antiviraler Strategien.

1 Introduction

Hepatitis B Virus (HBV) chronically infects 257 million individuals worldwide and is a major driver of end-stage liver disease, cirrhosis, and hepatocellular carcinoma (HCC) (WHO, 2019). Current therapies target viral replication but are ineffective in targeting episomal virus transcriptional templates in the nucleus of infected hepatocytes and curing infection (Jang et al., 2011). Studies to examine the mechanism of HBV entry are key to understanding viral tropism for the liver and for building antiviral screening platforms.

1.1 Hepatitis B virus (HBV)

The following chapter will introduce the Hepatitis B virus, discussing molecular biology and viral pathogenesis.

1.1.1 Classification

The small enveloped DNA virus human HBV belong to the *Hepadnaviridae* family that include mammalian and avian viruses that share properties in organ tropism, genome organisation and viral genome replication (Gust et al., 1986). The genus *Orthohepadnavirus* contain mammalian viruses, such as human HBV, woodchuck hepatitis virus (WHV), ground squirrel hepatitis virus (GSHV) and all viruses that infect Old and New World primates such as gibbons and chimpanzees (Schaefer, 2007, Summers et al., 1987). The genus *Avihepadnavirus* represent avian viruses such as duck hepatitis B virus (DHBV) and heron hepatitis B virus (HHBV) (Mason et al., 1980, Schaefer, 2007).

HBV can be divided into 9 genotypes (A-I) that differ in nucleotide sequence by more than 7.5 % (Kramvis, 2014, Velkov et al., 2018). The geographical distribution of genotype A is in Africa, Europe and America whereas B and C are more prevalent in Asia (Guettouche and Hnatyszyn, 2005, Kramvis, 2014, Velkov et al., 2018). Genotype D has its epicentre in the Mediterranean, India and America. HBV genotype E mainly exists in sub-Saharan Africa and genotype F in South and Central America. Genotype H is most common in Southern and Central America whereas genotype I is located in Asia. *Tatematsu et al*. introduced a putative new genotype ‘J’ that has been found in Japanese patients. It may have resulted from a recombination between genotype C and gibbon HBV (Lamontagne et al., 2016).

HBV can be classified into 4 subtypes adr, adw, ayr and ayw which are based on the antigenic variability of the hepatitis B surface antigen (Chu and Lok, 2002, Kramvis, 2014).

1.1.2 Morphology

HBV is a spherical, enveloped DNA virus with an approximate size of 42 nm and designated as the Dane particle (Dane et al., 1970). As depicted in figure 1 HBV consists of a viral capsid which is surrounded by an envelope. This envelope consists of small (S), middle (M) and large (L) HBV surface proteins (HBs) that are embedded in a lipid bilayer and share the C-terminal domain (Heermann et al., 1984, Nassal, 2015). The S proteins consists of the S-domain, the M-protein contains S- and preS2 domain and L-protein harbours S-, preS2 and the preS1 domain. The capsid has a T3 or T4 icosahedral symmetry consisting of 180 or 240 core subunits, respectively (Crowther et al., 1994, Kenney et al., 1995). The capsid harbours the viral genome, a relaxed circular DNA (rcDNA) with a covalently bound viral polymerase (Gerlich and Robinson, 1980, Robinson and Greenman, 1974). In addition to Dane particles non-infectious subviral particles (SVP) are produced (Bruss, 2004). These can exist in two forms: filaments that are mainly made up of S-proteins but also contain M and L-protein to a lower extend. Spheres are smaller in size and are primarily made of S-proteins but also contain M and L-protein in lower amounts. These SVPs can be produced in 100 to 10 000 fold excess compared to infectious viral particle, probably as a mechanism of immune evasion (Bruns et al., 1998).

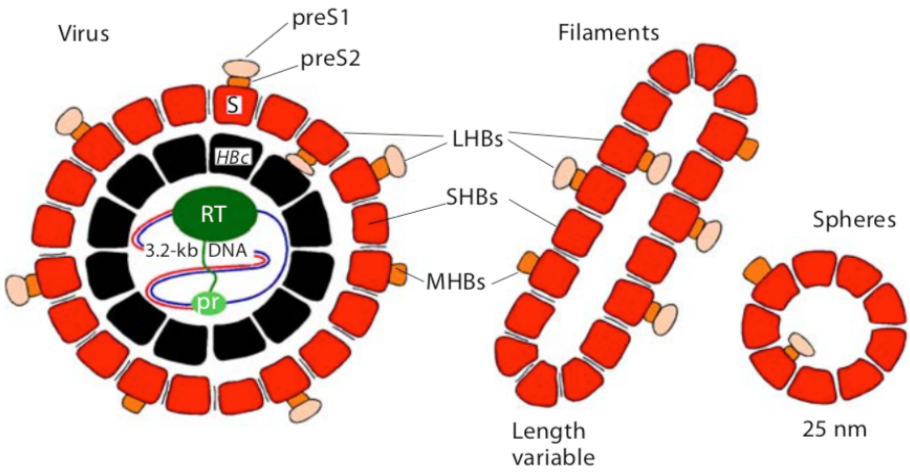

Figure 1: Structure of HBV and SVPs. HBV and SVPs consist of small (SHB), middle (MHB) and large (LHB) protein. Description in red represents S, orange preS2 and lighter orange preS1. The nucleocapsid contains the 3.2 kb viral genome that harbours the viral polymerase (RT, green) and primer domain (pr, light green) (Gerlich et al., 2010).

1.1.3 Genome organisation

HBV has a small 3.2 kb partially double stranded rcDNA consisting of a complete minus strand with a terminal redundancy of seven to nine nucleotides (nt) with the viral polymerase covalently attached (Fig. 2) (Gerlich and Robinson, 1980). The incomplete plus strand has a constant 5' end with the 3' varying in length (Hruska et al., 1977). Furthermore, the 5' end of the plus strand harbours a 18 nt long with mRNA-like cap structure (Seeger et al., 1986). The HBV genome encodes for four partially overlapping open reading frames (ORF) that encode for seven viral proteins (Glebe, 2006, Nassal, 2015). The largest ORF codes for the viral polymerase which harbours reverse transcriptase (RT), RNaseH and primer activity (Nassal, 2015). The second largest ORF gives rise to the viral envelope that comprises of L-, M- and S-protein. Further ORF encodes a pre-core protein, which is processed and secreted as hepatitis B e antigen (HBeAg), and the core protein which is a subunit of the viral capsid (Seeger and Mason, 2015). Last, the smallest ORF that encodes for the X-protein which is required for HBV replication (Lamontagne et al., 2016, Lucifora et al., 2011).

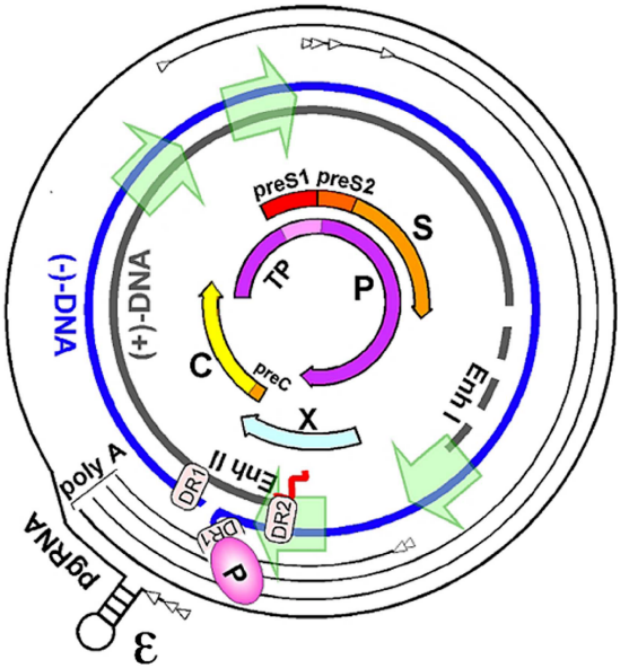

Figure 2: Genome organisation. The outer lines depict the viral transcripts with ε, the encapsidation signal, present on the pgRNA. The rcDNA is represented with minus strand that contains a nick and is attached to the viral polymerase (P), and an incomplete plus strand. The overlapping ORF on the cccDNA are depicted as arrows. Further transciptional enhancers Enh I/II ,direct repeats DR1/2 and the viral promoter regions (green arrows) are depicted (Nassal, 2015).

1.1.4 Viral life cycle

HBV initially interacts with heparan sulfate proteoglycans (HSPGs) via the viral L-protein and promotes enrichment of virions at the plasma membrane as a prerequisite for subsequent virus-receptor interactions (Fig. 3) (Leistner et al., 2008, Schulze et al., 2007). In a subsequent step the myristolylated preS1 domain of the L-protein binds to sodium taurocholate cotransporting peptide (NTCP) (Yan et al., 2012). The virus enters the host cells via the endocytic route where the importance of both clathrin- and caveolin mediated entry have been described for different cell types (Huang et al., 2012, Macovei et al., 2010). It still remains not precisely known when and how HBV uncoats releasing the viral capsid into the cytoplasm. It has been proposed that the viral capsid is directed to the nuclear pore complex (NPC) in an importin α/ β mediated manner through the nuclear localisation sequence (NLS) present on the core protein (Kann et al., 1999, Rabe et al., 2003). In the nucleus the viral genome, rcDNA, is converted into the episomal covalently closed circular DNA (cccDNA) by host cellular repair mechanisms (Guo et al., 2012). The cccDNA serves as a transcriptional template for viral replication causing persistence (Bock et al., 1994). cccDNA gives rise to pregenomic (pgRNA) and subgenomic RNA (sgRNA) that are transcribed by the cellular RNA polymerase II (Rall et al., 1983). All viral RNA consist of a 5' cap structure and are 3' polyadenylated (Huang and Yen, 1995). The mRNAs are exported to the cytoplasm without splicing where the pgRNA is translated into polymerase and core that are required for reverse transcription (Araki et al., 1989, Datta et al., 2012). Subgenomic RNAs give rise to the envelope and X proteins whereas the precore protein is proteolytically processed after translation and secreted as HBeAg (Fouillot et al., 1993).

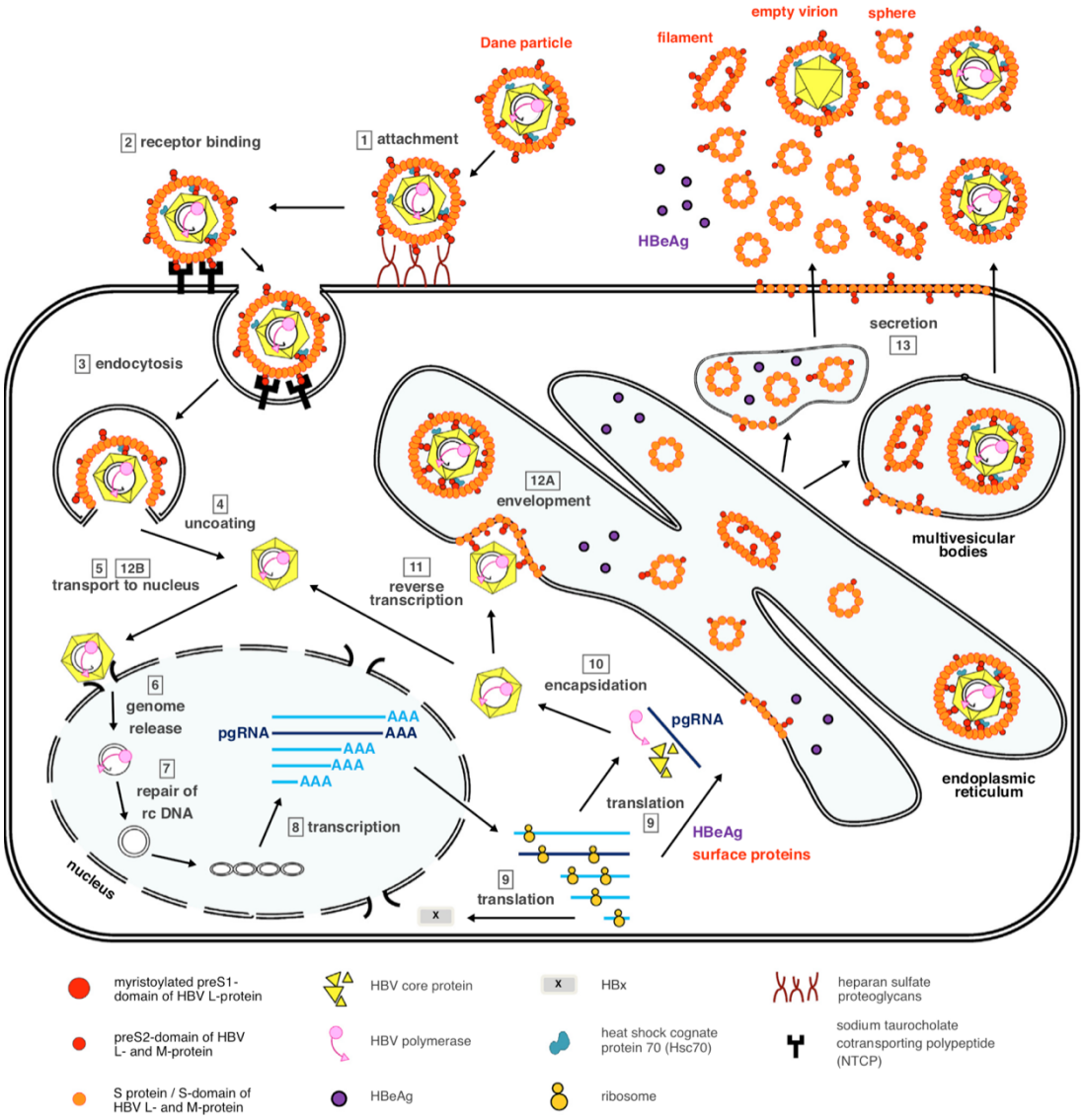

Figure 3: HBV life cycle in hepatocytes. (1) HBV attachment to HSPG with subsequent interaction with NTCP (2). Viral particle is endocytosed (3) and uncoated where the viral capsid is released into the cytoplasm (4). Capsid is trafficked o the the nucleus (5) whereupon the genome is released into the nucleus (6). In the nucleus rcDNA is repaired to cccDNA (7) which serves as a trancriptional template (8). Subsequently, translation (9), encapsidation (10) and reverse transcription (11) from pregenomic RNA occurs. Viral capsids are either enveloped (12A) and secreted (13) or reimported to the nucleus (12B) (Ko et al., 2017).

In addition to its role as mRNA, the pgRNA serves as template for reverse transcription (Fig. 4) (Nassal, 2015). The principle function of the polymerase is to convert pgRNA into rcDNA for incorporation into newly generated HBV virions. In the priming step the polymerase attaches to a stem loop structure at the 5' end of the pgRNA, designated ε, sequestering viral RNA and polymerase into newly generating nucleocapsids (Nassal, 2015, Seeger and Mason, 2000). One molecule of deoxyguanosine triphosphate (dGTP) binds covalently to the viral polymerase to form a base pair with a cytosine within the stem loop structure. Two molecules of deoxyadenosine triphosphate (dATP) are added to the guanosine to generate a three base-pair long primer (Nassal and Rieger, 1996). Subsequently, the polymerase translocates to a proximal 11-12 nt sequence homology referred to as the 3' direct repeat 1 (DR1) (Nassal, 2015). Extension from DR1 to the 5´ end of the pgRNA template yields a unit length DNA with a small ~10 nt terminal redundancy (DR2). The reverse transcription then occurs from the 5' end of the pregenome with the template being degraded by the polymerase harbouring RNase H activity and a minus strand DNA is generated with short redundancies. The 5' terminal 15-18 nt including the CAP and DR1 of the pgRNA are not degraded and serve as primer for plus strand DNA synthesis. This primer translocates to DR2 at the 5' end of the minus strand initiating plus strand synthesis. The plus strand synthesis stops before completion due to the packing of the incomplete plus strand preventing dNTP entry with the primer still bound at the 5' end (Siddiqui et al., 1979). The short redundancies in the minus strand and an intramolecular template exchange facilitate circularization of the DNA genome in the viral capsid (Modrow et al., 2011). This gives rise to a partially double stranded circular genome (rcDNA) that harbours covalently bound polymerase at the minus strand. When primer translocation and circularization fail a double-stranded linear genome can be formed that might play a role in host cell integration (Bill and Summers, 2004).

The newly synthesised DNA containing capsid can be reimported into the nucleus and contribute to cccDNA establishment (Ko et al., 2018, Lucifora and Protzer, 2016). These mature capsids can also be enveloped and further follow the secretory pathway via the endoplasmatic reticulum (ER) finally being secreted through multivesicular bodies as fully infectious virus (Ko et al., 2017).

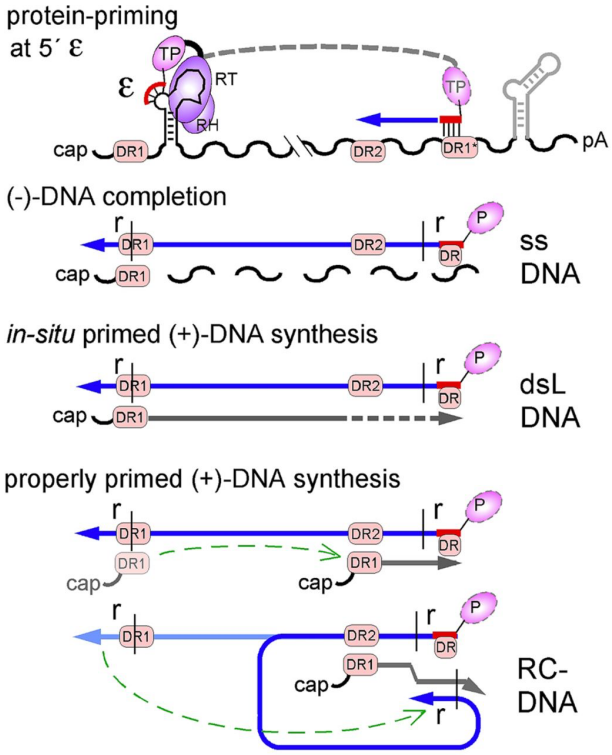

Figure 4: Reverse transcription. Reverse transcription is initiated via the binding of the polymerase to the 5' copy of the stem loop structure, ε, located at the terminal redundancy of the pgRNA. 3 nucleotides of the ε are copied with the polymerase translocating to DR1 in the 3' terminal redundancy. Reverse transcription continues and the pregenomic template is degraded by the RNaseH activity of the polymerase. Cap and DR1 are not degraded and translocate to DR2. Plus strand is synthesized and extends to 5' end of the minus strand. Circularization is enabled by the terminal redundancy on the minus strand. Plus strand synthesis is incomplete and packaging into the nucleocapsid occurs (Nassal, 2015).

1.1.5 Prevention and therapy

Prophylactic vaccines against HBV exist since 1982 that prevent disease and its long-term consequences (Lavanchy, 2004). The available vaccines largely consist of recombinant HBV surface proteins (Shouval et al., 1994). In most cases affecting adults, HBV infection is usually acute and self-limiting with no further treatments required (Hollinger and Lau, 2006, Lamontagne et al., 2016). In newborn and young children, however, HBV infection becomes chronic in >90 % of cases.

Although HBV infection can be prevented by vaccination chronic hepatitis B still remains a major health burden worldwide. Chronic carrier are at a high risk to develop liver fibrosis, cirrhosis and hepatocellular carcinoma causing an estimated 880 000 death a year (Jang et al., 2011). Current treatment consists of (PEGylated) interferon α (INFα) and nucleos(t)ide analogues such as Lamivudine, Adefovir, Entecavir and Tenofovir (Lavanchy, 2004, Nassal, 2015). INFα modulates immune response against HBV, however, the application comes with major side effects which have been described as flu-like symptoms (Tillmann, 2007, Trepo, 2014). The nucleos(t)ide analogues interfere with the viral polymerase blocking reverse transcription which as consequence hamper mature virion production. This application is well tolerated with minor side-effects but can promote HBV resistance rendering therapy ineffective (Tillmann, 2007) but fails to target

cccDNA which causes persistence and chronicity favouring a viral relapse after withdrawal of the treatment (Lempp and Urban, 2014). Therefore, combinatorial therapies targeting other steps in the viral life cycle are required. For instance, applying entry inhibitor to chronically infected patients can limit *de novo* infection and spreading into naïve hepatocytes. Myrcludex B is representative for novel HBV entry inhibitors that has been shown to inhibit HBV entry blocking interactions with NTCP (Ni et al., 2014). Myrcludex B is a myristolated preS1 peptide of the L-protein that has shown to block HBV and hepatitis D viral (HDV) infection both *in vitro* and *in vivo* and is currently in phase II clinical trials (Bogomolov et al., 2016, Glebe, 2006, Gripon et al., 2005).

1.2 Sodium-taurocholate cotransporting polypeptide (NTCP)

NTCP is encoded by the human SLC10A1 gene and is primarily involved in sodium dependent bile-acid transport from the blood contributing to the enterohepatic circulation and homeostasis of bile acids (Hagenbuch and Meier, 1994, Stieger et al., 2012). NTCP is a nine transmembrane protein embedded in the cellular membrane on the basolateral/sinusoidal side of hepatocytes (Fig. 5) (Anwer and Stieger, 2014). The entire structure is not known, however, it harbours a complex glycosylation pattern with potential four N-glycosylation site of which two N5 and N11 were confirmed (Hallen et al., 2002). In addition, it has been proposed that NTCP is present as a dimer on the cell surface (Bijsmans et al., 2012). Substrates specificity of NTCP ranges from unconjugated bile acids, glycine- and taurine-conjugated bile acids, steroid sulphate conjugate and certain drugs (Li and Tong, 2015, Stieger et al., 2012). NTCP expression was shown to be higher in differentiated HCC than lower differentiated cells (Kullak-Ublick et al., 1997). Further, isolation of primary hepatocytes displayed rapid loss in

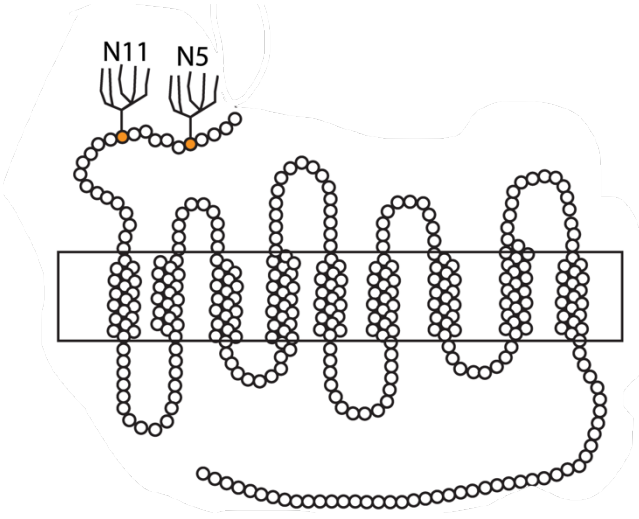

Figure 5: Structure of NTCP. Putative topology of NTCP at the plasma membrane. It is a nine transmembrane protein that resides at the basolateral/sinusiodal side of hepatocytes. N-glycosylation sites are indicated at position 5 and 11 (Appelman et al., 2017).

NTCP expression (Konig et al., 2014, Rippin et al., 2001). This might explain why hepatoma cells are non-permissive for HBV infection.

A combinatorial approach using biochemical and proteomic analysis discovered NTCP to be a bona fide receptor for HBV and HDV (Yan et al., 2012). The preS1 peptide ligand that consisted of the first 2-48 residues of preS1 was used as a bait and cross-linked with membrane proteins from primary tupaia hepatocytes (PTH). This discovery helped development of novel cell culture systems that support HBV infection such as the HepG2-NTCP K7 cells we described (Ko et al., 2018). Hepatoma cell line stably expressing NTCP have become an important tool for HBV studies (Li and Urban, 2016). Studies have shown that NTCP residues 157 – 165 are required for preS1-NTCP interactions highlighting the importance of NTCP in the HBV life cycle (Ni et al., 2014, Yan et al., 2012). Additional residues that promote sodium binding (Q68, S105N106, E257 and Q261) or bile acid binding (N262, Q293 and L294) are found to interfere with HBV infection (Yan et al., 2015). This indicates that HBV may follow the route of substrate transportation to enter hepatocytes. Interestingly, the single nucleotide polymorphism (SNP) at residue S267F of NTCP impairs bile acid transport and fails to support HBV infection in cell culture (Yan et al., 2014). This variant is most commonly found in the East Asian population and is associated with a resistance in developing chronic hepatitis B (Peng et al., 2014).

Inhibition of NTCP is a promising approach for HBV/HDV prevention. Targeting early steps in the viral life cycle can block cccDNA establishment in naïve or newly generated host cells (Li and Urban, 2016). Natural substrates such as conjugated bile salt can interfere with HBV infection at high concentrations (Yan et al., 2014). The concentrations required for inhibition exceed physiological bile acid concentration in the liver hence are not promising for therapeutic approaches (Li and Urban, 2016). Several pharmacological inhibitors that interfere with HBV infection by blocking NTCP have been reported. As already mentioned before targeting NTCP with Myrcludex B is a promising approach (Schulze et al., 2010). Ezetimibe that interferes with Niemann-Pick C1-Like 1 (NPC1L1) disrupting cholesterol transport has also been shown to block NTCP and HBV infection (Lucifora et al., 2013). The peptide Cyclosporine A (CSA) and its derivatives displayed antiviral activity inhibiting preS1-NTCP interaction and as a consequence blocking HBV infection (Watashi et al., 2014).

1.3 Epidermal growth factor (EGF) receptor

ErbB family of receptor tyrosine kinases are clustered into 4 related members one of which is the EGF receptor (EGFR) (Wieduwilt and Moasser, 2008). EGFR is a transmembrane receptor that resides at the plasma membrane (Fig. 6). Different ligand-receptor interactions determine different routes of receptor trafficking (Roepstorff et al., 2009). Ligands include EGF, heparin-binding EGF-like growth factor, transforming growth factor-α, amphiregulin, epiregulin, epigen, betacellulin and neuregulins. Ligand binding leads to activation of EGFR with subsequent dimerization, trans-phosphorylation and endocytic trafficking initiating a multi-step downstream signalling cascade (Atalay et al., 2003). In the acidic environment of the endosomal compartment EGFR-ligand complex dissociates followed by recycling of the receptor to the cell surface or lysosomal degradation (Herbst et al., 1994). Upon activation several signalling cascades are activated including Ras/MAPK, PI3K/Akt, PLCγ/PKC, and STAT pathway (Wieduwilt and Moasser, 2008). These pathways play an essential role in regulating cell proliferation, survival, differentiation and migration.

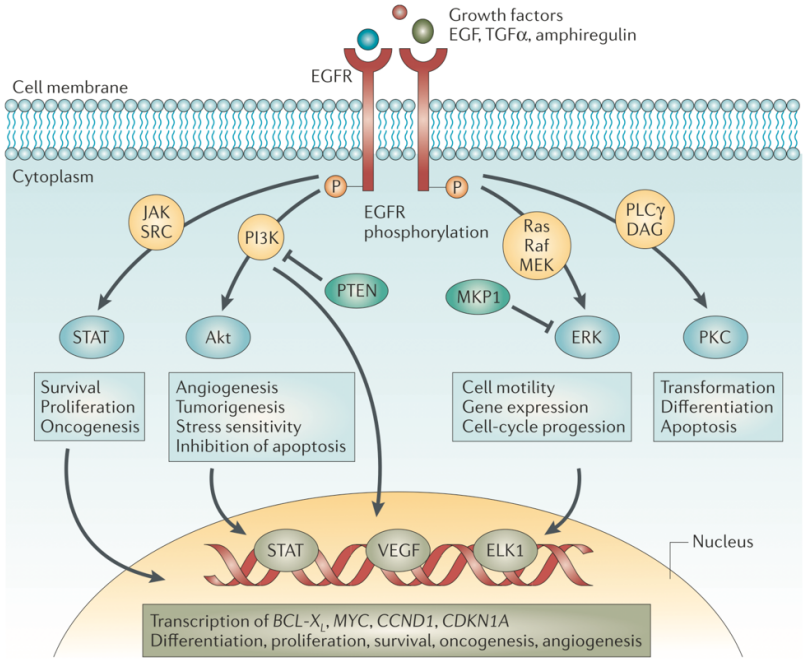

CCND1, gene encoding cyclin D1; *CDKN1A*, gene encoding p21; JAK, Janus kinase; TGFα, tranforming growth factor-α.

Figure 6: Signalling pathway regulated by EGFR. Ligand binding initiates dimerisation of EGFR resulting in autophosphorylation. This induces signalling pathways that are involved in cell proiferation, survival, differentiation and migration. PI3K: phosphatitylinositol 3- kinase; Ras: guanosine-nucleutide binding protein; Raf: proto-oncogene serine/theonine-protein kinase; MEK: mitogen activated protein kinase; PLC: phospholipase c- ; DAG: diacylglycerol; STAT: signal trasducer and activator of transciprion; Akt: protein kinase B; ERK: extracellular-signal-regulated kinase; PKC: serine/threonine kinase protein kinase-C; PTEN: phosphatase and tensin homologue; MKP1: MAPK phosphatase 1; VEGF: vascular endothelial growth factor (Nyati et al., 2006)

A recent study from *Iwamoto et al*. has identified the Epidermal Growth Factor Receptor (EGFR) as an additional entry receptor for HBV (Iwamoto et al., 2019). The study showed that stimulation of EGFR with its ligand EGF enhanced HBV infection. EGFR knockdown did not impair viral attachment but interfered with particle internalisation that was rescued with functional EGFR complementation. Additionally, the study showed that the HBV-NTCP complex colocalised with EGFR in endosomal compartments. Furthermore, point mutation in NTCP, the application of a decoy peptide and the pharmacological inactivation of EGFR with Gefitinib were able to disrupt EGFR-NTCP interactions.

1.4 Endocytosis and intracellular trafficking

Viruses utilise internalisation and trafficking machineries of the host cells to enter their correct replication site and proceed with the viral life cycle (Sieczkarski and Whittaker, 2002). In the following, pathways that are dependent on the GTPase dynamin, such as clathrin- and caveolin-mediated endocytosis and dynamin independent pathway, macropinocytosis, will be introduced (Fig. 7). Dynamin self-assembles and oligomerises promoting scission and budding of vesicles from invaginated membranes (Mettlen et al., 2009).

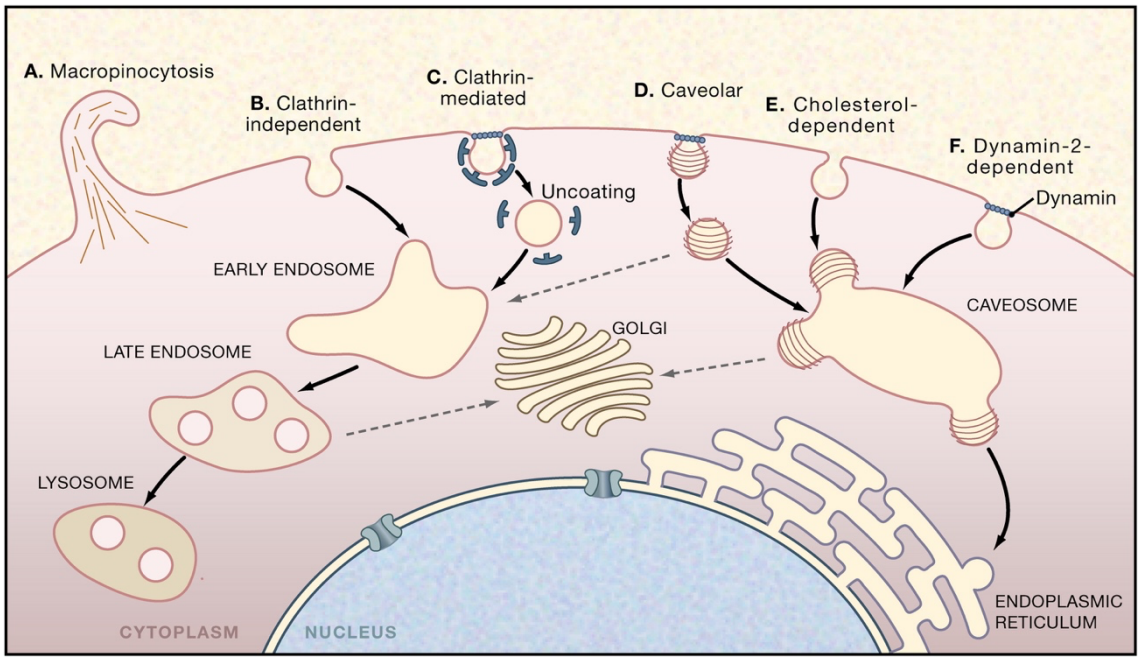

Figure 7: Endocytic pathways exploited by viruses. Many different endocytic routes are available for virus particle internalisation into mammalian cells such as (A) macropinocytosis, (B) clathrin-independent and (C) clathrin mediated entry, (D) caveolar pathway that is closley related to (E) cholesterol-dependent pathway and (F) Dyanmin-2 dependent pathway (Marsh and Helenius, 2006).

1.4.1 Clathrin-mediated endocytosis

Clathrin mediated endocytosis requires the involvement of clathrin that is a triskelion-shaped scaffold comprising of three heavy and three light chains (Edeling et al., 2006). During clathrin mediated endocytosis the receptor and its ligand is packaged into clathrin coated pits at the cytoplasmic face in the presence of adaptor and accessory proteins. The clathrin complex is initiated by the accumulation phosphatidyl-inositol-4,5-bisphosphate and adaptor proteins and accessory proteins including Epsins at the pinching site (Chang et al., 1993, Smythe et al., 1992). Scission is obtained through dynamin that gives rise to a clathrin coated vesicle. This vesicle uncoates and fuses to an endosome. Dependent on the cargo it undergoes lysosomal, recycling or trafficking pathways (Sorkin, 2004). Clathrin mediated endocytosis is a constitutive process that allows trafficking of receptors form the plasma membrane in a rapid and efficient manner. Thus, this pathway is exploited by the virus where the virus-receptor complex is transported into early and late endosomes (Marsh and Helenius, 2006). The exposure of the virus in the acidic environment of the endosome after rapid internalisation can induce changes in the viral envelope promoting viral infection (Marsh and Helenius, 1989). Several viruses have been shown to use this pathway for particle entry such as hepatitis C virus (HCV), human immunodeficiency virus (HIV) and vesicular stomatitis virus (VSV). Pharmacological agents that interfere with this pathway can be applied to identify the viral route of entry. For instance, Pitstop2 that competitively inhibits the terminal domain of clathrin interferes with clathrin mediated endocytosis therefore abolishing HIV entry (von Kleist et al., 2011).

1.4.2 Caveolin-mediated endocytosis

Caveolin endocytosis involves lipid rafts that are enriched in cholesterol and glycosphingolipids (Le et al., 2002). There are three mammalian caveolin proteins: Caveolin-1 (Cav-1) that is co-expressed with Caveolin-2 (Cav-2) in abundant cells such as fibroblast and endothelial cells whereas Caveolin-3 (Cav-3) is exclusively expressed in muscle specific tissues (Doherty and McMahon, 2009, Ikonen et al., 2004). Caveolin-1 phosphorylation at tyrosin14 is important for caveolar endocytosis through vesiculating (Orlichenko et al., 2006). Dynamin is required for the caveolar to pinch off from the membrane (Kirkham and Parton, 2005, Oh et al., 1998). The caveolar are very stable and immobile at the plasma membrane and bud less frequently than clathrin coated vesicles which indicated that this pathway is not involved in the continuous process of

endocytosis (Pelkmans and Helenius, 2002). Ligands such as cholera toxin B (CTB) or simian virus 40 (SV40) have been shown to enter the cell via caveolar endocytosis. The cargoes are either transported to the acidic early endosomes or to pH neutral caveosomes and subsequently trafficked to their penetration sites (Marsh and Helenius, 2006). Caveolar endocytosis inhibitors such as nystatin or methyl-beta cyclodextrin (MβCD) which deplete cholesterol from the membrane change the membrane composition preventing caveolar formation (Lajoie and Nabi, 2010). Different to clathrin-mediated endocytosis which is ubiquitous, caveolae are only present in limited cell types and not detectable in neuron, leukocytes and hepatocytes (Parton and Simons, 2007, Parton and Richards, 2003).

1.4.3 Macropinocytosis

Macropinocytosis is actin-dependent and promotes fluid and membrane internalisation into large vacuoles, designates macropinosomes (Schelhaas, 2010, Watts and Marsh, 1992). These macropinosomes form through membrane ruffling at the plasma membrane giving rise to cavities that are filled with fluids and closed by membrane fusion (Marsh and Helenius, 2006). These plasma membrane protrusions can form lamellipodia, filopodia or blebs (Mercer et al., 2010). The fate of these vesicles is cell type dependent, however, after entering the cytoplasm the vesicles are either being recycled back to the plasma membrane or follow the endosomal pathway (Hewlett et al., 1994, Racoosin and Swanson, 1993). Numerous factors and the mode of stimulation can contribute to macropinocytosis in various cell types (Mercer et al., 2010). Induction of macropinocytosis may involve cellular lipids, kinases, GTPases, Na+/H+ exchangers and more. In general, macropinocytosis does not rely on specific ligand-receptor interaction and is considered to be rather non-specific (Sieczkarski and Whittaker, 2002). Viruses can induce membrane ruffling entering the cell via macropinocytic endosytosis (Mercer et al., 2010). Viruses that have been reported to take this route are vaccinia virus, adenovirus type 3 and herpes simplex virus 1 (Mercer and Helenius, 2009). Most of these viruses depend on the Na+/H+ exchanger activity for particle internalisation. Perturbation analysis employing amilorides and derivates such as 5-(*N*-Ethyl-*N*-isopropyl) amiloride (EIPA) that inhibit Na+/H+ exchangers may help decipher dependency of the macropinocytic pathway for viral entry (Devadas et al., 2014, Meier et al., 2002, Dowrick et al., 1993).

1.4.4 pH dependency in viral entry

Following internalisation into the host cell the viral particle may be exposed to the acidic environment of the endosome. The pH in the endosomes can promote conformational changes in the virus or may be required for host enzyme activity to induce such changes facilitating viral penetration (Marsh and Helenius, 2006). The endosomal pathway traffics endocytic vesicles through compartments with increasing acidity from early to late endosome that in a subsequent step is either degraded in a lysosome or is recycled back to the plasma membrane (Gruenberg and van der Goot, 2006). Rab proteins are reliable markers to distinguish between different endosomal compartments that regulate vesicle formation, movement and membrane fusion (Stenmark and Olkkonen, 2001). In a Rab5-dependent manner the early endosome (pH 6.5-6) matures into the late endosome (pH 6- 5.5). Furthermore, the maturation is induced by the activity of the vacuolar membrane proton pump, v-ATPase, increasing acidity (Forgac, 2007). As a consequence, the endosomes lose Rab5 and acquire Rab7 that allows fusion with lysosomes. The viral penetration site for fusion and uncoating can depend on the pH level in these compartments inducing endosomal escape (Marsh and Helenius, 2006). Pharmacological intervention with e.g. Bafilomycin A1, which inhibits v-ATPase preventing acidification help to decipher the requirement for low pH in viral entry and productive infection (Drose and Altendorf, 1997). For various viruses, such as sindbis and influenza virus acidic pH in the endosomes is crucial for infection triggering fusion and uncoating (Smith and Helenius, 2004, White and Helenius, 1980).

1.4.5 Cytoskeleton in endocytic pathways

The cytoskeleton defines the cell shape mediating cell robustness, cell- to cell contact and promoting cell motion and organelles trafficking inside the cell (Pollard and Cooper, 2009). Viruses can hijack cytoplasmic membrane trafficking for intracellular transport (Dohner and Sodeik, 2005). During viral entry viruses often use the endocytic route to establish viral infection (Sieczkarski and Whittaker, 2002). Additionally, single viral components can directly interact with cytoskeleton network. Cytoskeleton filaments comprise of monomeric actin that can polymerise into microfilaments and dimeric tubulin that that polymerise to tube like structures (Welch and Mullins, 2002). Further, intermediate filaments are formed by keratin or vimentin (Dohner and Sodeik, 2005). Upon viral binding to the host cell cortical actin beneath the plasma membrane can contribute to particle internalisation and endocytosis (Doherty and McMahon, 2009,

Marsh and Helenius, 2006). Dynamic actin assembly contribute to vesicle formation and fission and play an important role in endosomal trafficking (Mercer et al., 2010, Smythe and Ayscough, 2006). Upon reaching the cytoplasm viruses and viral capsid require trafficking to defined locations in the cytoplasm or nucleus for viral replication. Many viruses such as herpes simplex virus 1 and adenovirus 2 move along the microtubules to reach the nucleus (Mabit et al., 2002). Application of pharmacological agents allow targeting of cytoskeleton proteins and deciphering the role in viral entry. For instance, cytochalasin and latrunculin interfere with actin polymerisation and colchicine and nocodazole depolymerise microtubules (Cooper, 1987, Jordan and Wilson, 1999).

1.5 *In vitro* model systems to study HBV

The paucity of appropriate cell culture models makes it difficult to study HBV infection at early stages and identifying novel host factors.

Primary human hepatocytes (PHH) are considered to be the most physiological system that are permissive for HBV infection supporting the entire life cycle (Gripon et al., 1988). The culturing and usage of PHH come with certain constrains. PHH do not expand in cell culture and harbour a limited time span requiring special culture condition (Verrier et al., 2016). Furthermore, HBV infection depends on the genetical background of the host and can vary due to the loss of cell polarisation after culturing (Glebe and Urban, 2007, Gripon et al., 1988). Interestingly, primary hepatocytes from the tree shrew *Tupaia belangeri* (PTH) are permissive for HBV infection (Su, 1987, Walter et al., 1996). PTH allowed the identification of NTCP as a novel receptor for HBV and HDV infection demonstrating a suitable system for viral analysis (Yan et al., 2012). Despite the limitations in using primary hepatocytes, these cells provide a physiological scenario that allows the study of HBV infection and the antiviral response (Luangsay et al., 2015).

Another cell model that displays more physiological features compared to hepatoma cell lines are HepaRG cells. These are liver progenitor cells that are derived from a hepatoma in a patient infected with hepatitis C virus (HCV) (Andersson et al., 2012). HepaRG cells can differentiate to hepatocyte-like cells and bile duct-like epithelial cells. These hepatocyte-like cells fully support HBV infection and can mount antiviral responses similar to those seen in primary cells (Shen et al., 2018). The limitations are long-time differentiation periods and low level of viral infection that make high-throughput screening difficult (Hu et al., 2019).

The hepatoma cell lines HepG2 and Huh7 cells engineered to stably express NTCP are most commonly used for HBV infection studies. These cells allow characterisation from

HBV attachment to cccDNA establishment and can be screened for antiviral agents (Ko et al., 2018, Verrier et al., 2016). The shortcomings of these cells are the oncogenic transformation that fail to reflect original hepatocyte physiology overexpressing NTCP and the incapability to induce immune responses (Hu et al., 2019).
In non-human cells in the presence of human NTCP, macaque and pig hepatocyte are able to promote infection, however, mice and rats failed to support HBV infection (Burwitz et al., 2017, Lempp et al., 2017). Fusion assays that included HepG2 and mouse cells displayed that infection in mouse cell is hampered by the lack of a host cell dependency factor. This indicates that apart from receptor specificity species dependent host factors play an important role in HBV infection.
Non-hepatic cells like HEK293T, that are human embryonic kidney cells, have been shown to support cccDNA formation from intracellular recycling pathway but do not support HBV entry and HBV transcription (Gao and Hu, 2007, Hu et al., 2019, Quasdorff and Protzer, 2010, Seeger and Mason, 2013). This indicates that non-hepatic cells might have host factors that could contribute to the HBV life cycle.
Comparative studies of human hepatic and non-hepatic cells for HBV permissivity might help identifying those tissue specific factors that are required for productive HBV infection.

1.6 Aim of the study

Our limited knowledge of the host pathways regulating HBV entry hinders the development of model systems that recapitulate the efficiency and dynamics of HBV infection in the liver. The identification of cellular factors regulating HBV entry will facilitate the generation of physiological *in vitro* systems, be key to develop suitable *in vivo* models and promote the development of preventive and therapeutic anti-viral strategies.

Current infection protocols require pre-differentiation of the cells with dimethyl sulfoxide (DMSO) and uses high viral titers and a long inoculation time with the addition of polyethylene glycol (PEG) to initiate infection (Michailidis et al., 2017, Ko et al., 2018). This approach is cumbersome and prohibitive to the study of HBV entry. Development of a sensitive assay that allows monitoring HBV entry in a synchronised manner is expected to allow characterising HBV trafficking pathway and unravel entry kinetics.
The aim of this study was to (I) develop a sensitive assay to analyse different steps of the HBV life cycle, (II) characterising features of NTCP for physiological functions and in

greater detail defining a distinct role in HBV entry and (III) examine the dynamic processes involved in HBV uptake.

Apart from NTCP being a key host factor required for HBV infection we consider an interplay with other potential co-receptors and molecules that are involved in HBV uptake receptors.

2 Results

2.1 Establishment of a synchronised uptake assay

We lack a detailed understanding as to how HBV entry and dissemination is regulated by host cellular pathways. This hinders the development of model systems that allow efficient HBV infection. Current HBV infection models and protocols require high MOI and a long exposure of viral inoculum in the presence of polyethylene glycol (PEG) which may alter HBV internalisation dynamics.

As a first step, we established an assay that allows synchronised HBV internalisation (Fig. 8). Cells were pre-chilled on ice and ice-cold HBV containing inoculum was added and incubated for 1 hour at 4 °C. This allowed the virus to attach at the cell surface without being internalised. After a medium exchange cells were shifted to 37 °C which allowed synchronised particle internalisation. Uptake kinetics were analysed in a 1-72 hours' time frame. At time of harvest cells were subjected to a short trypsinisation removing bound but non-internalised HBV particle. As output measurements, intracellular HBV DNA, cccDNA and HBeAg were analysed.

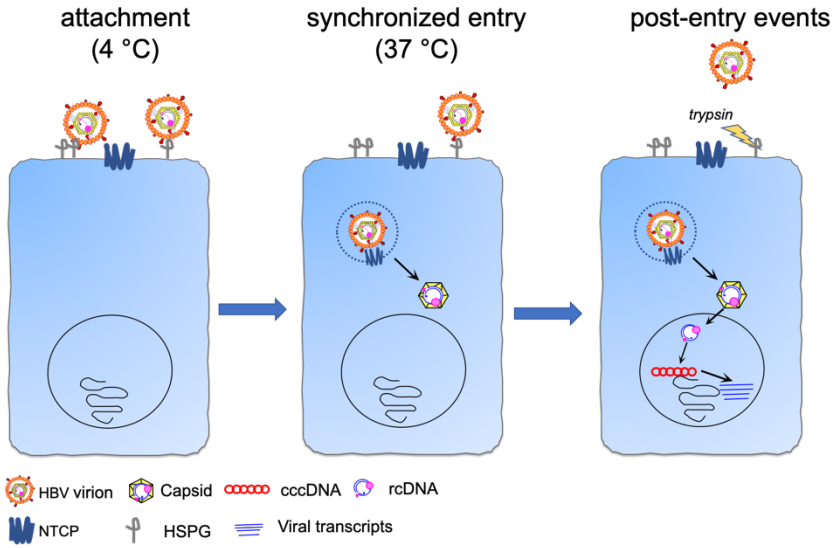

Figure 8: Synchronised HBV uptake assay. Pre-chilled cells are inoculated with HBV for 1 hour at 4 °C (attachment). This allows viral attachment to the cell surface without internalisation. Subsequently, cells are shifted to 37 °C promoting synchronous internalisation of viral particle (synchronized entry). Upon harvest at distinct time points cells are subjected to trypsinisation removing bound and non-internalised viral particle and analysed for HBV parameters (post-entry events).

To evaluate if this assay is suitable for HBV entry analysis I first examined viral attachment to the cell surface at 4 °C measuring cell-associated HBV DNA. Viral inoculum was added to HepG2 and respective cells that express NTCP (HepG2-NTCP K7) at 4 °C for 1 hour. Furthermore, trypsin, a protein digesting enzyme, was added to eliminate bound virus.

HBV attachment did not significantly differ between parental or NTCP-expressing cells (Fig. 9A). Trypsin treatment significantly reduced cell-bound virus up to 90 %. HBV attachment to the cell surface showed a MOI dependent increase (Fig. 9B). Further, the sensitivity of the virus infectivity to trypsin was investigated. Virus pre-treated with trypsin significantly lost infectivity by 90 % (Fig. 9C). This confirmed that trypsin was able to remove bound virus at the cell surface and rendered the virus non-infectious.

To investigate whether HBV particles were able to internalise into cells, virus was inoculated at 4 °C for 1 hour and either directly treated with trypsin to digest cell-bound virus or cells were subsequently shifted to 37 °C for 6 hours and trypsinised prior to harvest (Fig. 9D). Internalisation of the virus was measured by quantifying total intracellular HBV DNA in both HepG2 and HepG2-NTCP K7 cells. HBV uptake into HepG2 cells was significantly lower than in HepG2-NTCP K7 cells.

To investigate whether internalised virus could establish a productive infection cells, were then shifted for 1, 3 and 6 hours to 37 °C, subjected to trypsinisation at indicated time points and either harvested for intracellular DNA measurements or media was replaced and supernatants were analysed 3 and 7 days post inoculation for HBeAg secreted by HBV infected cells (Fig. 9E). Significantly increasing amount of total intracellular HBV DNA was detected within 1 – 6 hours compared to the 4 °C trypsinisation that was set as negative control. Respective HBeAg values showed a time dependent increase indicating that internalised virus from 1 hour onwards post trypsin treatment can lead to a productive infection.

In summary, the synchronised HBV uptake assay allows monitoring HBV kinetics spanning viral attachment, particle internalisation and establishment of a productive infection.

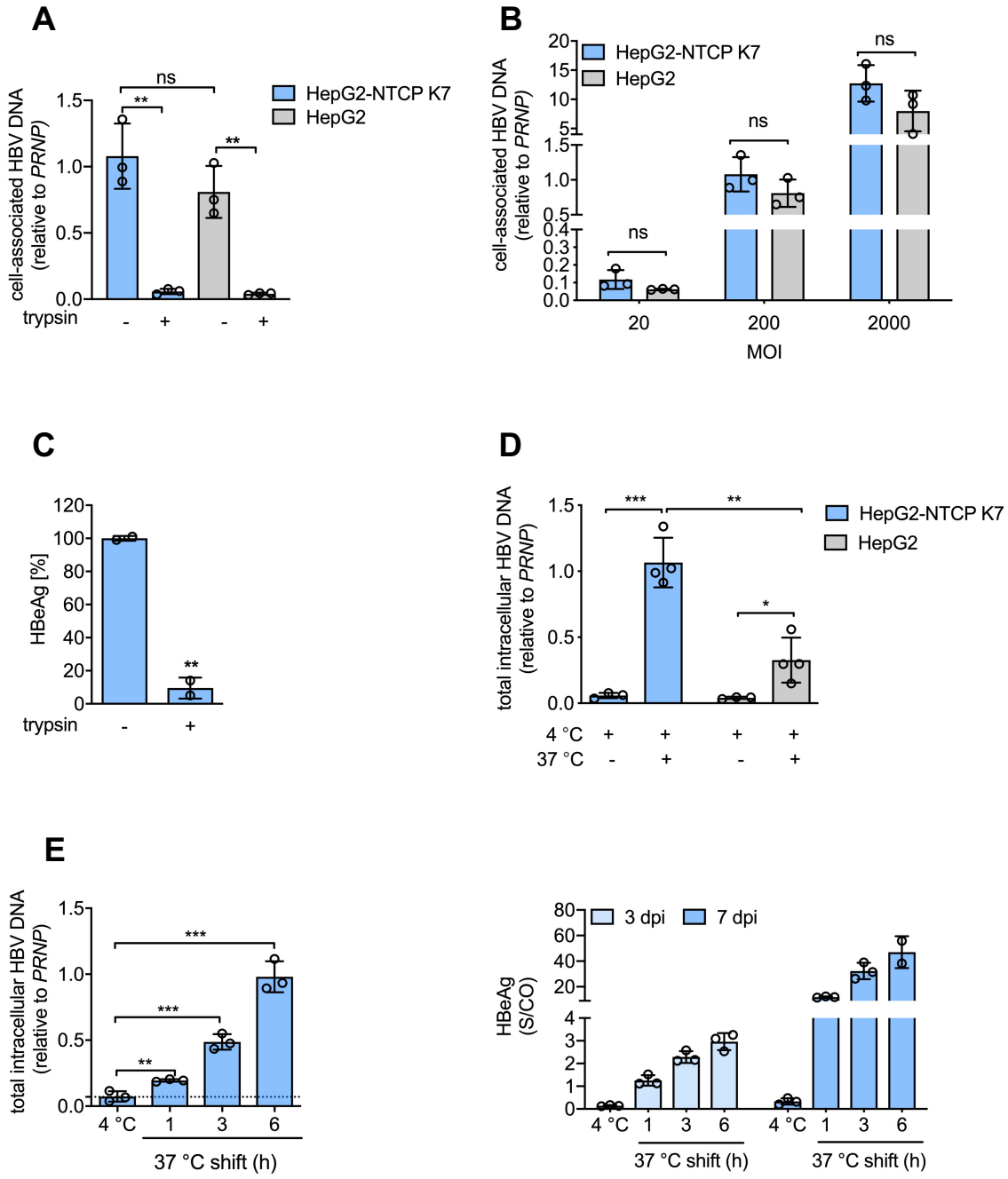

Figure 9: Characteristics of the synchronised HBV uptake assay. (A) HBV attachment (MOI 200) in HepG2-NTCP K7 and HepG2 cells was assessed. Cell-associated HBV DNA relative to *PRNP* (prion protein gene) was analysed in the presence and absence of trypsinisation after 1 hour at 4 °C. **(B)** HBV attachment with increasing MOI (20- 2000) was analysed measuring cell-associated HBV DNA relative to *PRNP*. **(C)** Effect of trypsin on viral infectivity was analysed via HBeAg measurements at day 5 post infection (p.i.). **(D)** HBV uptake assay was performed on HepG2-NTCP K7 and HepG2 cells. Cells were either harvested after 1 hour at 4 °C upon trypsinisation or shifted to 37 °C for 6 hours with subsequent trypsinisation and analysed for total intracellular HBV DNA relative to *PRNP*. **(E)** HBV uptake assay was performed and cells were either trypsinised and harvested after 1 hour at 4 °C or after shifting to 37 °C for 1, 3 and 6 hours harvested for total intracellular HBV DNA analysis. In the same experimental setup post trypsinisation fresh media was added and secreted HBeAg was measured at day 3 and 7 p.i. Data represent one independent experiment. In total three independent experiments with up to four biological replicates were performed. Statistical analysis: Student's unpaired *t*-test (ns: not significant, *p<0.05, **p<0.01, ***p<0.001).

To verify that the intracellular HBV DNA signal from internalised virus was dependent on viral encoded glycoproteins or NTCP, I employed reagents that are known to inhibit HBV infection (Fig. 10A). Heparin, that shields the virus from HSPG attachment, Myrcludex B, a preS1 peptide that specifically interferes with NTCP by blocking viral entry and Hepatect, a polyclonal antibody mixture known to neutralise infection were applied (Beckebaum et al., 2018, Lempp and Urban, 2014). All agents were able to significantly inhibit HBV entry to over 90 % and prevented subsequent cccDNA formation. Since heparin blocked entry and infection most efficiently it was further included as negative control for subsequent experiments.

HBV S-protein is known to be important in HBV attachment and entry (Lu and Block, 2004, Sureau and Salisse, 2013). Thus, I further investigated the effect of serum derived non-infectious subviral particles (SVP) that contain the S-protein on HBV entry (Fig. 10B). Purified serum derived SVP was used to circumvent adverse effects through bacterial or yeast residual proteins which can be an alternative source for SVP production. Subviral particles were applied in a dose dependent manner, ranging from 20 to 200 μg in the presence of HBV. At 20 μg subviral particles did not have an effect on HBV entry. However, with increasing HBs concentrations virus entry was significantly reduced which was confirmed with HBeAg measurements. This indicated competition of exogenous SVPs at higher concentrations with the viral envelope for viral receptors and confirmed that HBV entry in this assay is S-protein-dependent and thus specific for HBV.

As for the standard HBV infection protocol polyethylene glycol (PEG) and dimethyl sulfoxide (DMSO) are used I next investigated their impact on HBV entry. Both are not physiologically relevant to human infection but are required in *in vitro* systems. PEG significantly increased HBV uptake up to 8-fold which was specifically inhibited by heparin (Fig. 10C) (Ko et al., 2018). PEG is known to promote membrane fusion and may induce non-specific fusion between viral particle and the host membrane (Yang and Shen, 2006). The usage of PEG was therefore omitted in subsequent experiments to provide a more physiological setting and resemble natural human infection.

DMSO did not have an impact on HBV entry (Fig. 10D). However, for further experiments DMSO was included since it is known to be needed for downstream cccDNA transcription (Ko et al., 2018, Sainz and Chisari, 2006).

Altogether, these findings confirm that the established synchronised uptake assay is HBV specific and dependent on viral glycoproteins, showed HSPG mediated attachment and NTCP-mediated entry and can be further employed to investigate HBV internalisation kinetics.

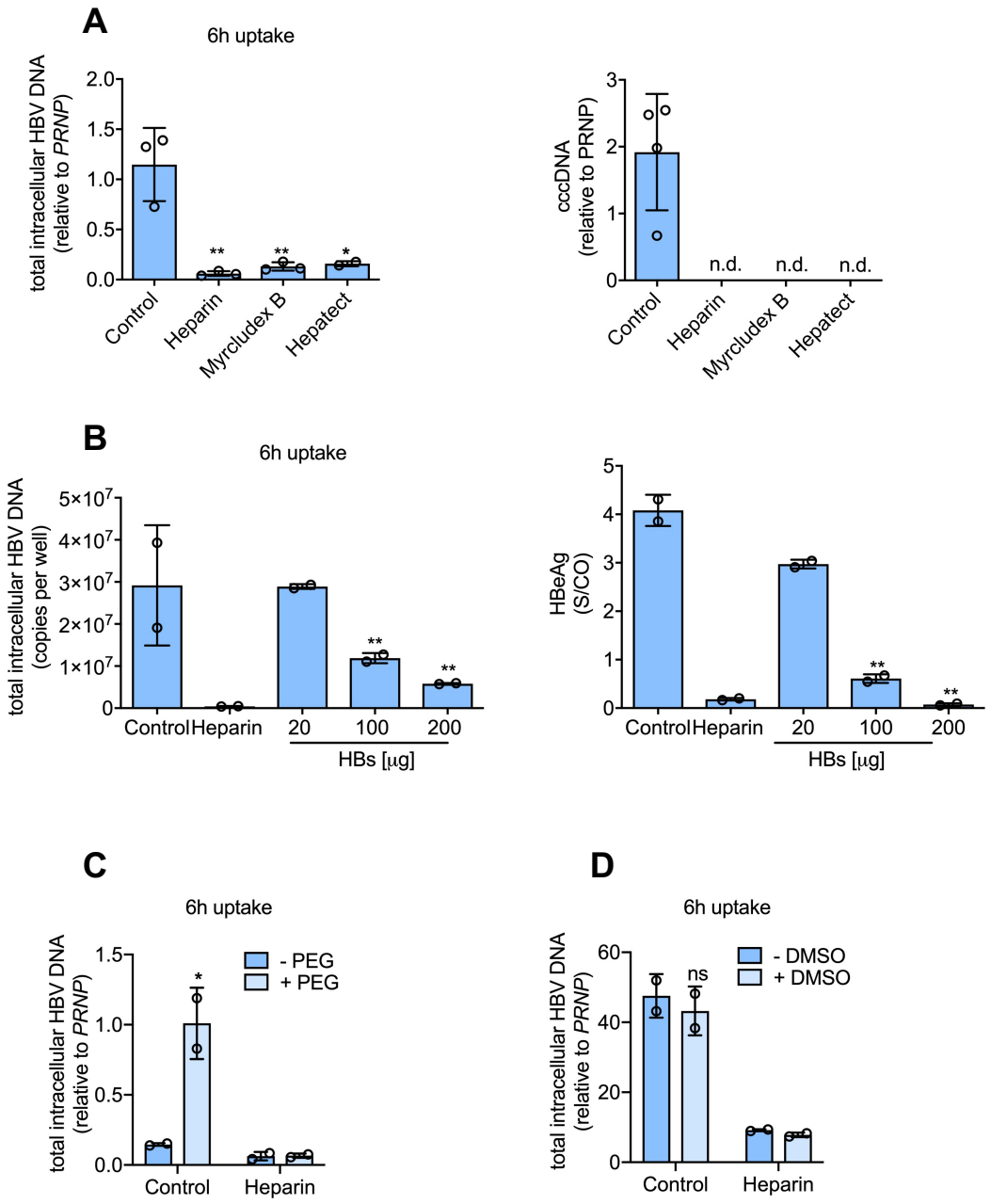

Figure 10: Specificity of the HBV uptake assay. **(A)** Analysis of HSPG, NTCP and viral glycoprotein dependency with known inhibitors heparin (50 IU/ml), Myrcludex B (200nM) and Hepatect (0.5 IU/ml), respectively, in the HBV uptake assay (MOI 200). Total intracellular HBV DNA at 6 hours post 37 °C shift and subsequent cccDNA at day 3 p.i. was measured relative to *PRNP*. **(B)** Evaluation of serum derived subviral particles (SVPs) on HBV uptake at 6 hours post 37 °C shift and infection at day 3 p.i. (MOI 200). Purified SVPs were co-treated in a dose dependent manner (20-200 µg) upon HBV inoculation. Effect of **(C)** 4 % PEG and **(D)** 2.5 % DMSO and on synchronised HBV uptake at 6 hours post 37 °C shift was investigated measuring total intracellular HBV DNA relative to *PRNP*. Data represent one independent experiment. In total three independent experiments with up to three biological replicates were performed. Statistical analysis: Student's unpaired *t*-test (ns: not significant, *p<0.05, **p<0.01, ***p<0.001); n.d.: not detectable.

2.2 HBV entry kinetics

To this date, HBV internalisation dynamics still remain unclear. The following chapter will address entry kinetics by employing the synchronised HBV uptake assay.

2.2.1 Evaluation of HBV uptake kinetics

To further characterise HBV entry kinetics, analysis on different hepatic and primary cells was obtained (Fig. 11). Virus was inoculated at 4 °C for 1 hour and shifted to 37 °C for indicated time points (0- 8 hours). At each time point the cells were trypsinised prior to harvest for total intracellular HBV DNA analysis. HepG2-NTCP K7 cells showed a time-dependent increase in total intracellular HBV DNA until 8 hours whereas the respective parental cell line, HepG2 cells, showed modest uptake capacity (Fig. 11A). The same kinetic profile was observed in Huh7-NTCP and the respective parental cell line (Fig. 11B). Further, entry kinetics was assessed in HepaRG cells and primary human hepatocytes (PHH) in order to provide a more physiological context (Fig. 11C-D). In order to obtain sufficient signal in these cells for analysis, PEG was required. In both cells similar kinetics as for HepG2 and Huh7 cells containing NTCP was observed with a time dependent increase in intracellular HBV DNA up to 6 hours for PHH, and 8 hours for HepaRG cells.

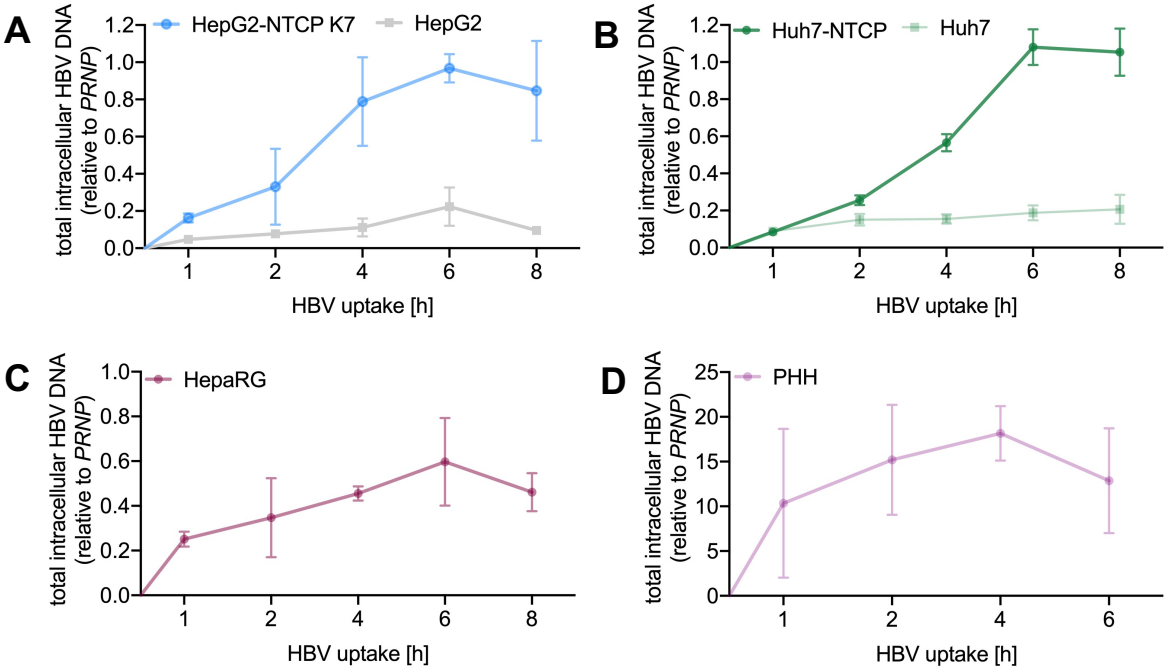

Figure 11: HBV internalisation kinetics into target cells. Synchronised HBV uptake (MOI 200) was assessed over time (0-8 hours) in **(A)** HepG2 and HepG2-NTCP K7 cells **(B)** Huh7 and Huh7-NTCP **(C)** HepaRG **(D)** and PHH. HBV uptake was measured analysing total intracellular HBV DNA relative to *PRNP* at indicated time points post 37 °C shift. Note, in HepaRG and PHH 4 % PEG was required for sufficient signal. Data from one representative experiment is shown. In total three independent experiments with up to four biological replicates were performed.

To further characterise HBV entry, I selected HepG2-NTCP K7 cells for subsequent analysis since HBV infection of these cells are very efficient (Ko et al., 2018). Internalisation was monitored measuring the following viral parameters, incoming HBV core and envelope proteins as well as intracellular HBV DNA in the first 24 hours post 37 °C shift (Fig. 12). For incoming HBV envelope and core protein an increase was observed until 8 hours post internalisation with a subsequent decrease (Fig. 12A). Interestingly, intracellular HBV DNA depicted a delayed peak at 12 hours (Fig. 12B).

To conclude, these data insinuate the time frame of viral uncoating in the cytoplasm and nuclear entry of the genome for cccDNA formation.

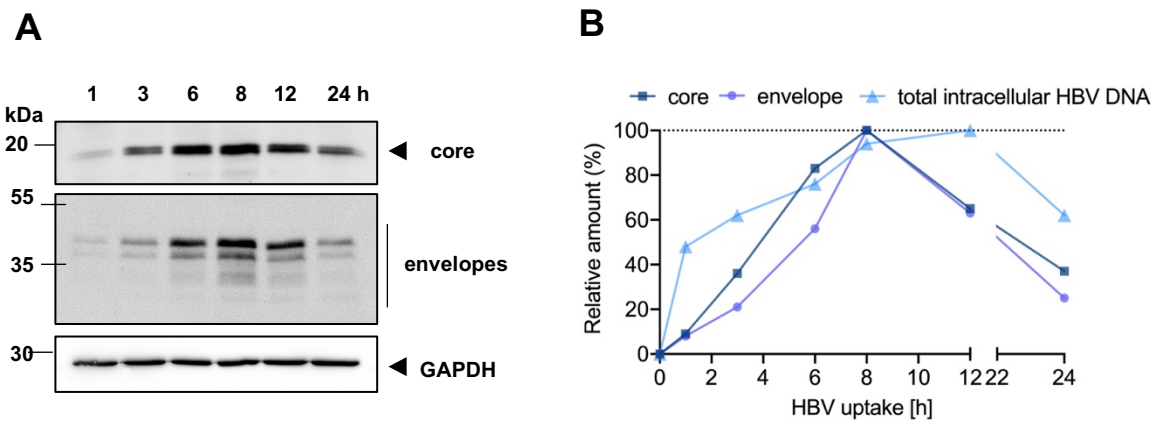

Figure 12: Characterisation of entry kinetics in HepG2-NTCP K7 cells. (A) Synchronised HBV uptake kinetics (MOI 200) was further dissected by analysing incoming HBV envelope and core protein over time (0-24h) via Western blot. **(B)** A summary of internalisation kinetics is depicted showing total intracellular HBV DNA, incoming HBV core and envelope protein kinetics. Bands determined at indicated time points in panel A for HBV core and envelope protein was quantified and plotted. The highest values at 8 hours were set to 100 %. For total intracellular HBV DNA the highest value at 12 hours was set to 100 %. Data from one representative experiment is shown. In total three independent experiments were performed.

2.2.2 Rate-limiting steps in the early HBV life cycle

To study the rate-limiting steps in HBV entry the distinct steps in the early viral life cycle was summarised. Table 1 displays the absolute numbers relative to cm^2 in total HBV DNA (input virus), cell-associated HBV DNA at 4 °C (attachment), total intracellular HBV DNA at 6 hours and cccDNA formation at 72 hours post 37 °C shift in HepG2 and HepG2-NTCP K7 cells. This data set combines the analysis of eight individual experiments with biological duplicates. Relative percentage values to the preceding step in viral entry has been calculated. In HepG2 cells 18 % of input virus was able to attach at the cell surface and 8 % was able to internalise. From total virus attached at the cell surface 45 % was able to internalise. However, internalised virus did not result in a productive infection since cccDNA was not detected at 72 hours. In HepG2-NTCP K7, 25 % of input virus was able to attach at the cell surface. In the presence of NTCP attachment was comparable to parental HepG2 cells. With NTCP, however, 83 % of attached viral particles were able to internalise. Subsequently, only 0.6 % from attached virus was able to form cccDNA at 72 hours p.i. in the presence of NTCP and none without NTCP.
A loss of 2 logs was observed between internalised virus and cccDNA formation. This indicated that degradation events may occur during viral entry, viral uncoating, nuclear import or rc- to cccDNA conversion.

Concluding my data indicate slow and inefficient processes are involved in the early HBV life cycle. Furthermore, they indicate that rc- to cccDNA conversion imposes a major restictrion in HBV infection efficacy.

	HepG2			HepG2-NTCP K7		
	Absolute copy number (relative to cm^2)	% from input virus	% from attached virus	Absolute copy number (relative to cm^2)	% from input virus	% from attached virus
Input	$1.5x10^8 \pm 2.9x10^7$	-	-	$1.5x10^8 \pm 2.9x10^7$	-	-
Attachment	$2.6x10^7 \pm 4.1x10^6$	18	-	$3.7x10^7 \pm 4.7x10^6$	25	-
Total intracellular HBV DNA (6h p.i)	$1.2x10^7 \pm 1.9x10^6$	8	45	$3.1x10^7 \pm 2.5x10^6$	21	83
cccDNA (72h p.i.)	n.d.	-	-	$2.2x10^5 \pm 3.8x10^4$	0.2	0.6

Table 1: Absolute quantification of early events in the HBV life cycle. Absolute copy numbers relative to cm^2 of total HBV DNA as input virus (MOI 200), cell-associated HBV DNA for 1 hour at 4 °C (attachment) and total intracellular HBV DNA after synchronised uptake at 6 hours post 37 °C shift is depicted. Absolute cccDNA values at 72 hours p.i. are displayed. Relative percentages from preceding step which was set to 100 % was calculated in HepG2 and HepG2-NTCP K7 cells. These data are presented as the mean ± SEM and combine eight independent experiment with biological duplicates. n.d.: not detected.

2.2.3 Subcellular localisation of HBV DNA

The time frame as to when HBV accesses the nucleus still is unknown. To investigate this, I analysed synchronised HBV uptake into subcellular compartments quantifying total intracellular HBV DNA and cccDNA. Whole cell lysates from HepG2-NTCP K7 cells were fractionated into cytoplasm and nucleus and purification assessed by measuring nuclear (lamin A/C) and cytoplasmic (α-tubulin) resident proteins (Fig. 13A). Analysis of *PRNP* gene, that is exclusively present in the nucleus, via qPCR at indicated time points was used as quality control confirming fractionation (Fig. 13B).

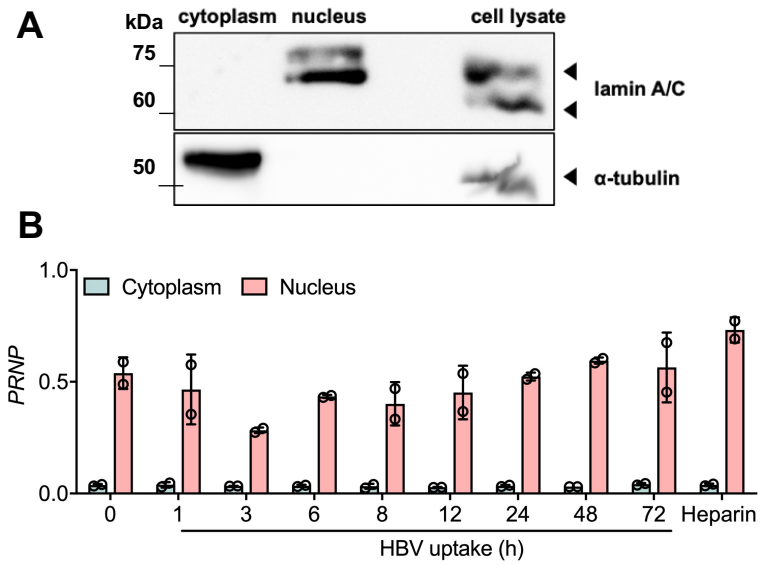

Figure 13: Subcellular fractionation into cytoplasm and nucleus. (A) Western blot targeting lamin A/C and α-tubulin that are nuclear and cytoplasmic resident protein, respectively. Whole cell lysate was included as a control. **(B)** Upon synchronised HBV entry samples were subjected to qPCR analysis of cytoplasmic and nuclear extracted DNA for *PRNP* at indicated time points post 37 °C shift. Data from one representative experiment is shown. In total three independent experiments with biological duplicates were performed.

HBV uptake post 37 °C shift was investigated from 0 - 72 hours. Samples were harvested post trypsinisation at indicated time points and separated into cytoplasmic and nuclear fractions and analysed for total intracellular HBV DNA or cccDNA (Fig. 14).

The levels of HBV DNA in the cytoplasm increased up to 12 hours and declined thereafter (Fig. 14A). In the nucleus HBV DNA was first detected between 3 and 6 hours post incubation at 37 °C that increased up to 24 hours with a subsequent decline. cccDNA was first detected 24 hours post 37 °C shift and increased until 72 hours in the nucleus and was negative in the cytoplasm (Fig. 14B). At 6 hours the absolute copies of HBV DNA in the nucleus was approximately one log lower than in the cytoplasm (Fig.

14A) indicating nuclear transport of rcDNA. When cytoplasmic HBV DNA reached a peak at 12 hours the amount of HBV DNA in the nucleus was an approximately 3-fold lower. HBV DNA in the nucleus reached its maximum at 24 hours, however, overall values were 2-fold lower compared to HBV DNA in the cytoplasm. Total cccDNA numbers from 24 – 72 hours were 4- to 2 -log lower compared to the corresponding HBV DNA values in the cytoplasm and nucleus, respectively (Fig. 14B). These results indicate degradation events occurring between particle internalisation and cccDNA formation (Fig. 14C).
The overall nucleus to cytoplasm ratio of HBV DNA increased until 48 hours with a subsequent decrease until 72 hours confirming rc- to cccDNA conversion.
In comparison to table 1 the total intracellular HBV DNA values at 6-hour p.i. in this experiment were 10-fold higher. This may be due to changes in the experimental setup e.g. sample separation into subcellular compartments, HepG2-NTCP K7 cell condition and general variations among individual experiments.

In summary, this data showed that the delivery of the viral genome from the cell surface to the nucleus took 3-6 hours. However, cccDNA was only detected at only 24 hours post 37 °C shift demonstrating that the conversion from rc- to cccDNA is slow and inefficient.

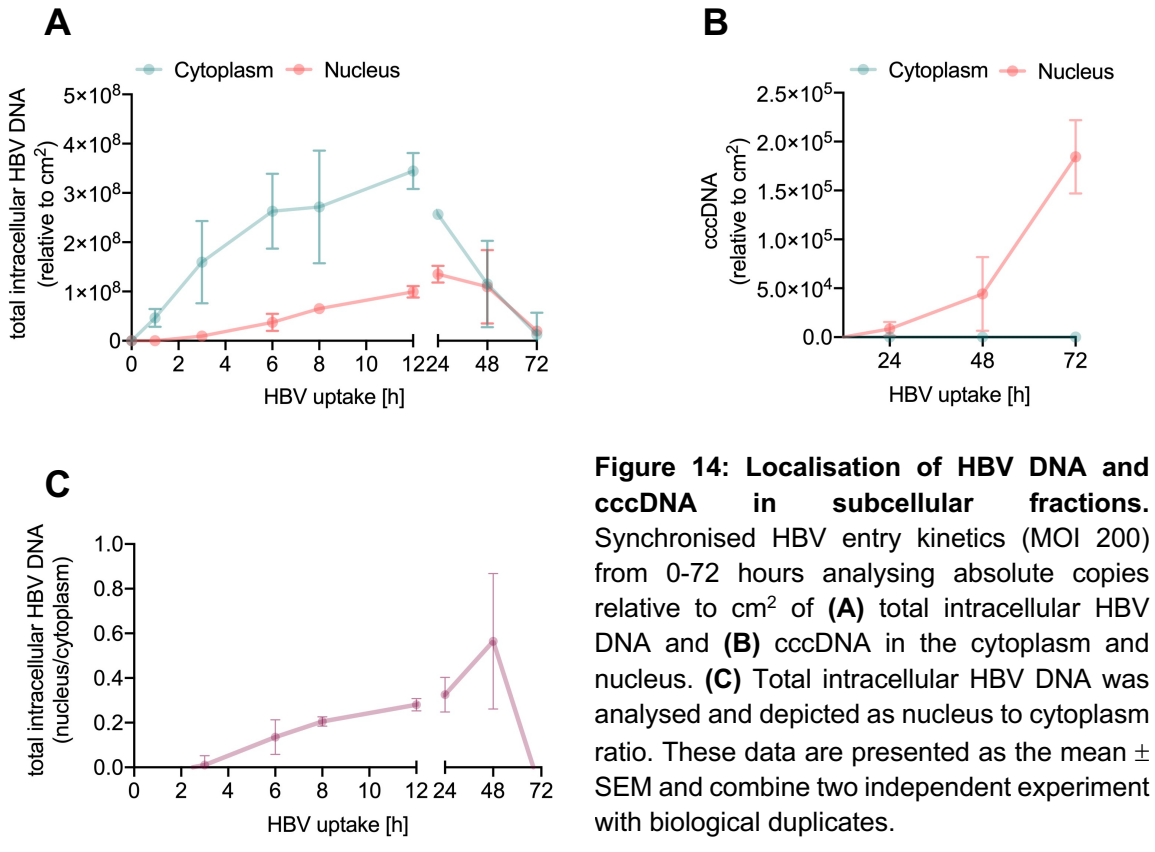

Figure 14: Localisation of HBV DNA and cccDNA in subcellular fractions. Synchronised HBV entry kinetics (MOI 200) from 0-72 hours analysing absolute copies relative to cm^2 of **(A)** total intracellular HBV DNA and **(B)** cccDNA in the cytoplasm and nucleus. **(C)** Total intracellular HBV DNA was analysed and depicted as nucleus to cytoplasm ratio. These data are presented as the mean ± SEM and combine two independent experiment with biological duplicates.

The rc- to cccDNA conversion may be time-limiting for two distinct reasons, first, the activation of host factors required for conversion or second, due to the viral genome uncoating from the capsid at the nucleus. To assess the latter, I employed a HBV core protein allosteric modulator (CpAM) that is primarily known to interfere with capsid assembly (Ko et al., 2019, Ruan et al., 2018). Recently, the heteroaryldihydropyrimidine (HAP)-type CpAM, HAP_R01 was shown to prevent the establishment of HBV infection (Ko et al., 2019). HAP_R01 at optimal dose (5 μM) was employed to investigate whether disrupting capsid integrity had an impact on cccDNA formation. I repeated subcellular fractionation as described in figure 14 and monitored synchronised HBV internalisation between 0-72 hours in the presence and absence of HAP_R01. Both in the cytoplasm and nucleus the HAP_R01 treated samples showed a time dependent increase until 12 hours in total intracellular HBV DNA similar to the untreated control (Fig.15A). However, total intracellular cytoplasmic HBV DNA had rapidly declined after 24 hours compared to untreated control. A rapid decline in nuclear HBV DNA in the presence of HAP_R01 was also observed after 24 hours (Fig. 15B). Compared to the untreated control, where cccDNA was present at 24 hours, cccDNA in HAP_R01 treated samples was detected only at 48 hours (Fig. 15C). Interestingly, a more than 2-fold reduction in cccDNA was observed when HAP_R01 was applied.

In summary, these data suggest that capsid integrity is required for efficient cccDNA establishment from incoming virus.

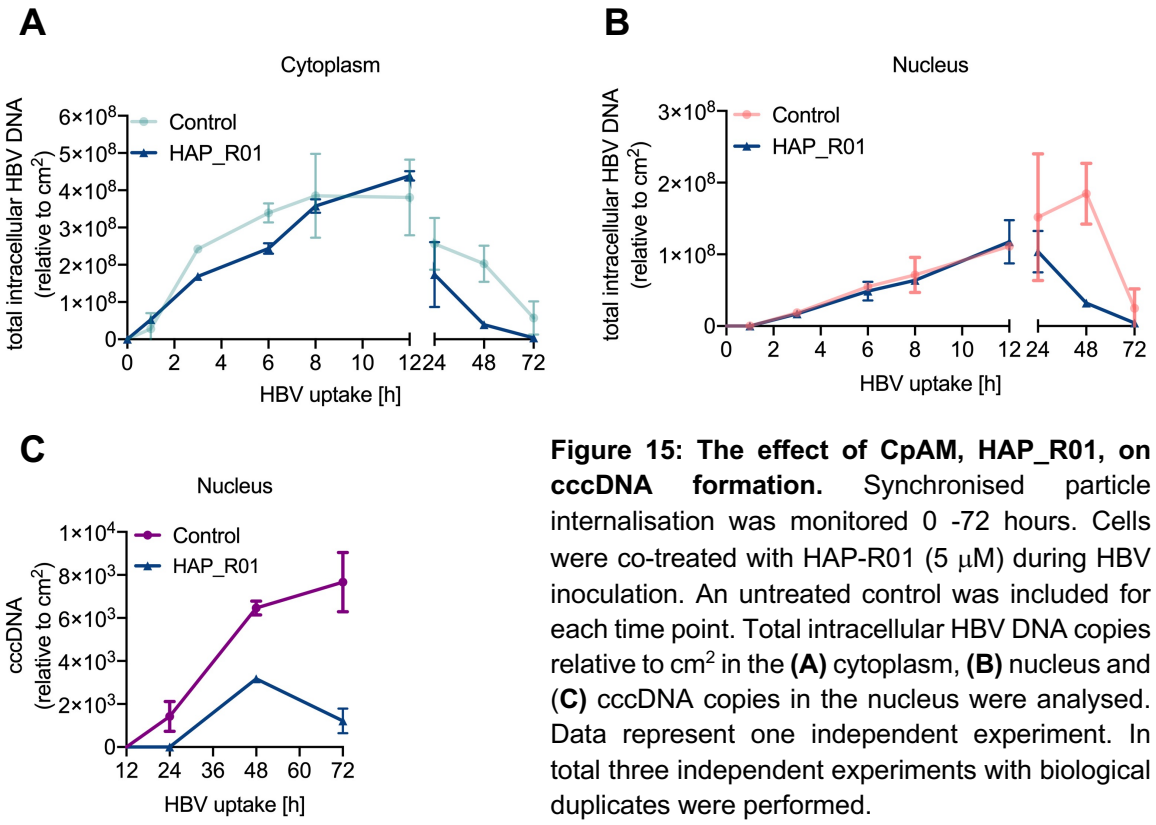

Figure 15: The effect of CpAM, HAP_R01, on cccDNA formation. Synchronised particle internalisation was monitored 0 -72 hours. Cells were co-treated with HAP-R01 (5 μM) during HBV inoculation. An untreated control was included for each time point. Total intracellular HBV DNA copies relative to cm^2 in the **(A)** cytoplasm, **(B)** nucleus and (**C)** cccDNA copies in the nucleus were analysed. Data represent one independent experiment. In total three independent experiments with biological duplicates were performed.

2.3 Visualisation of incoming viral particle

Imaging can contribute to a better understanding of a spatio-temporal resolution of virus –host interactions at its earliest time points. Visualisation of HBV entry would provide new opportunities to define the role of HBV receptors, uncoating of the viral capsid as well as nuclear import of the virus.

Several antibodies targeting HBV structural proteins such as core and envelopes are available. I assessed synchronised particle entry and stained for incoming core particle with a core-specific antibody (data not shown). Unfortunately, this approach was not successful, which may be due to antibody dependent sensitivity issues.

Next, I stained for incoming virus targeting HBV envelope protein with a specific antibody (H863) that recognises all three, small, middle and large surface proteins of HBV (Fig. 16A). To ensure sufficient signal for detection I used a high MOI of 1000 and included PEG for imaging. Synchronised viral uptake was monitored in HepG2-NTCP K7 cells for 1, 3 and 6 hours post 37 °C shift with heparin that blocks viral entry serving as a negative control. A time dependent increase in intracellular HBV envelope proteins was observed which confirmed kinetic analysis from figure 11 and 12. Heparin inhibited particle internalisation confirming uptake was HBV specific. Being able to visualise envelope proteins from incoming HBV particle gives us an insight of the cellular localisation of these proteins in the cell. However, this does not necessarily indicate the location of the intact virus. At some point in the early life cycle the viral capsid needs to be released in order to deliver the genome into the nucleus where the envelope of the virus remains in the cytoplasm.

To overcome this problem, I generated a virus that was labelled in the viral genome. The HBV producing cell line HepG2.2.1.5 was supplemented with 5-Ethynyl-2'-deoxycytidine (EdC) which incorporated into the genome of newly produced secreted virus. The visualisation of the viral genome is based on “click-chemistry”. The ethynyl containing DNA reacts with a biotin-azide in the presence of copper. As previously reported, to enhance sensitivity I added a strepatividin-Cy5 tag that binds to biotin-azide (Winer et al., 2018). I purified EdC containing virus secreted from treated HepG2.2.1.5 cells in parallel with untreated samples and checked for viral infectivity. EdC did not impair the viral infectivity as HBeAg levels upon infection into HepG2-NTCP K7 cells when compared to non-modified HBV (Fig. 16B). Based on this, I analysed synchronised entry into HepG2-NTCP K7 cells looking at 6 hours post 37 °C shift and included heparin as a negative control (Fig. 16C). After performing the “click reaction” samples were

subjected to confocal microscopy. EdC-HBV inoculated cells showed a positive Cy5 signal confirming viral entry. Heparin inhibited EdC-HBV entry into the cells.

These two staining protocols established will enable to dual stain for incoming HBV monitoring viral envelope and genome at the same time. These studies will give an insight into how and when HBV uncoating and the delivery of the genome in the nucleus occurs.

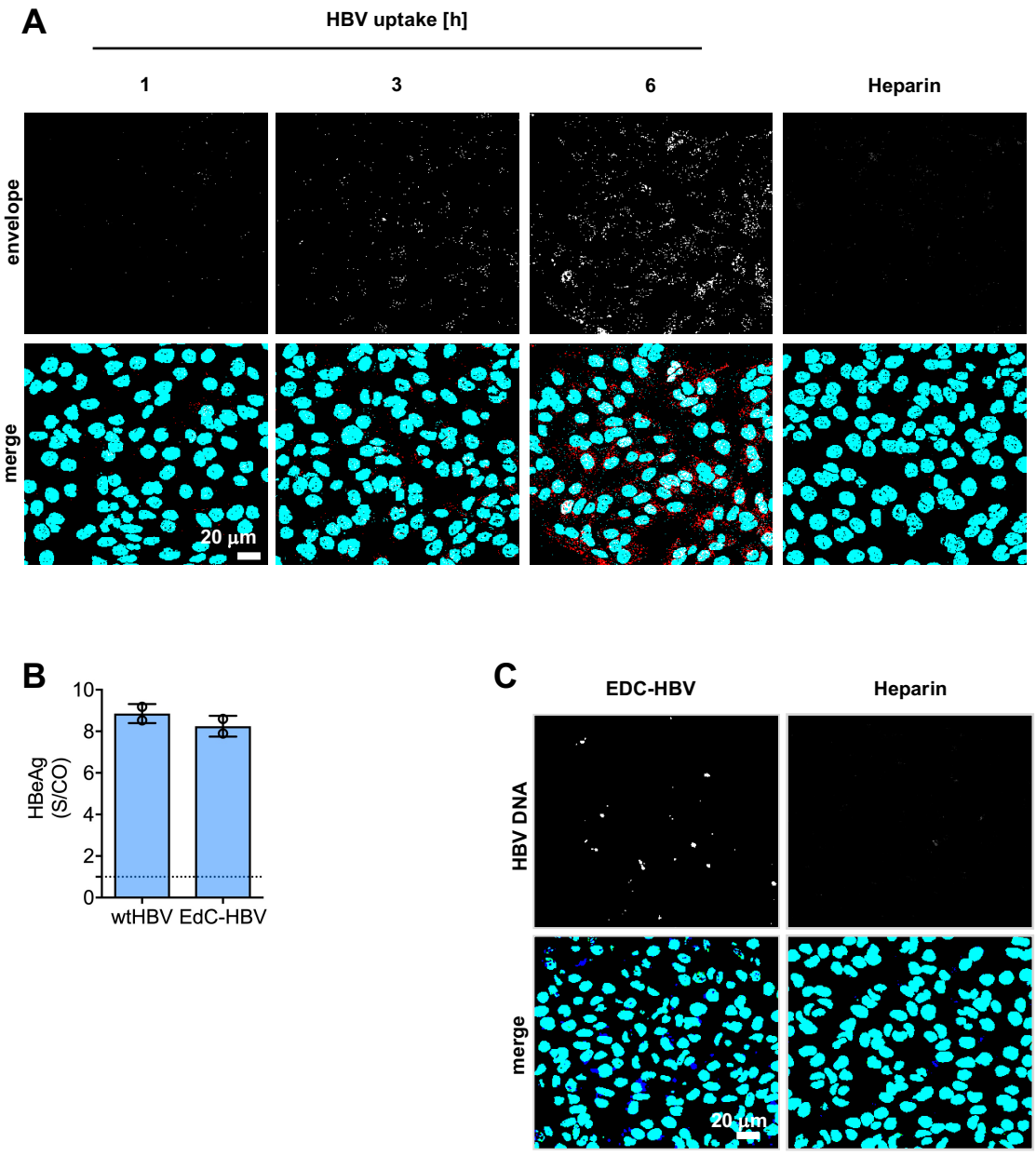

Figure 16: Tools to image HBV entry. (A) Synchronised HBV uptake (MOI 1000) was assessed in the presence of 4 % PEG. Incoming virus was stained for HBV envelope protein at the indicated time points post 37 °C shift (1-6 hours). Heparin was used as negative control. Envelope staining and a merge with DAPI is depicted. **(B)** Infectivity of EdC-HBV was compared to non-modified virus by measuring infection analysing HBeAg at day 5 p.i.. **(C)** Synchronised HBV-EdC internalisation at 6 hours post 37 °C shift is depicted showing Cy5 staining for HBV DNA with merge indicating nuclear DAPI staining.

2.4 Characterisation of entry pathway exploited by HBV

I investigated possible endocytic pathways involved in HBV entry by employing specific pharmacological inhibitors. Moreover, I studied the role of caveolin-1 and dependency on the cytoskeleton in HBV entry.

2.4.1 Cellular endocytic pathways required for HBV entry and infection

To investigate which cellular endocytic pathways are important for productive HBV entry and infection, the dependency of cholesterol-, dynamin-, clathrin- mediated pathways and macropinocytosis was analysed.

Synchronised particle internalisation at 6 hours post 37 °C shift measuring total intracellular HBV DNA in the presence of pharmacological inhibitors that interfere with the above mentioned pathways were employed. In parallel, the effect on HBV infection was monitored analysing HBeAg 5 days post inoculation. Pharmacological agents were used at concentrations where no cell toxicity was observed. Heparin and Myrcludex B that inhibit HBV entry were included as negative controls (Fig. 17). All inhibitors were tested on HepG2-NTCP K7, Huh7-NTCP and HepaRG cells at optimal dose.

MβCD, methyl-β-cyclodextrin, depletes cholesterol at the cell surface hence interferes with caveolin-mediated endocytosis downstream (Lajoie and Nabi, 2010). MβCD was pre-treated prior to HBV inoculation. It was able to significantly reduce HBV entry in all tested cell lines. This was confirmed with the reduction of HBeAg level upon viral infection (Fig. 17A-C).

Dynamin is a GTPase protein that is primarily involved in pinching off from the plasma membrane for both caveolin- and clathrin-dependent endocytosis. This can be perturbed using Dynasore that inhibits scission of endocytic vesicles (Mettlen et al., 2009).

Co-treatment of Dynasore during HBV inoculation significantly inhibited HBV entry and infection in HepG2-NTCP K7 and Huh-7 NTCP cells (Fig. 17A-B). It did not have an effect on HepaRG cells (Fig. 17C).

Furthermore, I tested Pitstop a selective inhibitor for clathrin-mediated endocytosis. Pitstop, that was co-treated during inoculation, reduced HBV entry and infection to 50 % in HepG2-NTCP and Huh7-NTCP cells. However, the inhibition was more pronounced in HepaRG cells.

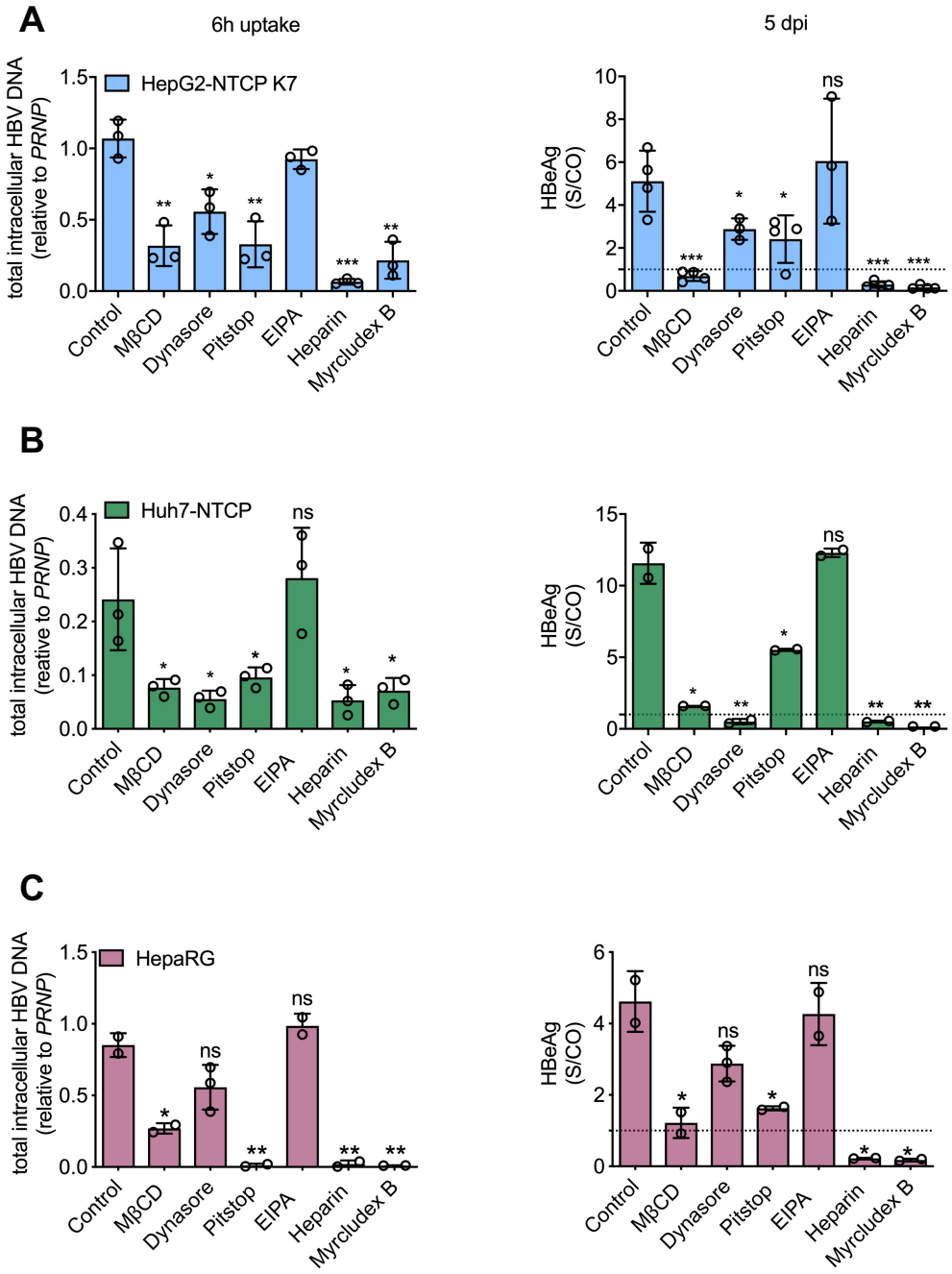

Figure 17: Characterising endosomal pathways exploited by HBV. To dissect the HBV entry pathway pharmacological agents targeting cholesterol-dependency (MβCD: 5 mM), dynamin- (Dynasore: 100 μM), clathrin- mediated endocytosis (Pitstop: 50 μM) and macropinocytosis (EIPA: 100 μM) were applied. Synchronised entry at 6 hour post 37 °C shift measuring total intracellular HBV DNA as well as HBV infection measuring HBeAg at day 5 p.i. was analysed in **(A)** HepG2-NTCP 7 cells, **(B)** Huh7-NTCP and **(C)** HepaRG cell**.** Data represent one independent experiment. In total three independent experiments with biological triplicates were performed. Statistical analysis: Student's unpaired *t*-test (ns: not significant, *p<0.05, **p<0.01, ***p<0.001).

Other mechanism of cellular entry such as macropinocytosis requires substantial rearrangements of the plasma membrane. To examine if HBV is taken up via macropinocytosis, I employed EIPA, ethyl-isopropyl amiloride, that inhibits the Na+/H+ exchanger (Devadas et al., 2014, Dowrick et al., 1993, Meier et al., 2002). In all tested cell lines co-treatment with EIPA did not affect HBV entry and infection.

As HepG2-NTCP K7 and Huh7-NTCP cells are cell lines easier to work with I continued characterising their requirement for clathrin in HBV entry.

To validate that these cells harbour functional clathrin pathway I tested labelled transferrin which is known to be taken up in a clathrin dependent manner (Fig. 18A). In both HepG2-NTCP K7 and Huh7-NTCP cells transferrin was taken up by the cells in a dose dependent manner. This indicated that both tested cell lines have an intact and functional clathrin pathway. Next, to confirm functionality of the compounds targeting clathrin mediated uptake, I used VSV pseudoparticles (VSVpp) in the presence of Dynasore and Pitstop (Fig. 18B). VSVpp have been reported to enter the cell in a dynamin- and clathrin-dependent manner (Meredith et al., 2016). The applied compounds were able to significantly inhibit VSVpp entry into HepG2-NTCP K7 cells proving functionality (Fig. 18C).

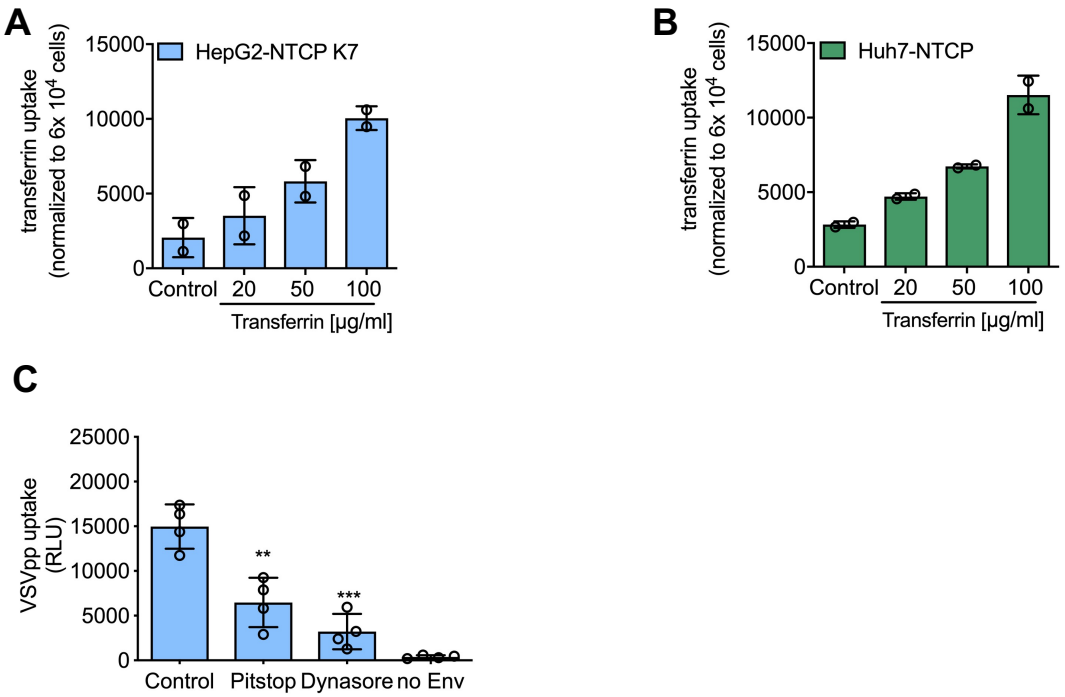

Figure 18: Verifying clathrin-dependent endocytosis. Labelled transferrin internalisation was measured in a dose dependent manner into **(A)** HepG2-NTCP K7 and **(B)** Huh7-NTCP cells with untreated cells set as control. Fluorescence values were normalised to 6x10^4 cells. **(C)** Inhibitory effect of dynamin and clathrin interfering agents Pitstop (50 µM) and Dynasore (100 µM), respectively, were verified in VSVpp entry measuring Relative Light Units (RLU) day 1 p.i.. Data represent one independent experiment. In total three independent experiments with up to four biological replicates were performed. Statistical analysis: Student's unpaired *t*-test (*p<0.05, **p<0.01, ***p<0.001).

Taken together, HBV entry in the tested cell lines required the presence of cholesterol at the plasma membrane. Dynamin played a role in HepG2-NTCP K7 and Huh7-NTCP cells with a subsequent clathrin-dependency in HBV entry.

Viruses often enter the cell in a pH-dependent manner. I next wanted to investigate whether HBV requires low pH for productive entry and infection. The lysosomotropic agent Bafilomycin A1, a specific v-ATPase inhibitor, raises the pH level in the early endosome and inhibits maturation to late endosome (Fig. 19). Synchronised HBV uptake and infection was assessed in HepG2-NTCP K7 cells in the presence of Bafilomycin A1. The entry inhibitors heparin and Myrcludex B were included as negative controls. Co-treatment with Bafilomycin A1 had a minimal effect on intracellular HBV DNA levels at 6 hours post 37 °C shift and increased HBeAg levels 5 days p.i. upon viral infection, suggesting that HBV internalisation was not pH-dependent.

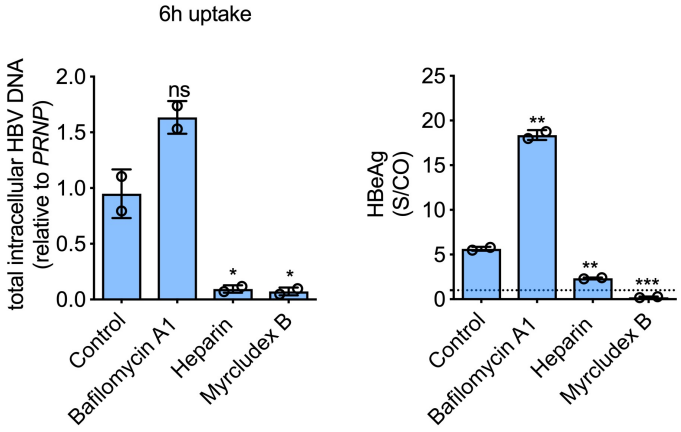

Figure 19: pH-dependency in HBV. Synchronised HBV uptake was assessed with the co-treatment of Bafilomycin A1 (100 nM) and analysed for total intracellular HBV DNA. HBV infection in the presence of Bafilomycin A1 was investigated measuring HBeAg at day 5 p.i.. Data from one representative experiment is shown. In total three independent experiments with biological duplicates were performed. Statistical analysis: Student's unpaired *t*-test (ns: not significant, *p<0.05, **p<0.01, ***p<0.001).

Altogether, this data indicates that stalling endocytosis at the stage of the early endosome may promote early endosomal release leading to a more productive viral infection.

2.4.2 Reconstitution of Caveolin-1 in HepG2-NTCP K7 cells

A study from *Macovei et al.* proposed that intact caveolin-1 is required for productive HBV infection in HepaRG cells. As mentioned before, in our cell culture system HBV entry was clathrin-dependent we next wanted to investigate the role for caveolin-1 in HBV entry. Caveolin-1 mediated routes may provide an alternative or additional route for a productive HBV infection. We first assessed the caveolin-1 expression in HepG2 and Huh-7 hepatoma cells as well PHH and HepaRG cells (Fig. 20). While high protein expression was detected in HepaRG cells no caveolin-1 was detected in any of the hepatoma cell lines or PHHs.

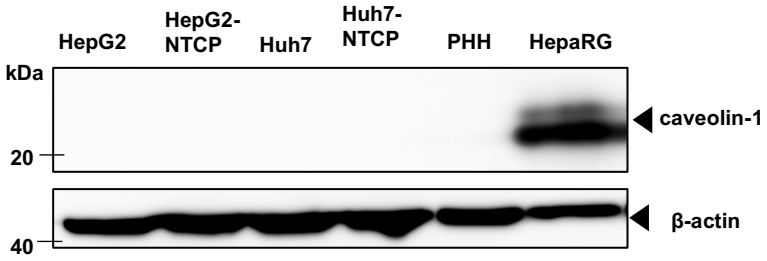

Figure 20: Caveolin-1 expression in hepatic cell lines. Western blot analysis was performed to detect caveolin-1 in HepG2, HepG2-NTCP, Huh7, Huh7-NTCP, PHH and HepaRG. β-actin was used as a reference protein.

As caveolin-1 expression is negative in hepatoma cell lines it may play a crucial role in viral entry *in vivo*. Thus, I reconstituted caveolin-1 into HepG2-NTCP K7 cells and studied HBV entry. Jochen M. Wettengel kindly generated HepG2-NTCP K7 cell clones that harboured either caveolin-1 or caveolin-1 with a RFP-tag. For visualising NTCP at the cell surface I applied labelled Myrcludex B staining and confirmed expression in all cell clones (Fig. 21A). All cell clones were screened for caveolin-1 protein expression by Western blot (Fig. 21B). Clone 5, 11, 12 and 13 expressed caveolin-1 expression and were studied further. A frequently used molecule to investigate caveolin mediated endocytosis is cholera toxin B (CTB). Labelled CTB at optimal dose was incubated with all cell clones and subjected to FACS analysis (Fig. 21C). As expected the parental HepG2-NTCP K7 cells were negative for CTB uptake. C5, C13 and C12 were positive and C11 cells were negative for CTB internalisation. However, total percentage of CTB positive cells in all clones was below 20 % unfortunately, indicating low caveolin-1 functionality in our cell clones. Thus, no final conclusion on the role of caveolin can be drawn.

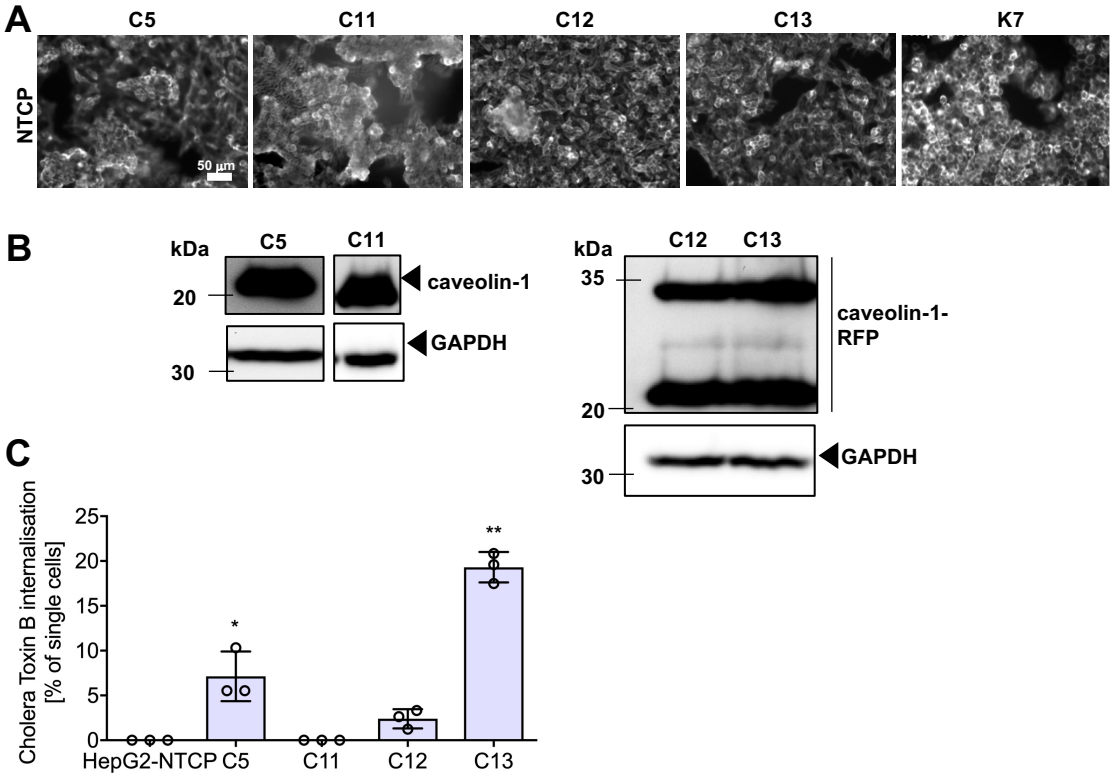

Figure 21: Generation of HepG2-NTCP clones that express caveolin-1. (A) Caveolin-1 cell clones (C5, C11, C12 and C13) were stained for NTCP expression at the cell surface applying labelled Myrcludex B and analysed via microscopy. **(B)** Western blot analysis of HepG2-NTCP with caveolin-1 or caveolin-1-RFP. GAPDH was included as a reference protein. **(C)** Caveolin-1 functionality was confirmed with labelled Cholera Toxin B (CTB) uptake into all cell clones via FACS analysis. CTB internalisation is depicted in % of single cells. Data represent one independent experiment. In total three independent experiments with biological triplicates were performed. Statistical analysis: Student's unpaired *t*-test (*p<0.05, **p<0.01, ***p<0.001).

Next, I investigated the effects of caveolin-1 on synchronised HBV entry analysing total intracellular HBV DNA at 6 hours post 37 °C shift (Fig. 22A). In addition, Pitstop that inhibits clathrin-mediated internalisation, was added as control in order to differentiate clathrin- from caveolin mediated effects. The overall HBV uptake capacity of the cell clones was similar and Pitstop showed comparable inhibitory activity with the caveolin-1 expressing clones as the parental cells. Subsequently, cccDNA formation from internalised virus was measured (Fig. 22B). Compared to HepG2-NTCP K7 cells C5, C12 and C13 displayed higher cccDNA levels. In addition, the application of Pitstop did not show any difference in cccDNA levels among all clones. Next, all caveolin-1 cell clones were subjected to HBV infection (Fig. 22C). HBeAg levels were significantly higher in C5, C12 and C13 compared to HepG2-NTCP cells. The high cccDNA and

HBeAg levels in these cells may be a clonal effect that is independent from caveolin-1 expression.

In summary, reconstituting caveolin-1 into HepG2-NTCP K7 cells did not render the cells more effective for HBV entry and infection. Higher cccDNA and HBeAg levels observed in C5, C12 and C13 may be due to a clonal effect, since the functionality of caveolin-1 expressed in these cells were relatively low.

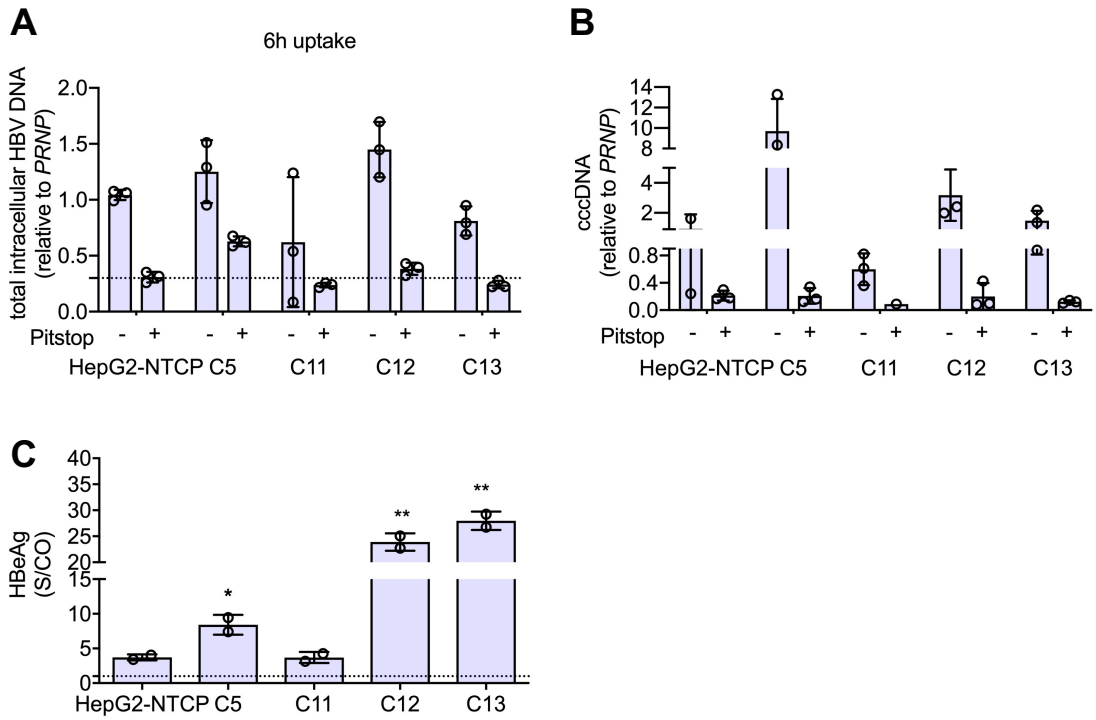

Figure 22: HBV entry and infection in HepG2-NTCP-K7 clones harbouring caveolin-1. (A) Synchronised HBV uptake was analysed at 6 hours post 37 °C shift measuring intracellular HBV DNA. Pitstop (50 μM) was added as control to differentiate between caveolin-1 and clathrin mediated effects. **(B)** Subsequent cccDNA from internalised virus was measured. **(C)** All caveolin-1 clones were tested for HBV infection analysing HBeAg at day 5 p.i.. Data from one representative experiment is shown. In total three independent experiments with up to four biological replicates were performed. Statistical analysis: Student's unpaired *t*-test (ns: not significant, *p<0.05, **p<0.01, ***p<0.001).

2.4.3 Involvement of the cytoskeleton in HBV entry

The cytoskeleton is made up from filamentous proteins, like actin and tubulin which contribute to stability and motility of the cell. To investigate whether the virus exploits the host cytoskeleton during viral entry I determined the effect of agents that interfere with the cytoskeleton. In untreated cells filamentous distribution of actin was observed (Fig. 23A left panel). Upon Cytochalasin D treatment, that depolymerises actin filaments, these filaments were disrupted and displayed a granular morphology.
Nocodazole, is a pharmacological reagent that disrupts polymerisation of tubulin filaments. Compared to untreated cells the addition of Nocodazole led to a diffused pattern of the microtubule filaments (Fig. 23A, right panel).
Next, I investigated whether HBV entry is dependent on the actin and tubulin network. Cells were co-treated with Cytochalasin D and Nocodazole upon HBV inoculation and harvested after 6 hour synchronised internalisation and analysed for total intracellular HBV DNA (Fig. 23B). Nocodazole and Cytochalasin D significantly reduced HBV entry in the first 6 hours. In HBV infection both reagents were able to significantly reduce HBeAg levels (Fig. 23C).

In conclusion, the cytoskeleton plays an important role in the first 6 hours of particle internalisation. This indicates motility of the virus across endosomes and further the transport of the viral capsid to the nucleus occurring at very early stages in viral entry requires both intact actin and tubulin filaments.

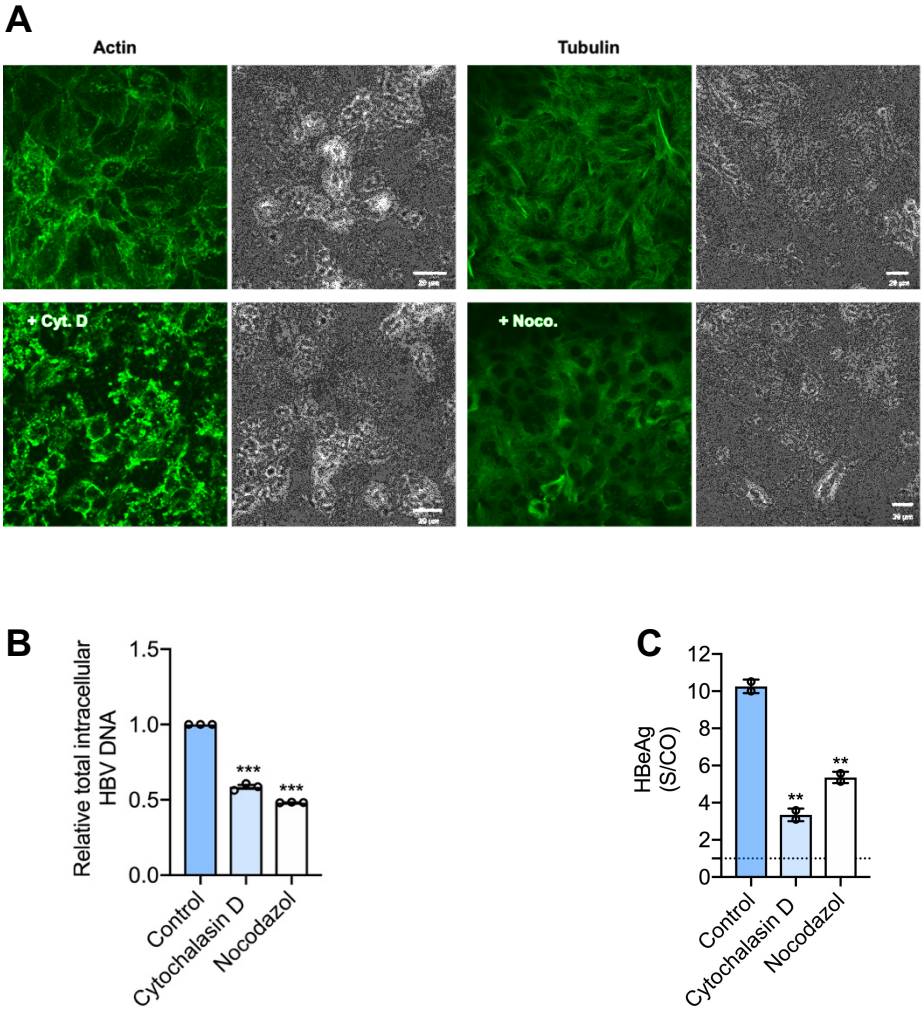

Figure 23: Role of actin and tubulin in HBV entry. (A) HepG2-NTCP K7 cells were stained for actin and tubulin and analysed via confocal microscopy. Cytochalasin D (Cyt.D) and Nocodazole (Noco.) ,50μM each, disrupted actin and tubulin filaments, respectively. **(B)** Synchronised HBV uptake assay was performed in the presence of Cytochalasin D and Nocodazole and cells were harvested at 6 hours post 37 °C shift measuring total intracellular HBV DNA. An untreated control was included for each time point and was set to 1. **(C)** HBV infection in the presence of Nocodazol and Cytochalasin D was performed and HBeAg levels were analysed at day 5 p.i.. Data represent one independent experiment. In total three independent experiments with up to three biological replicates were performed. Statistical analysis: Student's unpaired *t*-test (*p<0.05, **p<0.01, ***p<0.001).

2.5 HBV entry receptor

NTCP has been identified as an important cellular receptor for HBV and determines liver tropism and species specificity (Watashi and Wakita 2005). A deeper understanding into the functional role of NTCP will help to further examine the mechanisms of HBV-receptor interactions. More recently, EGFR has been reported to be a host entry cofactor that promotes HBV uptake (Iwamoto et al., 2019). In the following section the role of NTCP and EGFR in HBV entry has been characterised.

2.5.1 NTCP as the HBV entry receptor

The identification of NTCP has improved cell culture systems which make it possible to study HBV entry. In the following chapter I will first discuss the requirement of posttranslational modifications of NTCP in HBV infection. Secondly, the role of NTCP expression levels on HBV entry and finally the potential intracellular role for NTCP in HBV entry was investigated.

2.5.1.1 Effects of N-glycosylation of NTCP on HBV infection

NTCP harbours two N-linked glycosylation sites, however, the role of glycans in the context of protein trafficking and role for HBV infection has not been previously characterized.

In collaboration with the group of Stan van de Graaf, Amsterdam, we published the functional role of glycosylation of NTCP for HBV entry (Appelman et al., 2017). Mutants of NTCP harbouring either single- (NTCP-N5Q, NTCP- N11Q) or double- (NTCP-N5,11Q) mutations at the glycosylation sites were generated and expressed in HepG2 cells. Cells expressing NTCP with a mutated single glycosylation expressed protein at the cell surface (Fig. 24A) and internalised bile acids displaying physiological function consistent with their trafficking to the plasma membrane (Fig. 24B). However, glycosylation-deficient NTCP showed low cell surface expression and reduced bile acid transport. HBV infection was assessed by quantifying cccDNA and HBeAg levels (Fig. 24C-D). Both levels were comparable to wildtype in single glycosylation mutants, however, the double mutants displayed significantly low cccDNA and HBeAg levels (Appelman et al., 2017).

These data suggest that N-glycosylation is required for membrane localization, bile acid transport and HBV infection. Mutant NTCP harbouring a single glycan moiety is sufficient to preserve physiological and HBV receptor function.

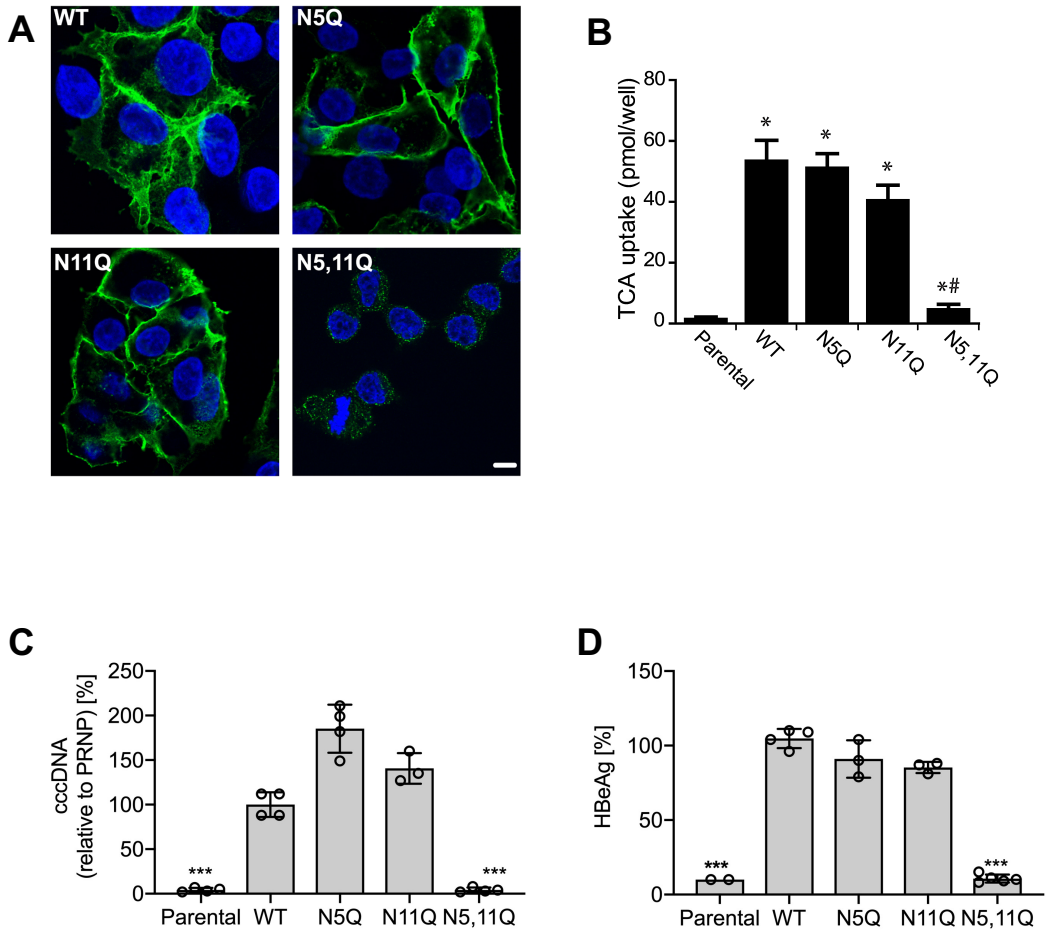

Figure 24: Effect of post-translational modification of NTCP on HBV infection. Wildtype HepG2-NTCP cells or cells harbouring single (N5Q, N11Q) or double (N5,11Q) N-glycosylated NTCP mutants were analysed for: **(A)** distribution at the plasma membrane, **(B)** bile acid uptake, **(C)** and HBV infection assessed by cccDNA and HBeAg expression. Data represent one independent experiment. In total three independent experiments with up to four biological replicates were performed. Statistical analysis: Student's unpaired *t*-test (*p<0.05, **p<0.01, ***p<0.001) (published in Appelman et al., 2017).

2.5.1.2 NTCP expression levels regulate HBV uptake

The generation of hepatoma cell lines to express NTCP has been used to study HBV infection and entry. These systems overexpress NTCP which is located throughout the entire plasma membrane. The question arose whether NTCP overexpression is required for productive HBV entry and infection. I analysed different in-house generated HepG2-NTCP clones and confirmed NTCP expression at the cell surface using labelled Myrcludex B. Three different cell clones K3, K6 and K9 were compared to the standard cell line used in our lab, HepG2-NTCP K7 cells. Confocal microscopy as well as FACS

analysis showed higher levels of NTCP expression in K3 and K6 and low expression in K9 compared to the K7 clone used in *Ko et al.* (Fig. 25A-B). Next, synchronised HBV entry at 6 hours post 37 °C shift was analysed for total intracellular HBV DNA. Heparin that inhibits viral entry was included as a negative control. We noted that HBV internalization into K3 was comparable to K7 cells. Viral entry into K6 was about 2 -fold lower compared to K7 cells (Fig. 25C). K9 did not promote viral entry. HBeAg upon infection however was similar between K3, K6 and K7 and was negative for K9 (Fig. 25D).

These results indicate that a certain threshold of NTCP molecules at the cell surface is required to promote viral infection. As currently cells that stably overexpress NTCP e.g. HepG2-NTCP K7 cells are used for HBV studies I was interested to examine if the quantity of NTCP is a regulating factor for efficient HBV uptake.

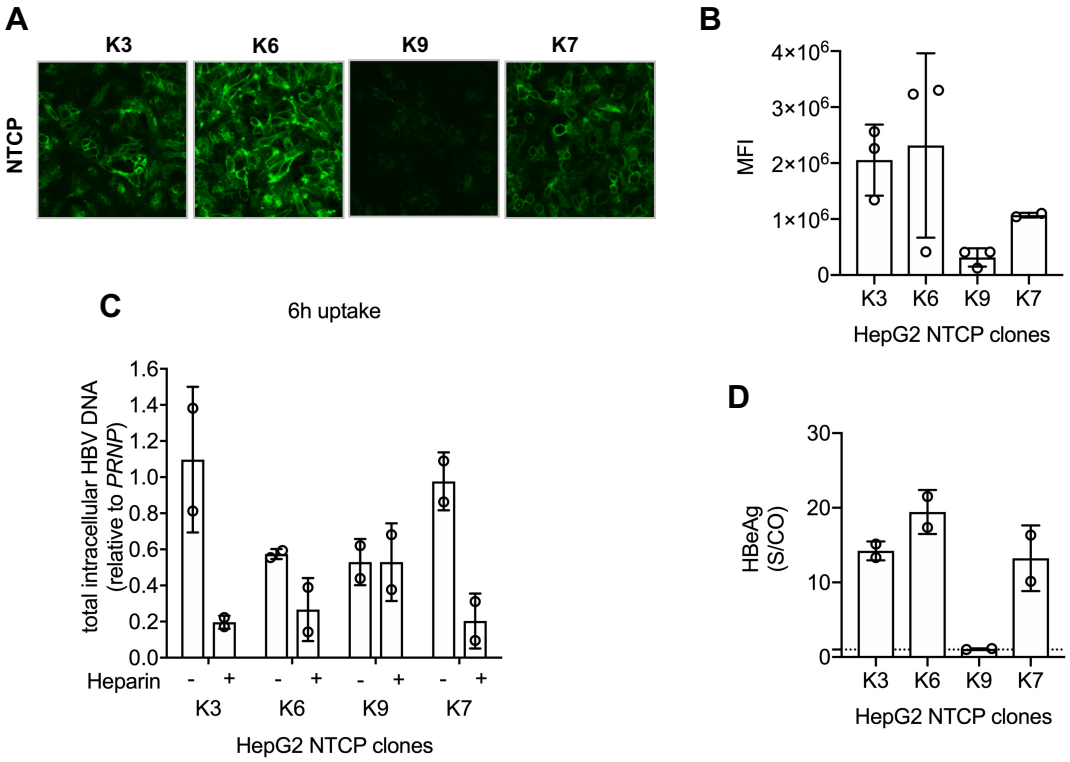

Figure 25: Characterisation of different HepG2-NTCP clones. (A-B) HepG2-NTCP cell clones (K3, K6, K9 and K7) were stained for NTCP at the cell surface with labelled Myrcludex B and analysed via confocal microscopy and FACS analysis. **(C)** Synchronised HBV uptake was analysed measuring total intracellular HBV DNA at 6 hours post 37 °C shift. Heparin was included as a negative control. **(D)** All HepG2- NTCP clones were subjected to HBV infection and measured for HBeAg at day 5 p.i.. These data represent one independent experiment. In total three independent experiments with up to three biological replicates were performed.

Next, I investigated whether cell surface NTCP expression levels define the efficiency of HBV uptake. This was a joint project with Andreas Oswald (PhD student, Institute of Virology, TUM). We employed transient mRNA transfection to express NTCP at the cell surface in HepG2 cells. NTCP mRNA was transfected into HepG2 cells ranging from 1000 - 3.9 ng. Untreated parental HepG2 and HepG2-NTCP K7 served as negative and positive controls, respectively. Previous time course experiments showed that NTCP protein expression was at maximum 24 hours post mRNA transfection (data not shown). Hence, we transfected mRNA 24 hour prior to characterising the cells for NTCP expression and bile acid uptake. Different NTCP mRNA concentration ranging from 1000-3.9 ng transfection did not impair cell viability (Fig. 26A). NTCP expressed from transfected mRNA migrated at the correct molecular weight and glycosylation pattern compared to HepG2-NTCP K7 cells (Fig. 26B), showing multiple bands ranging from 35-60 kDa reflecting different N-glycosylation patterns. Samples were treated with PNGaseF that cleaves N-glycans, resulting in a shift to 35 kDa in all samples confirming comparable glycosylation patterns. Next, NTCP expression at the cell surface was analysed applying labelled Myrcludex B in FACS analysis (Fig. 26C). A decrease from 1000 - 3.9 ng in the Mean Fluorescent Intensity (MFI) was observed confirming dose dependent NTCP expression at the cell surface. Next, we investigated the functionality of NTCP by measuring bile acid uptake capacity in collaboration with Dr. Yi Ni from Prof. Stephan Urbans group (Fig. 26D). As a negative control Myrcludex B was included that interferes with bile acid internalisation through NTCP binding. A dose dependent bile acid uptake was observed. However, only 1000 – 15.6 ng with NTCP mRNA transfected samples could be significantly blocked by Myrcludex B indicating the range of protein functionality.

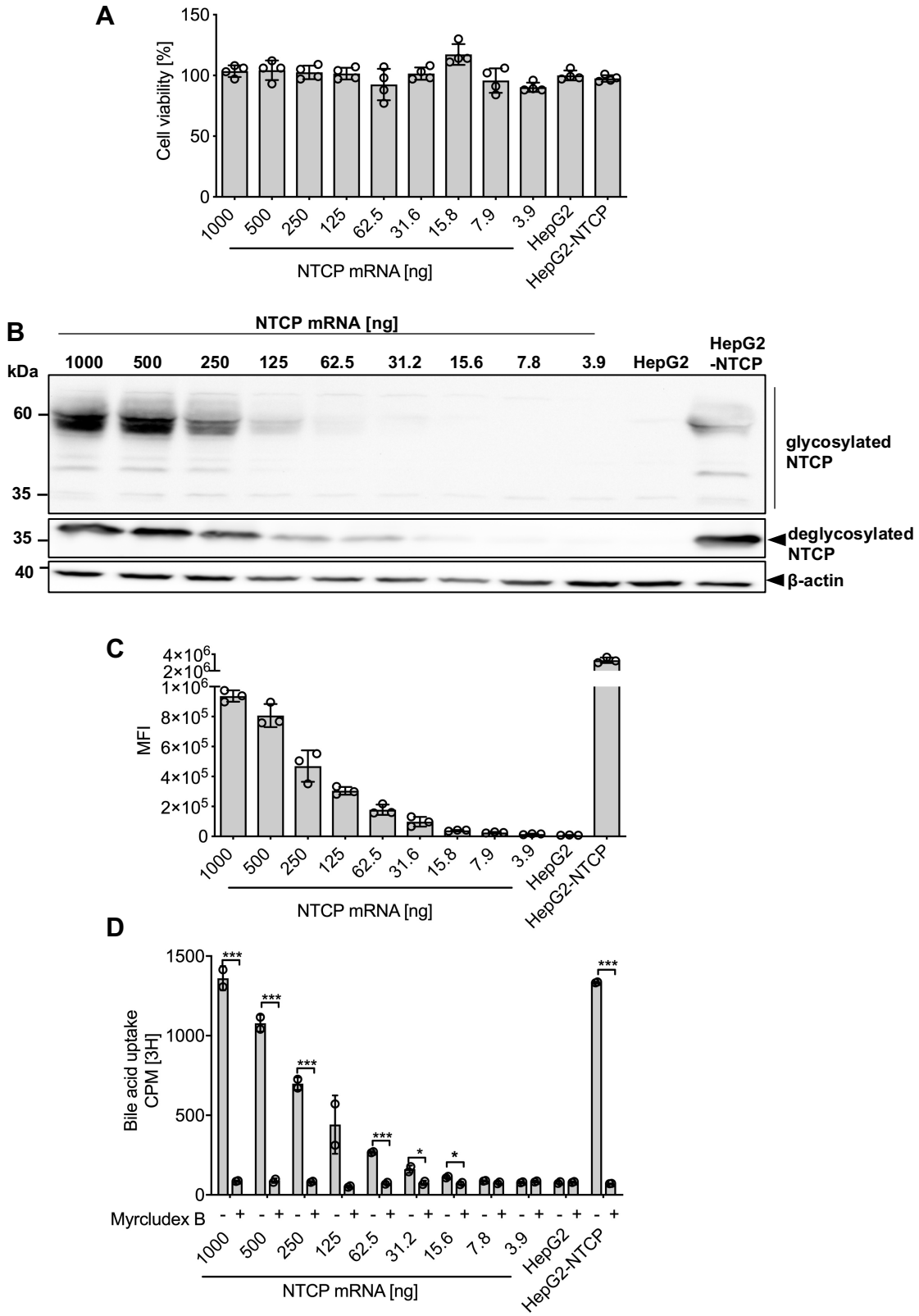

Figure 26: mRNA transfection to express NTCP in HepG2 cells. NTCP mRNA was transiently transfected into HepG2 cells 24 hours prior to performing experiments. A dose dependent titration (1000 – 3.9 ng) of NTCP mRNA was performed and analysed for **(A)** cell viability, **(B)** NTCP protein expression by Western blot and **(C)** NTCP expression on the cell surface employing labelled Myrcludex B via FACS analysis and **(D)** bile acid uptake. Data represent one independent experiment. In total up to three independent experiments biological triplicates were performed. Statistical analysis: Student's unpaired *t*-test (*p<0.05, **p<0.01, ***p<0.001).

After confirming that the transfected NTCP mRNA displayed proper protein expression and functionality, HBV parameters were assessed. Synchronised HBV uptake was performed and at 6 hours post 37 °C shift we measured total internalised HBV DNA after dose dependent transfection of NTCP mRNA. Myrcludex B was included as negative control for each sample. In line with the bile acid uptake data, samples ranging from 1000 – 15.6 ng were permissive for HBV internalisation that was significantly reduced by Myrcludex B (Fig. 27A). Further, HBV infection was assessed by quantifying cccDNA and HBeAg (Fig. 27B-C). A concentration dependent decrease in both parameters was observed. Interestingly, the sample transfected with the lowest concentration of 3.9 ng NTCP mRNA displayed very low levels in cccDNA and HBeAg that could be significantly inhibited by Myrcludex B.

In summary, these results demonstrate that NTCP expression levels define HBV entry and infection. Transient NTCP mRNA expression can be used as an alternative to overexpression systems reducing clonal effects in experiments.

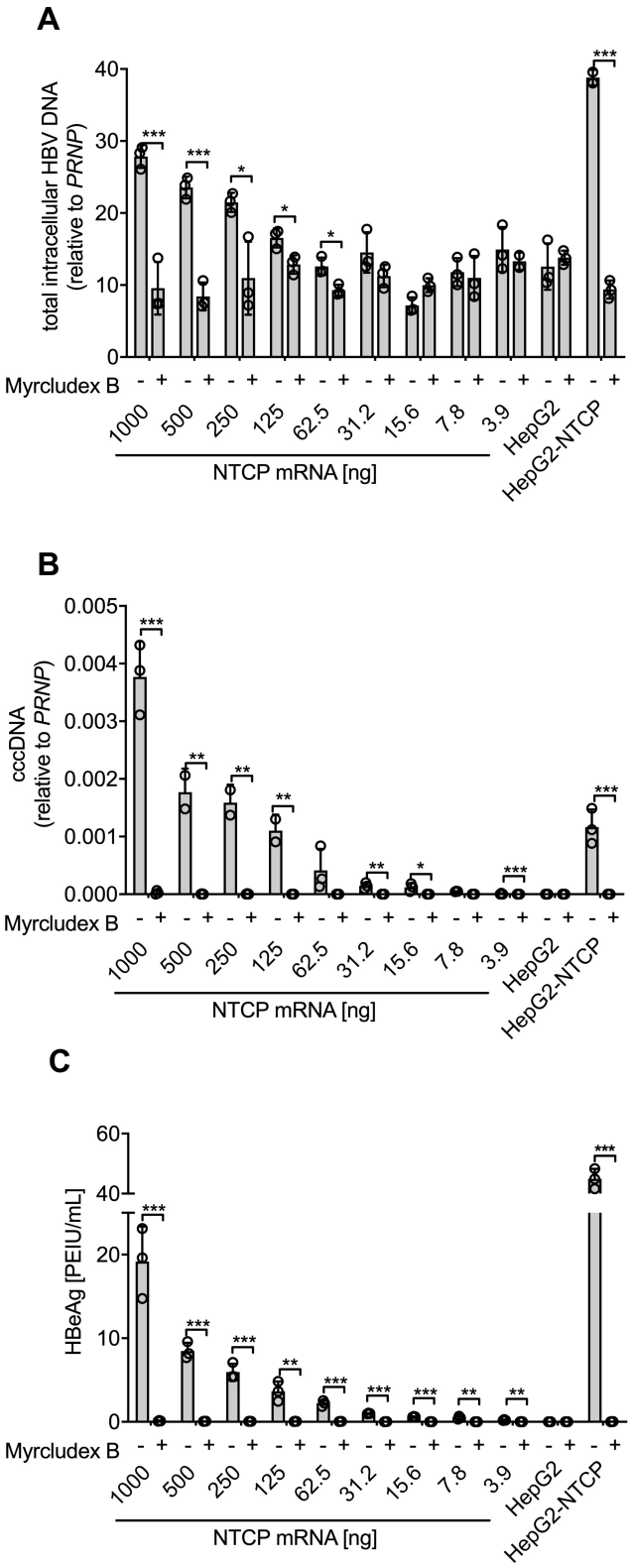

Figure 27: NTCP expression levels define HBV entry and infection in HepG2 cells. NTCP mRNA was transiently transfected into HepG2 cells in a dose dependent manner (1000 – 3.9 ng). After inoculation with HBV with a MOI of 200 cells were subjected to **(A)** HBV synchronised entry analysing total intracellular HBV DNA at 6 hours and **(B-C)** infection measuring cccDNA and HBeAg at day 5 p.i.. In all experiments Myrcludex B was added as negative control. Data represent one independent experiment. In total three independent experiments with biological triplicates were performed. Statistical analysis: Student's unpaired *t*-test (*p<0.05, **p<0.01, ***p<0.001).

2.5.1.3 Potential intracellular role for NTCP in HBV entry

While NTCP was identified as an essential HBV receptor its distinct role in HBV entry still remains elusive. Observations throughout this study indicated a potential intracellular role for NTCP in HBV entry. Kinetics studies performed in HepG2 cells lacking NTCP displayed modest uptake capacity (Fig. 11A). Analysis of synchronised HBV uptake at 6 hours post 37 °C shift in the presence of Myrcludex B displayed up to 80 % inhibition whereas heparin was able to block HBV entry up to 95 % in HepG2-NTCP K7 cells (Fig. 28A). The low uptake levels we observed when Myrcludex B was present never resulted in a productive cccDNA formation. This finding was confirmed by Western blot analysis targeting incoming HBV core protein and confocal microscopy staining for incoming envelope protein where low levels of entry were observed (Fig. 28B-C). This incomplete block of Myrcludex B in HBV entry indicated a potential intracellular role for NTCP.

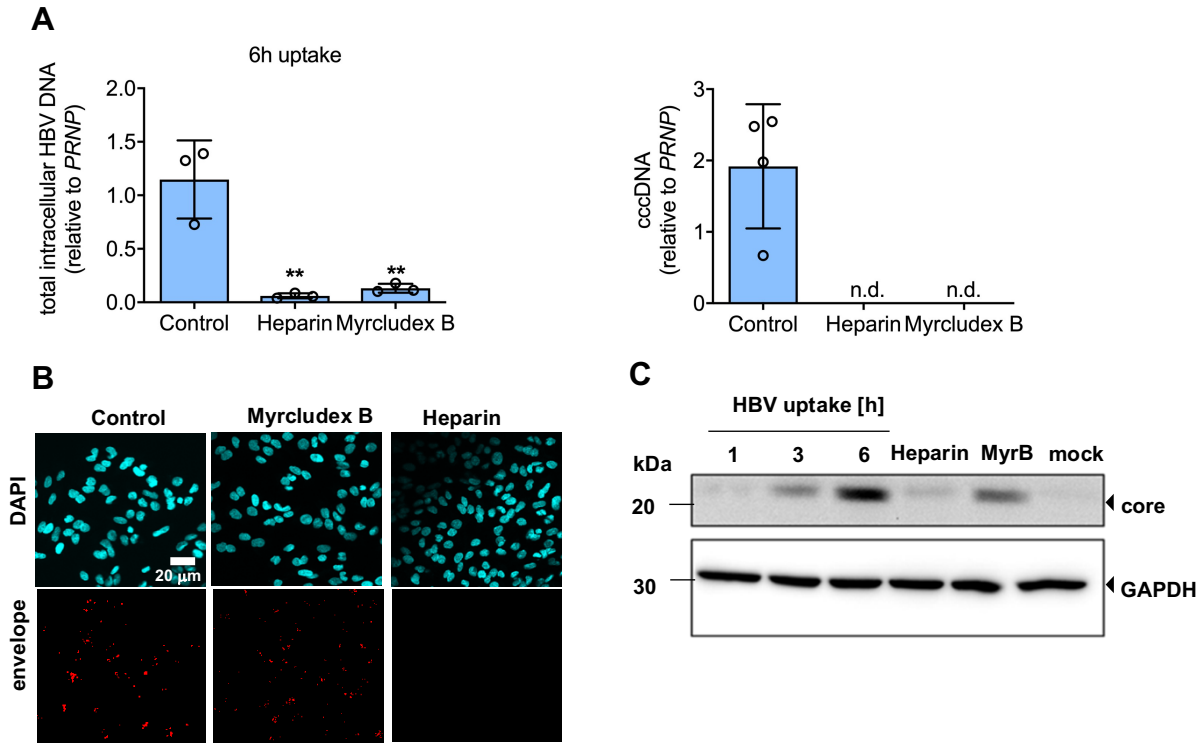

Figure 28: Potential intracellular role for NTCP in HBV entry. Synchronised HBV uptake was analysed where cells were harvested at 6 hours post 37 °C shift in the presence of Heparin (50 IU/ml) and Myrcludex B (200nM). **(A)** Total intracellular HBV DNA at 6 hours and subsequent cccDNA formation was measured at day 3 p.i.. **(B)** In addition, confocal microscopy was performed staining for incoming HBV envelope protein at 6 hours post 37 °C shift. **(C)** Western blot analysis was performed on incoming HBV core protein at 1, 3 and 6 hours post 37 °C shift. Heparin, Myrcludex B and untreated mock were included as controls. Data represent one independent experiment. In total three independent experiments with up to four biological replicates were performed. Statistical analysis: Student's unpaired t-test (*p<0.05, **p<0.01, ***p<0.001); n.d.: not detectable.

To further narrow down the time frame as to when NTCP is required for productive HBV infection synchronised HBV uptake was monitored. HepG2-NTCP K7 cells were inoculated at 4 °C for 1 hour and subsequently shifted to 37 °C. At indicated time points cells were subjected to short trypsinisation removing bound but non-internalised virus and replaced with Myrcludex B containing media. Subsequently, HBV infection from internalised viral particle was monitored until 5 days post internalisation. Myrcludex B containing media added 1 hour post 37 °C shift significantly reduced HBeAg levels at day 5 p.i. up to 40 % compared to untreated control (Fig. 29A). However, addition of Myrcludex B 3 and 6 hours post 37 °C shift did not have an effect on HBeAg levels.
To confirm these findings with a more sensitive read-out I repeated this experiment applying the HBV reporter that encodes Gaussia Luciferase in the viral genome (Fig. 29B) (Untergasser and Protzer, 2004). Upon infection, cccDNA is established expressing Gaussia Luciferase that is secreted into the supernatant. The same experimental setup as described above was applied using the HBV reporter virus measuring luciferase activity at day 5 p.i. with the addition of the 0.5 hour post 37 °C shift time point. From 0.5 to 1 hour HBV internalisation was significantly reduced in the presence of Myrcludex B compared to untreated control. At 1 hour luciferase signals were 50 % reduced compared to the control. At 3 and 6 hours post 37 °C shift Myrcludex B was not able to reduce luciferase activity hence did not interfere with viral entry confirming previous results.

Altogether, these results displayed that Myrcludex B was able to interfere with HBV entry in the first hour of particle internalisation hindering subsequent HBV infection. This might indicate the time frame when NTCP is required for HBV entry and needs further characterisation.

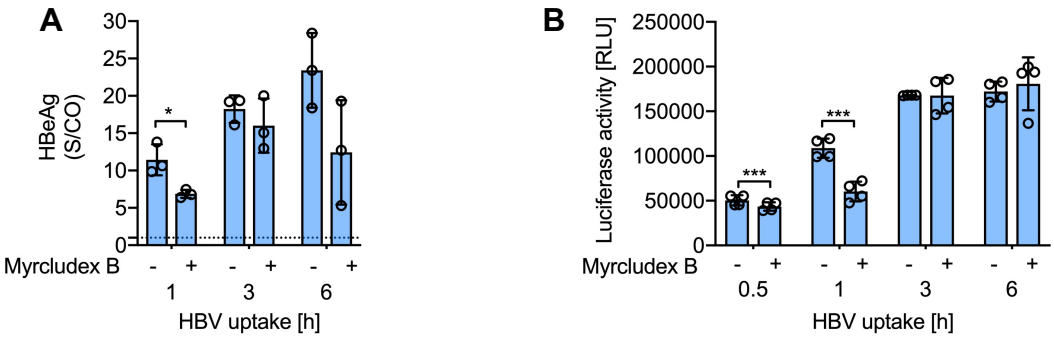

Figure 29: Myrcludex B add-in assay. Synchronised HBV assay was performed with a MOI of 200 in HepG2-NTCP K7 cells and were trypsinised at indicated time points post internalisation. Subsequently media containing Myrcludex B was added and HBeAg for wildtype infection **(A)** and luciferase activity for reporter HBV virus **(B)** was measured at day 5 p.i.. Data represent one independent experiment. In total two independent experiments with up to four biological replicates were performed. Statistical analysis: Student's unpaired *t*-test (*p<0.05, **p<0.01, ***p<0.001).

2.5.2 The role for EGFR in HBV entry

Recently, an interplay between EGFR and NTCP in HBV entry has been reported (Iwamoto et al., 2019). I wanted to verify these findings in our cell culture model. First, EGFR mRNA expression was assessed in HepG2 and Huh7 cells and those engineered to express NTCP as well as HepaRG cells (Fig. 30A-B). In parental HepG2 cells EGFR levels were low whereas in HepG2-NTCP K7, EGFR mRNA expression was higher. However, Huh7 cells displayed higher EGFR levels compared to Huh7-NTCP arguing for a cell clone specific effect. HepaRG cells were positive for EGFR. These results were confirmed by EGFR protein expression analysis via Western blot (Fig 30B). These results show that different cell lines express different levels of EGFR.

In addition, the study of *Iwamoto et al.* showed EGFR priming with its ligand EGF increased HBV entry into hepatocytes (Iwamoto et al., 2019). To confirm this, HepG2-NTCP K7 cells were primed with EGF prior to analysing synchronised HBV internalisation measuring total intracellular HBV DNA at 6 hours post 37 °C shift (Fig. 30C). Heparin and Myrcludex B which both inhibit viral entry were included as negative controls. However, upon EGF priming no significant increase in HBV internalisation was observed in our experiments.

In summary, I was not able to confirm that EGFR priming leads to an increase of viral internalisation. Further studies showing EGFR signalling need to be performed that help analysing this data.

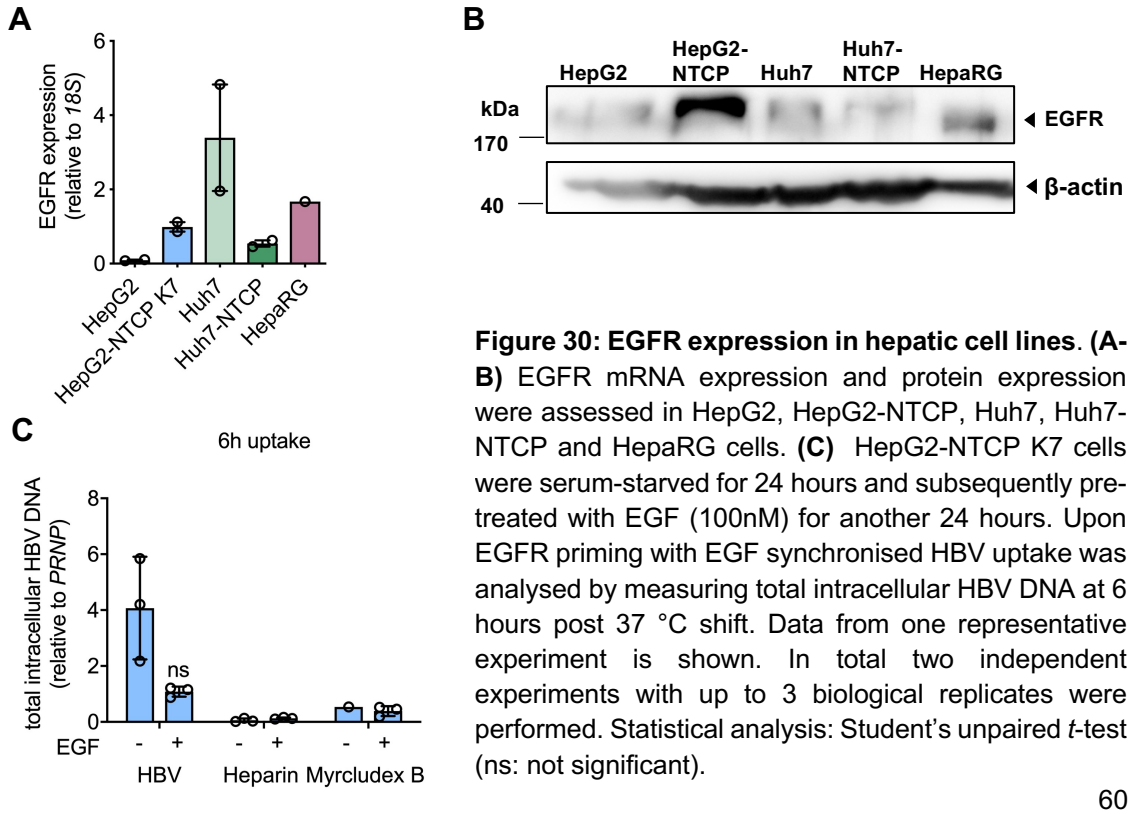

Figure 30: EGFR expression in hepatic cell lines. **(A-B)** EGFR mRNA expression and protein expression were assessed in HepG2, HepG2-NTCP, Huh7, Huh7-NTCP and HepaRG cells. **(C)** HepG2-NTCP K7 cells were serum-starved for 24 hours and subsequently pre-treated with EGF (100nM) for another 24 hours. Upon EGFR priming with EGF synchronised HBV uptake was analysed by measuring total intracellular HBV DNA at 6 hours post 37 °C shift. Data from one representative experiment is shown. In total two independent experiments with up to 3 biological replicates were performed. Statistical analysis: Student's unpaired *t*-test (ns: not significant).

2.6 HBV entry into non-hepatoma cell lines

Next, we raised the question whether NTCP, as the hepatic tropism factor for HBV, expressed in non-liver cells will support HBV uptake and infection. To address this hypothesis, the group of Stan van de Graaf engineered non-hepatoma cells to stably express NTCP. The following cell lines were chosen to work with:

HeLa	human epithelia cells from cervical cancer
HEK293T	human bone osteosarcoma epithelial cells
A549	human adenocarcinomic alveolar basal epithelial cells
U2OS	human bone osteosarcoma epithelial cells

Table 2: Non-hepatoma cells engineered to express NTCP

When checked for cell surface expression of NTCP with labelled Myrcludex B in these engineered cells, I observed differences in expression levels (data not shown). All cell lines except U2OS-NTCP cells displayed low to no NTCP mRNA or protein expression. As NTCP is liver specific, different expression levels may be explained by the non-susceptibility of overexpressed NTCP accompanied by rapid protein degradation.
To overcome this issue, together with Andreas Oswald we engineered non-hepatoma cells to transiently express NTCP applying mRNA transfection. NTCP mRNA (500ng) was transfected 24 hours prior to performing experiments. In all experiments HepG2-NTCP K7 and HepG2 cells transfected with NTCP mRNA were included as positive controls. Parental HepG2 cells served as negative controls. mRNA transfection in all cell lines did not impair cell viability (Fig. 31A). Next, the NTCP expression was determined by Western blot (Fig. 31B). All untreated parental cells were negative for NTCP expression, however, all cells transfected with NTCP mRNA expressed protein at comparable levels to HepG2-NTCP K7. Upon PNGaseF treatment all samples shifted to the same size indicating correct glycosylation patterns. Subsequently, we checked for NTCP expression at the cell surface using labelled Myrcludex B (Fig. 31C). Fluorescence microscopy showed comparable NTCP expression at the plasma membrane in all non-liver cells. This was further quantified with FACS analysis that showed comparable MFI values with a 100 % coverage of NTCP positive cells confirming similar NTCP expression among all cells (Fig. 31D). The physiological function of NTCP was assessed in the non-hepatoma cells. Bile acid uptake was measured in all parental cells and respective cells harbouring NTCP. In addition, Myrcludex B was added as a negative control that binds and interferes with NTCP disrupting bile acid transport (Fig. 31E). All non-liver parental cells were negative for bile acid uptake.

NTCP transfected cells displayed bile acid uptake at comparable levels that was inhibited by Myrcludex B.

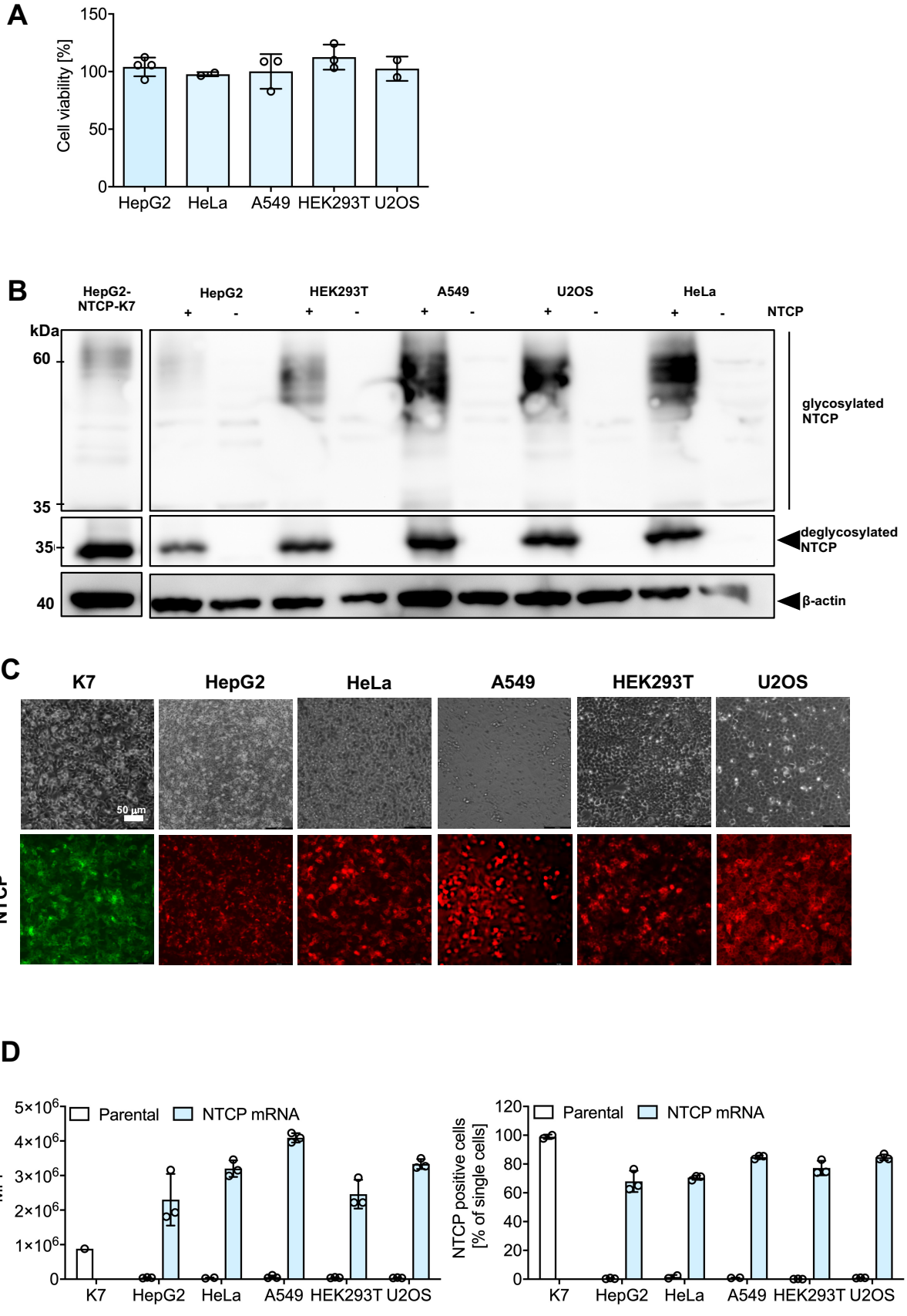

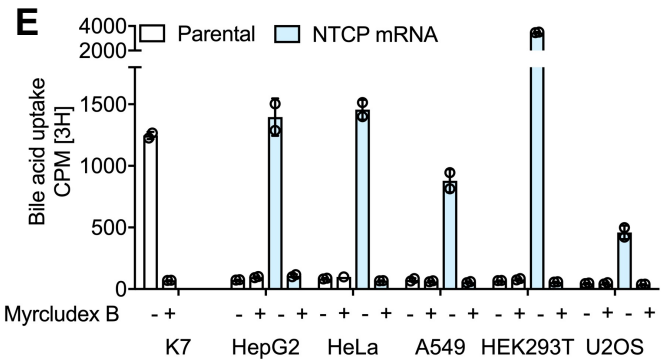

Figure 31: NTCP expression in non-hepatoma cell lines. 500 ng mRNA transfection of NTCP into HepG2, HeLa, A549, HEK293T, U2OS and SAOS2 cells. 24 hours post NTCP mRNA transfection the following parameters were analysed: **(A)** cell viability, **(B)** NTCP protein expression via Western blot, **(C-D)** NTCP expression at the cell surface determined by labelled Myrcludex B via microscopy and FACS analysis and **(E)** bile acid uptake capacity. Data represent one independent experiment. In total two independent experiments with up to three biological replicates were performed.

Having confirmed NTCP expression and functionality, we analysed HBV entry and infection. Synchronised HBV uptake at 6 hours measuring intracellular HBV DNA was analysed in both parental cells and those harbouring NTCP (Fig. 32A). Heparin and Myrcludex B were included as negative controls. All tested non-hepatoma cells showed modest HBV entry capacity in the presence of NTCP that was inhibited by heparin and Myrcludex B. Interestingly, parental A549 and U2OS cells were able to promote HBV internalisation suggesting non-specific uptake.

Upon HBV infection all non-hepatoma cells were negative for HBeAg levels (Fig. 32B). In order to verify that factors required for HBV genome transcription were present we transduced all cells with an adenovirus that harboured the HBV1.3L$^-$ genome (Ad-HBV1.3L$^-$) (Fig. 32C). All non-liver cells were able to transcribe the HBV genome as reflected in positive HBeAg levels.

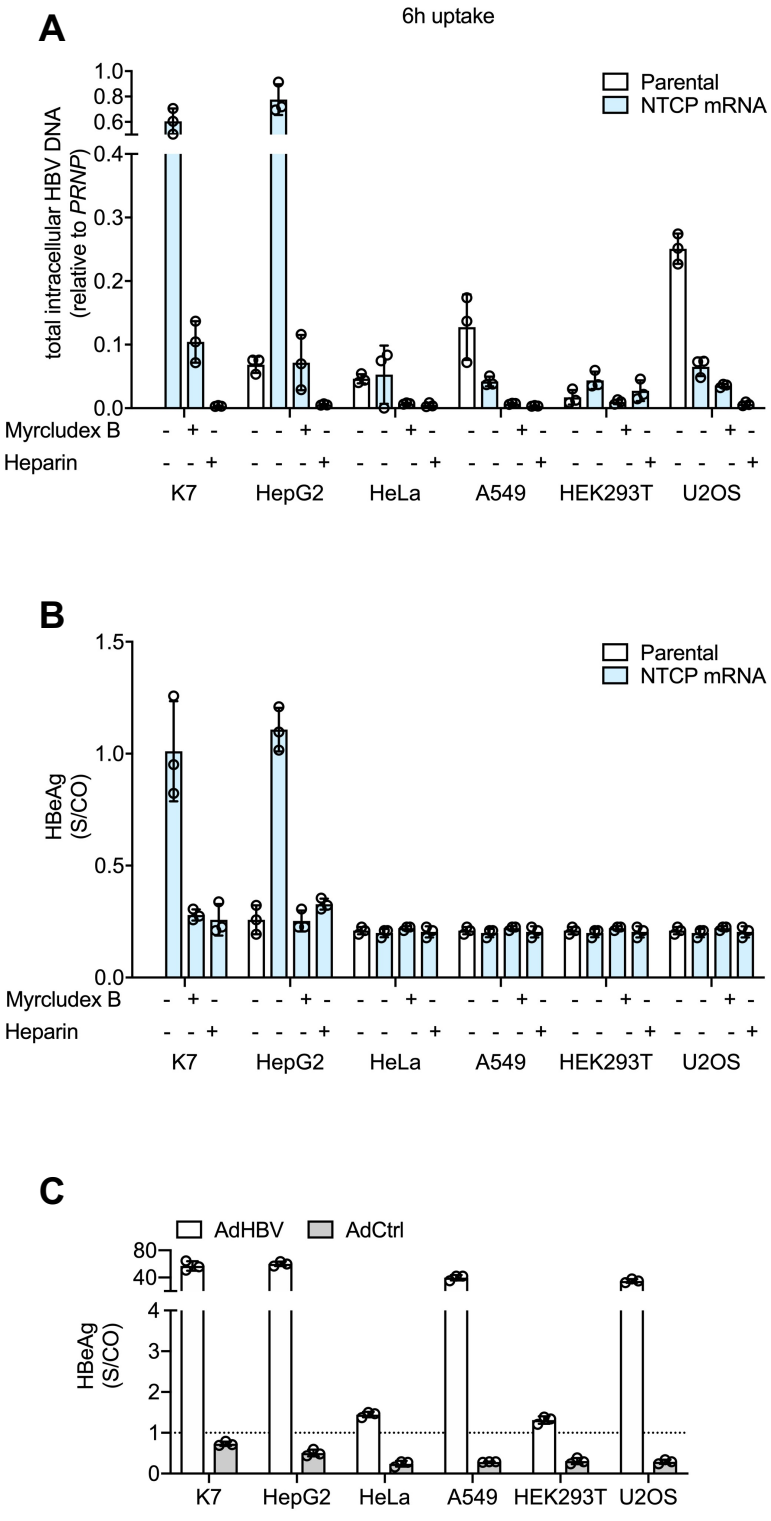

Figure 32: Effect of HBV entry and infection on non-hepatoma cells harbouring NTCP. **(A)** Synchronised HBV uptake was analysed for total intracellular HBV DNA at 6 hours post 37 °C shift. Respective parental cells, heparin and Myrcludex B were included as negative controls. **(B)** In addition, HBV infection was monitored at day 5 p.i. measuring HBeAg. **(C)** Non-hepatoma cells were transduced with either Ad-HBV1.3L- or AdCtrl and analysed for HBeAg at day 5 p.i.. Data represent one independent experiment. In total two independent experiments with biological triplicates were performed.

As earlier mentioned the only non-hepatoma cell generated by Stan van de Graaf's group stably expressing NTCP was U2OS cells. Interestingly, these U2OS-NTCP cells showed high HBV uptake capacity comparable to hepatoma cell line HepG2-NTCP K7 whereas the parental cell line was negative (Fig. 33A). Both, U2OS and U2OS-NTCP were negative for HBeAg (Fig. 33B). Since U2OS-NTCP were negative for HBeAg expression it was unclear which step of the HBV life cycle was restrictive. Thus, U2OS-NTCP cells were transduced with an adenovirus Ad-HBV1.3L$^-$. The genome was delivered directly into the nucleus and served as a template for HBV transcripts where HBeAg served as a stable read out. Transduced U2OS-NTCP cells were able to produce HBeAg supporting HBV transcription and translation (Fig. 33C).
When NTCP was transiently introduced into U2OS it did not have an effect on HBV entry, however, when stably expressed high HBV uptake capacity was observed. The long exposure of NTCP in U2OS stably expressing NTCP may have altered cellular properties promoting HBV uptake suggesting a clonal effect.

Taken together, the transient expression of NTCP in non-hepatoma cells displayed sufficient NTCP protein expression and confirmed physiological bile acid activity. However, HBV uptake and infection were limited suggesting additional liver specific factors besides NTCP are required for productive HBV infection.
Additionally, the stable cell line U2OS-NTCP supported HBV uptake but not infection may be used to study additional host and restriction factors required for HBV infection.

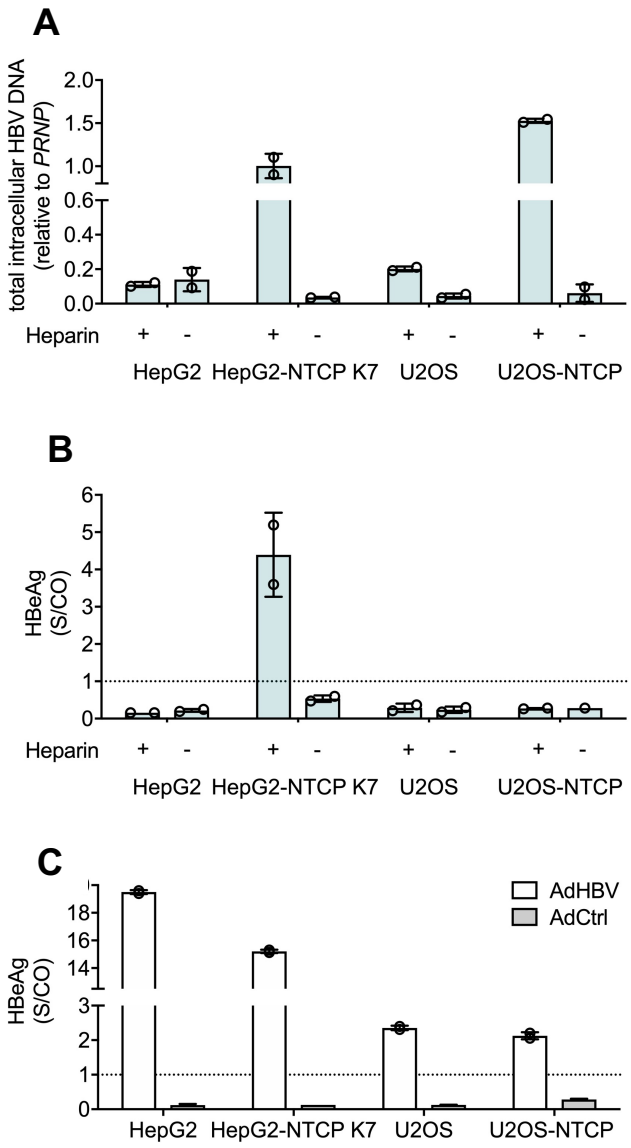

Figure 33: Effect of HBV entry and infection into U2OS-NTCP cells. **(A)** Synchronised HBV uptake assay was performed and cells were analysed for total intracellular HBV DNA at 6 hours post 37 °C shift. Respective parental cells and heparin was included as negative controls. **(B)** In addition, HBV infection was monitored at day 5 p.i. measuring HBeAg. **(C)** U2OS/NTCP cells were transduced with either AdHBV1.3L- or AdCtrl and analysed for HBeAg at day 5 p.i.. Data represent one independent experiment. In total two independent experiments with biological duplicates were performed.

3 Discussion

Molecular characterisation of viral-host interactions in the early steps of the HBV life cycle are key in understanding host specificity and viral tropism. I will discuss my results on HBV entry kinetics in the light of published data and how this informs our understanding of HBV infection.

3.1 HBV entry kinetics highlight slow and inefficient steps in the early life cycle

To investigate HBV entry, I established an assay that monitors particle internalisation in a synchronised fashion. HBV attachment to the cell surface at 4 °C displayed a MOI dependency and was NTCP independent, suggesting a role for HSPGs in the initial attachment stage. This indicated that HSPG binding is sufficient for viral attachment. It has been reported that the S and preS1 region of the HBV surface proteins are crucial for HSPG binding and are essential for HBV infection (Schulze et al., 2007, Sureau and Salisse, 2013). Since HSPG are ubiquitously present on various cell types a novel mechanism for HBV to avoid non-hepatic attachment was reported (Seitz et al., 2016). *Seitz et al.* showed two distinct HBV particle forms that mature from HSPG-non-binding to HSPG-binding particles. In this maturation process the viral particle undergo conformational changes in the preS region rendering the virus infectious and enable HSPG interaction on hepatocytes. This study demonstrates the importance of initial HBV binding to HSPG to hepatocytes. Furthermore, studies performed with recombinant HBV particle confirmed HSPG dependency for HBV attachment suggesting an intracellular role for NTCP (Somiya et al., 2016). In general, HSPG dependency has been reported for various viruses such as herpes simplex virus (HSV), human papilloma virus (HPV) and dengue virus (DENV) (Cagno et al., 2019). Viruses exploit the weak interaction with HSPG to increase viral concentration at the cell surface increasing the chance to interact with a subsequent more specific entry receptor (Birkmann et al., 2001, Rusnati and Urbinati, 2009, Shukla et al., 1999).

Analysing particle uptake kinetics I observed a time dependency in HBV entry into hepatocytes. HBV uptake into HepG2-NTCP K7 cells showed that viral particles internalized as early as 1 hour after transferring the cells to 37 °C and these particles were able to establish a productive infection. Further investigations in HepG2-NTCP K7 cells showed an increasing amount of intracellular HBV DNA until 12 hours, however intracellular viral proteins were already declining after 8 hours (Fig. 12). Total

quantification of HBV entry from 8 independent experiments showed that particle internalisation from attached virus was efficient (Table 1). However, a low conversion of internalised rcDNA to cccDNA was observed. This indicates restrictive processes in the cytoplasm might be a cause for low cccDNA formation. Of note, the applied HBV DNA and cccDNA specific qPCRs are of different efficiency, which needs to be considered for comparisons.

In vivo, HBV infection occurs through the basolateral membrane of hepatocytes and required cell polarisation (Schulze et al., 2012). A study in HepaRG cells showed that HBV infection is restricted to differentiated cells with a PHH-like polarisation displaying canalicular structures (Schulze et al., 2012). The formation of hepatocyte-like structures and the membrane polarity was shown to be important for the virus to access the entry receptor at the basolateral membrane. The cell polarisation status of the hepatoma cell lines used in our study still remains unclear. Cell polarisation is important for cellular trafficking pathway that might be key for productive HBV entry and infection.
Alternatively, low cccDNA levels may be explained through the loss of 'unrepaired' rcDNA in the nucleus via degradation processes. Subcellular fractionation of the infected cells enabled us to investigate the location of intracellular HBV DNA and showed genome delivery from cell surface to the nucleus within 3 - 6 hours (Fig. 14). However, cccDNA in the nucleus was only detected after 24 hour confirming studies from *Ko et al*.. Similar kinetics was observed in DHBV entry into PDH (Funk et al., 2004). Here, internalisation of DHBV required a maximum of 3 hours with a subsequent nuclear import of the genome that lasted for a period of 14 hours. Another study showed DHBV synchronised internalisation into PDH was more rapid (> 0.5 hours) with translocation of DHBV DNA into the nucleus by 4 hours (Qiao et al., 1999). In line with our observation, cccDNA formation was delayed and only detected at 48h.

Viral infection kinetics *in vivo* is thought to differ from the currently used *in vitro* models where a single duck hepatitis B virus particle was sufficient to establish infection in neonatal ducks (Jilbert et al., 1996). When adult ducks were infected cccDNA was detected after 6 hours in the liver (Qiao et al., 1999). In chimpanzees, approximately 10 viral genome copies are sufficient to induce acute HBV infection (Komiya et al., 2008). These studies show that productive infection *in vivo* is more effective compared to *in vitro.*

3.1.1 rc- to cccDNA conversion is a rate limiting step in vitro

Upon uncoating the genome containing capsid is delivered to the nucleus via the nuclear basket (Gallucci and Kann, 2017). Once the rcDNA is in the nucleus the partially double stranded genomes are repaired and converted into cccDNA in a multi-step process. In this study, I demonstrate that the rc- to cccDNA formation in our cell culture system is slow and ineffective.
The delay in rc- to cccDNA formation may be explained by 1) delays in genome trafficking from viral capsid across the nuclear membrane or 2) delays in DNA repair mechanisms for cccDNA formation.

The viral capsids are directed to the nuclear pore complex (NPC) in an importin α/ β mediated manner through the nuclear localisation sequence (NLS) present on the core protein to the nuclear basket Nup153 (Gallucci and Kann, 2017, Kann et al., 1999, Rabe et al., 2003). To assess whether genome uncoating from viral capsid was rate-limiting I investigated whether disrupting HBV capsid integrity with a CpAM had an effect on cccDNA formation. HAP_R01 (CpAM) treatment in HepG2-NTCP K7 cells during HBV entry delayed and reduced cccDNA formation in the nucleus. This finding highlights that capsid integrity is key for efficient cccDNA formation from incoming virus. These results are in line with recently published findings from *Ko et al.* where a dual role for HAP_R01 targeting incoming capsids with a subsequent impact on cccDNA formation and modulation in capsid assembly was described (Ko et al., 2019).

Studies with WHV showed genome delivery from nucleocapsid to the nucleoplasm was slow compared to soluble HBV DNA-polymerase complex that was transported rapidly (Kann et al., 1997). Furthermore, this study indicated that a large number of genome containing capsids remained in the cytoplasm with only a minor fraction translocating to the nucleus indicating a rate limiting step in WHV entry which may be similar to HBV.

The rcDNA is partially single stranded and harbours the HBV polymerase at the 5' end and a redundant sequence on both ends of the minus strand (Guo et al., 2007, Nassal, 2015, Seeger and Mason, 2000). The 3' end of the plus strand is a few nucleotides shorter and consists of a covalently attached RNA primer at the 5' end. The mechanism how rcDNA is concerted into cccDNA is not fully understood. However, five distinct steps have been described that are required for cccDNA formation (Gao and Hu, 2007, Hu et al., 2019b, Mitra et al., 2018): [1] the removal of the viral polymerase; [2] the removal

of the terminal redundancy; [3] completion of the plus strand; [4] elimination of the RNA primer and finally the ligation of both strands. It has been indicated that host DNA repair mechanism and other enzymes are involved in this process(Guo and Guo, 2015). It has been reported that tyrosyl DNA phosphpdiesterase 2 (Tdp2), that is known to remove topoisomerase II from DNA adducts, is involved in the cleavage of the viral polymerase from the rcDNA (Cui et al., 2015, Koniger et al., 2014). Recently, the cellular flap-like structure specific endonuclease (Fen1) was reported to play a role in the removal of one terminal redundant sequence as well as the cleavage of the RNA primer (Hu et al., 2019b, Kitamura et al., 2018). Furthermore, DNA ligase (Lig) I and III are involved in ligating either of the both strands (Long et al., 2017). Host polymerase κ has been reported to be involved in cccDNA formation (Qi et al., 2016).

The aforementioned factors need to be present upon HBV inoculation. It is well known that DMSO is required to enhance HBV infection, however, its entire mode of action is not well characterised (Ko et al., 2018). DMSO is required to polarize HepaRG and PHH cells and further promotes HBV replication in HepG2 cells (Schulze et al., 2012, Urban et al., 2014, Verrier et al., 2016). The interplay between the genome delivery into the nucleus and the application of DMSO might trigger these factors to be active promoting conversion and persistence of cccDNA. Furthermore, DMSO arrests the cell cycle in G0/G1 phase inhibiting cell division (Sainz and Chisari, 2006). Since cccDNA is not tethered to chromosomal DNA when a cell divides the cccDNA is not distributed equally among daughter cells (Allweiss and Dandri, 2017). Hence, an asynchronous cccDNA loss in proliferating cells was observed both *in vitro* and *in vivo* (Allweiss et al., 2018). This is an additional reason why DMSO is required for *in vitro* cell experiments to ensure productive infection.

Aforementioned, the cell cycle status of hepatocytes may have an impact on the establishment of HBV infection. For cell lines such as Huh7 infected with HBV and HepG2.2.15 expressing HBV it was reported that HBV stalled cell cycle progression before entering the S-phase (Friedrich et al., 2005). Furthermore, a HBV mediated cell cycle arrest in G1 was observed in HepG2.2.15, however, in Huh7 cells and primary marmoset hepatocytes stalling occurred in G2 phase (Chin et al., 2007, Wang et al., 2011). Despite different reports on the cell cycle status these observations show that HBV replication increased in G1 and G2 phase with a decrease in the S-phase (Lamontagne et al., 2016).

More recently *Xia et al.* reported the shift from uninfected PHH in G0/G1 phase to an enrichment in G2/M phase when infected with HBV. The study showed deregulation of cell cycle associated genes in HBV infected PHH that are important for viral infection (Xia et al., 2018).

DNA damage responses have been well described stating that upregulation of host factors involved in DNA repair are cell cycle dependent (Hustedt and Durocher 2016). The aforementioned host factors that contribute to rc- to cccDNA conversion most probably require a specific cell cycle state for optimal activity.
To study whether delays in the host repair mechanism occur during rc- to cccDNA conversion the use of pharmacological inhibitors that interfere with this step may provide a more detailed insight. Screening for such compounds showed that sulphonamides (DSS) interfered with rc- to cccDNA conversion, however the exact mode of action still remains unclear (Cai et al., 2012). Further screening platforms gave rise to hydrolysable tannins that have been proposed to interfere with cccDNA formation and its decay (Liu et al., 2016). Including these compounds in the experimental setup analysing HBV DNA and cccDNA in subcellular fractions may help distinguish whether genome uncoating or rc- to cccDNA conversion as rate-limiting steps.

Subcellular fractionation (Fig. 14) showed a major difference between internalised HBV DNA and cccDNA formation. It has been proposed that different PF-rcDNA species can lead to a productive or non-productive conversion to cccDNA (Hu et al., 2019b, Luo et al., 2017). The low numbers in cccDNA established from incoming virus can be a result of a rcDNA species that follow a dead-end pathway with subsequent degradation.

3.2 Imaging HBV entry into cells

An approach to investigate viral entry is imaging of labelled virus that give more insights to viral-host interactions. Multicolour labelling of virus and host structures might unravel spatio-temporal information of viral entry. In this study, I showed two distinct methods to image incoming viral particle. Targeting HBV envelope protein with a specific antibody allowed visualisation of particle entry in a time-dependent manner. However, the localisation of the surface protein does not necessarily give information of the entire viral particle. At some point in HBV entry the virus uncoats whereupon the viral capsid is released into the cytoplasm. Thus, the viral envelope is retained in an endosomal compartment. To overcome this caveat, I used the previously described EdC labelling of

the HBV genome (Winer et al., 2018). The ‘click reaction’ enables visualisation of the viral genome allowing monitoring via microscopy. Supplementing EdC to the HBV genome did not impair viral fitness and was comparable to wildtype. This method allows sensitive detection of HBV DNA in the cells. The combined application of the HBV envelope protein targeted by an antibody and genome labelling can give more insights as to when viral uncoating occurs. Furthermore, capsid trafficking in the cytoplasm as well as genome delivery into the nucleus can be monitored. One advantage this system offers is the application of this cell culture derived labelled virus in animal models. *Winer et al.* injected EdC-HBV into their newly generated model hNTCP/BAC transgenic mice harbouring human NTCP and showed HBV DNA positive murine hepatocytes.

To this date, many efforts in labelling HBV have been made. HB virions tagged with GFP at the S-protein at the N-terminus allowed particle binding to HepG2 cell (Lambert et al., 2004). Similar approach in tagging N-terminal M-protein with GFP has been reported (Zhang et al., 2016). However, the infectivity of GFP labelled HBV was not addressed. In another study capsid like particles containing GFP was reported. Due to steric hindrance these particles could not be enveloped, however, this approach might give insights into capsid trafficking post uncoating. A rather small tag, a tetracystein (TC) tag, was incorporated into HBV core protein that can be labelled with biarsenical dyes (Sun et al., 2014). These biarsenical labelled HBV particles were able to internalise, however, viral infectivity needs further investigation. Until now single viral components were used for labelling. One of the missing links in the early HBV life cycle is viral uncoating. For instance, for Influenza virus fusion events were determined inserting octadecyl rhodamine B chloride (R18) into the viral envelope at concentration where self-quenching occurs (de Lima et al., 1995, Nunes-Correia et al., 2002). Upon viral fusion with unlabelled target membranes a fluorescent signal can be measured. This application can be both used as a marker for fusion site and can be used to check for inhibitors that interfere with early events of the HBV life cycle.

3.3 Cellular pathways exploited for HBV to enter cells

Viruses are known to utilise cellular trafficking pathways to enter their host cells. After having characterised HBV kinetics, I investigated pathways that are involved in HBV entry.

3.3.1 HBV requires cholesterol at the plasma membrane

In all tested cells cholesterol depletion with MβCD at the plasma membrane significantly impaired HBV entry and infection. Liver and specifically hepatocytes play an important role in cholesterol homeostasis and uptake (Ikonen, 2018). Hepatotropic viruses may highjack cellular cholesterol pathways for viral entry. For HCV it has been well characterised that cholesterol and lipoprotein have an impact on viral entry. Both receptors involved in lipid metabolism, low density lipoprotein receptor (LDLR) and scavenger receptor class B I (SRBI), are required for HCV entry (Albecka et al., 2011, Grove et al., 2007, Kapadia et al., 2007, Molina et al., 2007). In this context, I tested Huh7 cells harbouring either LDLR, SRBI or double knockouts for HBV entry and did not observe any impairment (data not shown). This infers that HBV does not require LDLR or SRBI for productive infection.

It has been reported that Apolipoprotein H and E are associated with HBV particles and are required for productive infection (Mehdi et al., 1994, Qiao and Luo, 2019). Moreover, one study showed that hydrolysis of neutral lipids had an impact on HBV infection (Esser et al., 2018). The lipid lipase inhibitor, orlistat reduced HBV infection in a dose dependent manner, suggesting that HBV uptake is associated to the hepatotropic lipoprotein metabolism. Additionally, Ezetimibe, a small molecule that interferes with cholesterol transport and binds NTCP was reported to reduce HBV entry and infection (Dong et al., 2013, Lucifora et al., 2013). Bile acids are synthesised from cholesterol and are primarily transported by NTCP (Chiang, 2009). Thus, it has been reported that HBV required cholesterol transport pathways prior to hepatocytes infection via transcytosis through liver macrophages (personal communication with K. Esser and X. Cheng).

These studies provide evidence that cholesterol metabolism and homeostasis are important for HBV infection and progression.

3.3.2 Cellular dynamin and clathrin are required for productive HBV entry

Employing pharmacological inhibitors helped to dissect cellular pathways that are required for HBV entry and infection. In all tested cell culture systems HBV entry and infection was dependent on dynamin and clathrin-mediated endocytosis. Reconstitution of caveolin-1 into HepG2-NTCP K7 cells did not enhance HBV internalisation efficiency. Hepatoma cells do not express caveolin-1 and may have further cellular restrictions in e.g. membrane composition that per se cannot promote effective caveolin-1 function when reconstituted (Parton and Richards, 2003, Parton and Simons, 2007). In literature both clathrin- and caveolin-mediated pathway have been described to be involved in HBV entry. *Macovei et al.* demonstrated that dominant-negative mutants of caveolin-1 inhibited HBV infection of HepaRG cells. In contrast, *Huang et al.* showed clathrin-dependent HBV uptake into HuS-E/2 immortalised PHHs (Huang et al., 2012). As hepatoma cell lines lack sufficient caveolin-1 expression it might be that both pathways can be exploited and can result in productive HBV infection.

After particle internalisation the genome containing capsid is released into the cytoplasm prior to translocating to the nucleus. However, the underlying mechanisms are unclear. Bafilomycin A1 inhibits the transition from early to late endosome by increasing the vesicular pH (Bayer et al., 1998). In this study, Bafilomycin A1 did not reduce HBV entry or infection. This suggested that HBV entry does not require low pH for internalisation and may indicate an endosomal escape in the early endosome. The enrichment of early HBV containing endosome through Bafilomycin A1 may enhance productive HBV infection.

The direct endosomal processes are still unclear, however, an involvement of the small GTPases Rab5 and 7 in HBV uptake was observed (Macovei et al., 2013). Rab5 promotes early endosome formation whereas Rab7 is involved in endosomal maturation from late endosome to lysosome (Hayes et al., 2016). Studies silencing either Rab5 or Rab7 in HepaRG cells impaired HBV infection suggesting that viral translocation into the late endosomes is required to establish infection (Macovei et al., 2013). Furthermore, the study localised HBV particles in the lysosomes which the authors concluded to be a dead-end pathway. This may explain why I see a drop from internalised HBV DNA to cccDNA formation as a consequence of HBV being in a non-productive compartment during particle internalisation. Further experiments to co-localise HBV with endosomal markers in our cell culture system would help support our conclusion. The finding that HBV DNA first appeared between 3 and 6 hours in the nucleus suggests that endosomal

trafficking occurs very early during HBV entry. My attempts to colocalise HBV particles with Rab5 and 7 protein via super-resolution microscopy failed (data not shown). This might be due to the fact that concentration of internalised virus in a single cell is very low. Overall, further characterisation as to how HBV escapes the endosomal compartments and uncoats in the cytoplasm needs to be performed. Further studies employing a dual staining for viral envelope and genome may help to further decipher viral uncoating in a spatio-temporal manner.

3.3.3 Role of cytoskeleton in HBV entry

The host cytoskeleton is of great importance in transporting the virus across the cell. Most commonly actin and microtubule are exploited by viruses for motility (Marsh and Helenius, 2006). In this study, I investigated the dependency of HBV entry on the cytoskeleton in a defined time frame. Actin and tubulin were important in the first 6 hours of HBV internalisation. The dynamics of actin play a crucial role for clathrin mediated endocytosis indicating that clathrin- mediated endocytosis already occurred in the first 6 hours of particle entry (Smythe and Ayscough, 2006). This time frame correlates with the data that HBV DNA was first detected between 3 and 6 hours post internalisation in the nucleus. Not much studies have been performed to dissect distinct role of the cytoskeleton in different stages of HBV entry. Incoming DHBV particles into PDH was shown to depend on microtubule based trafficking (Funk et al., 2004). Further, lipid-mediated introduction of HBV capsid into cells showed that microtubules are important for capsid trafficking towards the nucleus (Rabe et al., 2006).

3.4 NTCP

The following will discuss different aspects of NTCP characteristics that are involved in HBV infection.

3.4.1 Single N-glycosylation of NTCP is sufficient for HBV infection

Together with Stan van de Graaf's group we have shown the importance of N-glycosylation on NTCP in HBV infection (Appelman et al., 2017). NTCP harbours two N-glycosylation sites at residues N5 and N11 (Hagenbuch and Meier, 1994). We investigated the effect of mutating NTCP at residues N5, N11 or both on bile acid transport and HBV infection (Appelman et al., 2017). Single glycan variants were still

able to transport bile acids and locate at the plasma membrane. Furthermore, NTCP with a single glycan was sufficient to promote HBV infection. However, glycosylation deficient NTCP lacked bile acid transporter function and showed limited expression at the plasma membrane with rapid degradation in the lysosome. Here, HBV infection was impaired arguing that HBV requires sufficient NTCP expression at the plasma membrane and is unlikely to use the lysosomal degradation pathway for particle entry. A recent study by *Lee at al.* reported that N-glycosylation was not important for HBV infection (Lee et al., 2018). They observed that NTCP expressed on HepaRG cells was glycosylation deficient but still permissive for HBV infection. Further introduction of single and double glycan mutant did not impair NTCP expression and localisation in HepG2 cells in their study. However, this study did not analyse physiological bile acid transport in their mutant cells. Furthermore, they used NTCP constructs that included a bovine rhodopsin epitope at the C-terminus. However, they did not show whether the C-terminal tag had an impact on NTCP glycosylation. These inconsistent findings need to be further investigated since vector delivery as well as cellular background of investigated cells differed from our setting.

3.4.2 NTCP expression levels regulate HBV entry

Since the discovery that NTCP is required for productive HBV infection, cell culture models overexpressing NTCP have been used to study HBV replication. HepaRG cells, a non-transformed and more physiological system as it shares similar characteristics of primary human hepatocytes, express lower levels of NTCP upon differentiation and yet support efficient HBV infection (Marion et al., 2010). Most commonly used NTCP overexpressing cell lines may result in alterations in cellular properties, e.g. through higher bile acid accumulation in these cells. It has been shown that increased bile acid concentration in cells have an impact on antiviral activity of interferons (Podevin et al., 1999). In addition, *Zhao et al.* found that NTCP interfered with HBV transcription that was dependent on its bile acid transporter function (Zhao et al., 2018). Therefore, NTCP overexpression in cell lines may limit the investigation of HBV infection in a more physiological environment.

To investigate how NTCP levels regulate HBV infection we used transient mRNA transfection as a tool to express NTCP in HepG2 cells. We noted a clear dose-dependency of mRNA and NTCP protein expression. High amounts of NTCP mRNA (≤1000 ng) resulted in NTCP levels comparable to the cell line stably expressing NTCP (HepG2-NTCP K7) in physiological bile acid transport, NTCP expression and localisation

as well as HBV entry and infection. However, transfection of low mRNA concentrations (≤15.6 ng) were still able to display physiological function and interestingly also promoted HBV entry and infection at very low levels. These results indicated that a certain threshold of NTCP molecules at the plasma membrane was sufficient to promote productive HBV entry and infection.

In this context, it would be interesting to quantify absolute numbers of NTCP molecules present on cell surface that are required for HBV entry. One possibility to address this would be the application of fluorescence correlation spectroscopy (FCS). In a homogenous solution this approach combines spectroscopy/microscopy systems with labelled proteins and can give information of particle or protein concentration at the cell surface (Altan-Bonnet and Altan-Bonnet, 2009, Li et al., 2016). In this context, either NTCP harbouring a fluorescent protein or labelled Myrcludex B that directly binds to NTCP could be applied. These quantifications could help to determine physiological numbers of NTCP and help the development of more physiological cell culture system to study HBV permissivity.

3.4.3 Potential intracellular role for NTCP in HBV entry

Having shown that HBV binding to the cell surface is HSPG mediated but NTCP independent I further characterised the role of NTCP in HBV entry. Observations of modest uptake capacity when NTCP was not present or when NTCP was blocked with Myrcludex B suggested possible alternative routes for HBV internalisation. In the absence of functional NTCP the viral particle may be taken up and degraded in the lysosomal pathway indicating that NTCP may play a role in endosomal escape. Alternatively, the internalised particle may be transported back to the cell surface via recycling endosomes.

Myrcludex B add-in assay on HepG2-NTCP K7 cells showed that HBV entry was reduced within the first hour of internalisation. The rational for these experiments was to determine at which time point upon viral entry NTCP becomes dispensable for productive infection. The incomplete block may be explained by a concentration of Myrcludex B which was not sufficient to entirely compete with virus. However, these findings suggest that NTCP plays a role post binding in an intracellular compartment. Similar findings were reported by *Somyiya et al.* employing HBV mimicking particles, i.e. bio-nanocapsules coupled with myristoylated L-protein (Somiya et al., 2016). They

showed that uptake of these particles into hepatoma cells solely depends on HSPG not NTCP.

A deeper understanding of intracellular trafficking pathway of NTCP may help to elucidate cellular processes involved in HBV entry. It has been described that NTCP colocalises with Rab4 in the early endosome and with Rab11 in the recycling endosome (Sarkar et al., 2006). These endosomes required intact microtubules for trafficking which was regulated by the PI3 kinase/PKCζ pathway (Dranoff et al., 1999, McConkey et al., 2004, Sarkar et al., 2006). However, NTCP was not detected in late endosomes (Sarkar et al., 2006). These finding support my results that HBV escapes the early endosomes in the presence of NTCP.
Another study showed Ca^{2+} dependent PKC-α induced endocytosis of NTCP, thereby lowering bile acid uptake (Stross et al., 2010). In rats a dileucine motif at 221 and 222 in NTCP determined plasma membrane retention or endocytosis (Stross et al., 2013). A subsequent PKC activation lead to endocytosis of NTCP in a clathrin dependent manner with subsequent lysosomal degradation. The involvement of PKC mediated endocytic pathways can be further investigated in the context of HBV internalisation.

It is known that enveloped viruses require complex formation that promotes viral fusion and uncoating. It would be interesting whether intracellular multimerization of NTCP is required for HBV entry and viral uncoating. The presence of NTCP dimers in rat liver membranes and U2OS cells expressing exogenous NTCP has already been reported (Bijsmans et al., 2012). Through immunoprecipitation analysis it was shown that NTCP can form heteromeric complexes with other members of the SLC10A family. More recently, *Funkano et al.* showed NTCP oligomerisation in the presence of HBV preS1 that was disrupted by troglitazone (Fukano et al., 2018). Interestingly, troglitazone did not impair HBV attachment but preS1 internalisation suggesting that intracellular oligomerisation of NTCP may be required for HBV entry.

Altogether, this leads to the assumption that initial HBV-NTCP interaction occurs at the plasma membrane with a still unknown intracellular role for NTCP in HBV entry and may need undergo endocytosis to fulfil its role as a receptor.

3.5 EGFR did not play a role in HBV entry

Additional host factors other than NTCP are thought to be necessary for efficient HBV uptake into cells. The identification of such host factors is required for a better understanding of viral entry and dissemination as well as for the establishment of experimental systems to study infection.
A recent study reported an interaction of NTCP and EGFR that regulates HBV entry (Iwamoto et al., 2019). To confirm these findings, I screened hepatoma cells for EGFR expression at RNA and protein level. An overall diverse EGFR mRNA and protein expression was observed in all tested cells. HepG2-NTCP cells displayed higher EGFR expression compared to parental cells. Parental Huh7 cells displayed higher levels of EGFR compared to when NTCP was present. Differentiated HepaRG cells displayed lower level of EGFR expression compared to HepG2-NTCP K7 cells. A NTCP dependent expression of EGFR was not observed in all tested cell lines. The differences in EGFR expression can be explained as cell clonal or population specific effect.

An earlier study reported co-trafficking of NTCP and EGFR in endosomal compartments (Wang et al., 2016). The study also showed that EGFR and NTCP both are present in a steady state, between cell surface and endosomal compartments. These findings suggest a role for EGFR and NTCP in trafficking HBV into endosomes.
Iwamoto et al. showed an increase in preS1 internalisation upon EGFR activation with its ligand EGF. However, in our laboratory treating HepG2-NTCP K7 with EGF had negligible effects on HBV uptake. I did not confirm EGF signalling which limits the interpretation of my data. Compared to the study from *Iwamoto et al.* where only preS1 trafficking was assessed I used authentic HBV which also might explain different results. Further experiments such as introducing NTCP mutants or the application of pharmacological agents that abolish EGFR interaction are required.

For HCV it has been shown that EGFR is activated upon cluster of differentiation 81 (CD81) interactions with the virus (Diao et al., 2012). When EGFR endocytosis was inhibited by kinase inhibitors, HCV infection was disrupted. Further, antibodies targeting the EGFR ligand binding site impaired viral entry, demonstrating a role for EGFR in HCV entry. Similar to HCV EGFR-NTCP may play an intracellular role in HBV entry and viral uncoating into the cytoplasm.
Altogether, there are implications that an interplay of NTCP and EGFR is required to promote HBV particle internalisation and infection.

3.6 Approaches to identify host factors involved in HBV entry

While NTCP is a key factor that is required for HBV entry into hepatocytes we hypothesize that additional host factors may regulate HBV uptake, uncoating of the viral particle into the cytoplasm and rc- to cccDNA conversion.
In this study, human non-hepatoma cells engineered to express NTCP have been used to decipher possible restricting host factors that is required by HBV. We therefore investigated whether NTCP supported HBV uptake in a non-hepatic background and whether this is the sole factor required.
NTCP expression in non-hepatoma cells conferred bile acid uptake but displayed limited evidence for specific HBV uptake that could be blocked by Myrcludex B or heparin. Parental U2OS and A549 had a high background level of HBV uptake that did not lead to a productive infection suggesting unspecific internalisation events.
HBV genome introduction with an adenovirus circumventing the HBV specific entry pathway showed that all non-hepatoma cells were able to promote viral transcription.
These data support the model that additional liver specific factors in addition to NTCP are required for HBV uptake. A possible approach to identify such liver specific factors can be the delivery of a liver expression library (e.g. cDNA library) into a non-hepatoma cell expressing NTCP that did not support HBV entry e.g. HEK293T-NTCP cells. This would allow screening for liver specific factors that govern HBV uptake and infection.

Interestingly, U2OS cells stably expressing NTCP that were already used for mechanistic NTCP studies (Bijsmans et al., 2012, Donkers et al., 2019, Donkers et al., 2017) in my studies were able to internalise HBV comparable to HepG2-NTCP K7 cells. However, U2OS-NTCP cells failed to establish cccDNA. Adeno-transduction of HBV genomes into the nucleus promoted viral transcription. These findings did not confirm results obtained from transient NTCP expression in U2OS suggesting a clonal effect.
However, these results in U2OS cells stably expressing NTCP suggest a blockage in viral uncoating into the cytoplasm, nuclear import or rc- to cccDNA conversion. Subcellular localisation for HBV DNA in U2OS-NTCP cells may help narrow down whether restriction occurs in the cytoplasmic or nuclear fraction.
U2OS-NTCP cells may be used to additionally screen for missing host factor(s) that support HBV uptake.

It is known that U2OS cells in general harbour multiple chromosomal aberrations (Ozaki et al., 2003). This has been used to study other virus host interactions in U2OS cells.

For instance, U2OS lack the transcriptional regulator ataxia telangiectasia and Rad3-related protein (ATR) that promotes DNA repair in the cell (Dilley et al., 2016). For adenovirus and for human papillomavirus virus replication in U2OS and the involvement of functional ATR and its importance in the DNA repair machinery has been already described (Kivipold et al., 2015, Schreiner et al., 2013). HBV rc- to cccDNA conversion requires a functional host DNA repair pathway. The aberrant DNA repair pathway in U2OS might be an additional reason why cccDNA was not established.

Most recently, *Kostyusheva et al.* showed that ATR signalling is important for HBV replication (Kostyusheva et al., 2019). Re-introducing DNA repair response factors into U2OS-NTCP cells may help find missing factors that are responsible for rc- to cccDNA conversion.

In summary, engineered non-hepatoma cell lines can be used as a tool to identify additional factors that contribute to HBV entry and infection.

3.7 Conclusion

In this study, I have established a robust assay that will allow further characterisation of HBV entry using several approaches ranging from analysing HBV parameters, tracking viral particle via microscopy to screening for novel entry inhibitors.
My data indicate that initial HBV attachment to the cell surface is HSPG mediated but independent of NTCP (Fig. 34). However, NTCP is required for HBV particle internalisation that is dependent on dynamin and clathrin but independent of caveolin. Here, a single N-glycosylation of NTCP is sufficient to promote viral infection. Further, my data proposes an early endosomal escape of the viral particle which may be facilitated by a potential intracellular role of NTCP. HBV DNA from the cell surface reaches the nucleus within 3 hours, however, cccDNA was only detected between 24 – 72 hours.

Collectively, this study illustrates gaps in our knowledge to understand host factors that are involved HBV entry and dissemination. Detailed entry kinetic analysis identified early steps of the HBV life cycle including the rc- to cccDNA conversion to be rate and time limiting. Tools generated in this thesis such as the synchronised uptake assay and visualising labelled viral particle will further allow to dissect host pathways that are required in viral entry. Identifying limiting steps and host factors involved will allow the generation of more physiological cell culture and *in vivo* models. This will also help advancing our knowledge in the development of preventive and therapeutic antiviral strategies.

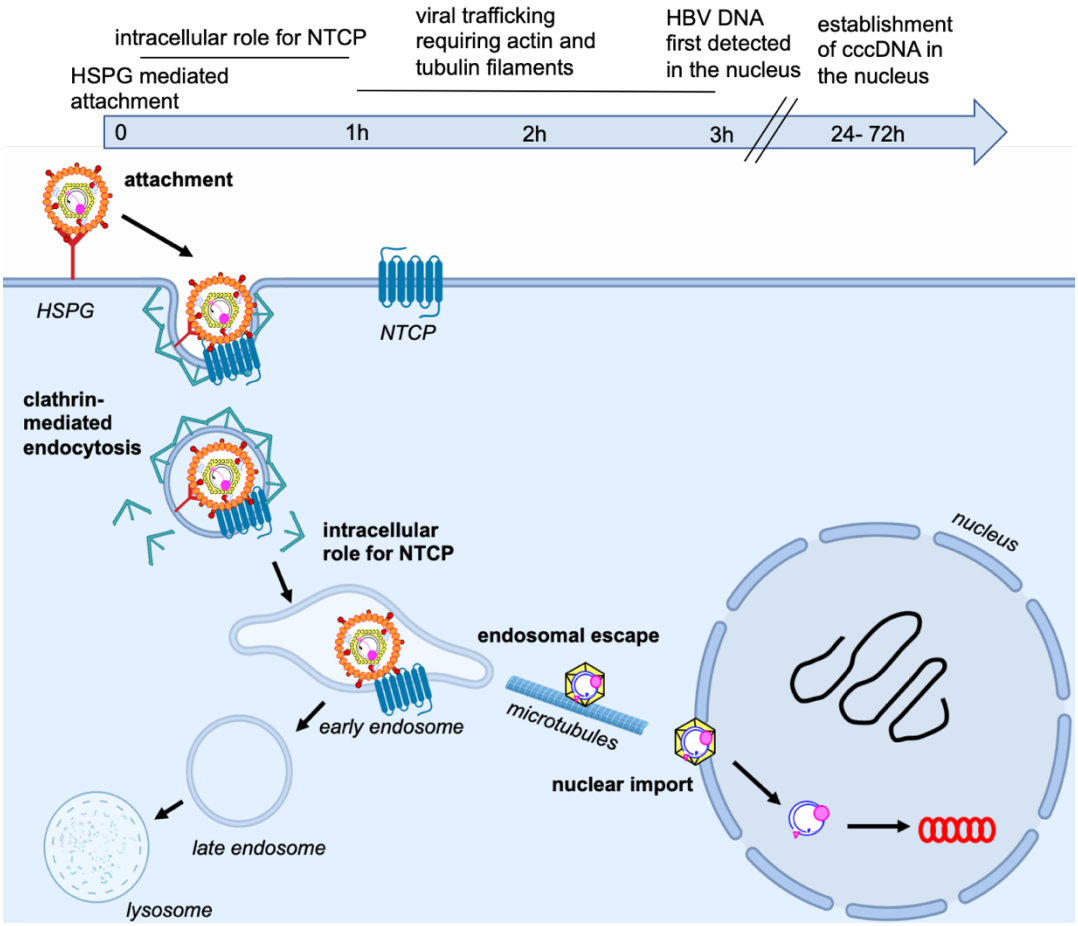

Figure 34: Proposed HBV entry pathway into HepG2-NTCP K7 cell. Details are given in the main text (Created with BioRender.com).

4 Material and methods

4.1 Material

4.1.1 Laboratory equipment and consumables

Product	Supplier
Amersham Hybond PVDF membrane	GE Healthcare Life Sciences
Amersham nylon membrane Hybond N+	GE Healthcare Life Sciences
BEP (HBeAg measurement)	Siemens Molecular Diagnostics
Cell culture flasks and plates	TPP
Cell culture incubator HERAcell 150i	Thermo Scientific
Centrifuge 5417C / 5417R	Eppendorf
Cryo vials	Greiner Bio One
ELISA 96well plates Nunc	Thermo Scientific
Falcon tubes 15ml, 50ml	Greiner Bio One
Fluorescence microscope Leica DM8	Leica
Gel chambers (agarose gel electrophoresis)	Peqlab
Gel chambers (SDS-PAGE)	Bio-Rad
Hyperflask	Corning
Light Cycler 480 II	Roche
Pipette “Accu-jet pro”	Brand
Pipette filter tips	Starlab
Pipette tips 2 - 50ml	Greiner Bio One
Pipettes	Eppendorf
PVDF membrane	Bio-Rad
qPCR 96-well plates	4titude
Reaction tubes	Eppendor
Sterile filters 0.45µm	Merck, Millipore
Sterile hood	Heraeus
Tecan plate reader Infinite F200	Tecan
Ultracentrifuge Beckman SW40 rotor	Beckman Coulter
Western Blotting Chamber (Wet Blot)	Bio-Rad
Whatman paper	Bio-Rad

4.1.2 Chemicals and reagents

Name	Supplier
5-Ethynyl-2'-deoxycytidine (5-EdC)	Jena Bioscience
Agarose	Peqlab
Amersham ECL Prime Western Blotting Detection Reagent	GE Healthcare Life Sciences
Ampicillin	Roth
APS	Roth
Blasticidin S HCl	Invitrogen
Cholera Toxin B (CTB) Alexa Flour 488	Thermo Fischer Scientific
Collagen R	Serva Electrophoresis
CsCl	Roth
DMEM-F12	Thermo Fischer Scientific
DMSO	Sigma-Aldrich
Dulbecco's Modified Eagle's Medium	Gibco/Invitrogen
EGF	Sigma-Aldrich
Ethanol	Roth
Ethidium bromide	Merck
FBS Fetalclone II, Hyclone	GE Healthcare Life Sciences
FCS (heat-inactivated)	Gibco/Invitrogen
Fish (herring) sperm DNA	Invitrogen
Fluoromount G	Thermo Fischer Scientific
Formaldehyde	Roth
Geneticin (G418)	Thermo Fisher Scientific
Glutamine	Sigma-Aldrich
Glycine	Roth
HBsAg	Roche
Hydrocortisone	Pfizer
Isopropanol	Roth
Lipofectamine 2000	Life Technologies
Methanol	Roth
Milk powder	Roth
NaCl	Roth
NaOH	Roth
Non-essential amino acids	Gibco/Invitrogen
OptiMEM	Gibco/Invitrogen
Page Ruler Plus Prestained protein ladder	Thermo Fischer Scientific
PBS	Gibco/Invitrogen
PEG6000	Merck
Penicillin/streptomycin	Gibco/Invitrogen
Pierce RIPA buffer	Thermo Scientific
PNGase F	New England BioLabs

Polyacrylamide	Roth
Protease inhibitor (Complete)	Roche
SDS	Roth
T5 exonuclease	New England Biolabs
TEMED	Roth
Transferrin From Human Serum, Alexa Fluor™ 488 Conjugate	Life Technologies
Tris HCl	Roth
Trypan blue	Gibco/Invitrogen
Trypsin	Gibco/Invitrogen
Tween 20	Roth
William's medium E	Gibco/Invitrogen

4.1.3 Cell culture media

HepG2/NTCP; Huh7/NTCP, HEK293T, A549, U2OS, HeLa cells	DMEM-F12 10 % FCS Penicillin/streptomycin (100 U/ml)
HepaRG culture media	William's E medium 10 % FBS Fetalclone II Penicillin/streptomycin (100 U/ml) Glutamine (2mM) Human insulin (0.023 U/ml) Hydrocortisone (4.7 µg/ml) Gentamicin (80 µg/ml)
HepaRG differentiation media	William's E medium 10 % FBS Fetalclone II Penicillin/streptomycin (100 U/ml) Glutamine (2mM) Human insulin (0.023 U/ml) Hydrocortisone (4.7 µg/ml) Gentamicin (80 µg/ml) 1.8 % DMSO
HBV production media	William's E medium 5 % FCS Penicillin/streptomycin (100 U/ml) Glutamine (2mM) Non-essential amino acids (1x) Sodium pyruvate (1mM) Hydrocortisone (4.7 µg/ml) 1 % DMSO

4.1.4 Kits

Name	Supplier
AllPrep DNA/RNA Kit	Qiagen
LightCycler 480 SYBR Green I Master mix	Roche
NucleoSpin RNA isolation Kit	Macherey-Nagel
NE-PER™ Nuclear and Cytoplasmic Extraction Reagents	Thermo Fischer Scientific
NucleoSpin Tissue Kit	Macherey-Nagel
SuperScript III First-Strand Synthesis	Invitrogen

4.1.5 Antibodies

Name	Supplier	Application
α-tubulin	Sigma-Aldrich	Western blot (1:500)
AD53	Provided by M. Nassal	Western blot (1:500)
Anti-mouse	Sigma-Aldrich	Western blot (1:10 000)
Anti-rabbit	Sigma-Aldrich	Western blot (1:10 000)
β-actin	Sigma-Aldrich	Western blot (1:300)
Caveolin 1	Cell Signaling	Western blot (1:1000)
EGFR	Cell Signaling	Western blot (1:1000)
GAPDH	Acris	Western blot (1:5000)
HBV core (HBcAg)	DAKO	NAGE (1:300)
Hepatect CP	Biotest	Uptake assay (1:100)
H863	Provided by S. Urban	Immunofluorescence/ Western blot (1:500)
K9	Provided by B. Stieger	Western Blot (1:500)
Lamin A/C	Thermo Scientific Fischer	Western blot (1:500)

4.1.6 Inhibitors

Name	Supplier	Application
Bafilomycin A1	Sigma-Aldrich	100 nM
Dynasore hydrate	Sigma-Aldrich	100 μM
Cytochalasin D	Sigma-Aldrich	50 μM
EIPA	Sigma-Aldrich	100 μM
HAP_R01	Roche	5 μM
Heparin	Ratiopharm	50 U/ml

MβCD	Sigma-Aldrich	5 mM
Myrcludex B	Provided by S. Urban	0.2 μM
Nocodazole	Sigma-Aldrich	50 μM
Pitstop2	Sigma-Aldrich	50 μM

4.1.7 Primer sequences

Name	Sequence
18S fw	AAACGGCTACCACATCCAAG
18S rev	CCTCCAATGGATCCTCGTTA
cccDNA 2251+	AGCTGAGGCGGTATCTA
cccDNA 92-	GCCTATTGATTGGAAAGTATGT
EGFR fw	TTCCTCCCAGTGCCTGAA
EGFR rev	GGGTTCAGAGGCTGATTGTG
HBV DNA 1745	GGAGGGATACATAGAGGTTCCTTGA
HBV DNA 1844	GTTGCCCGTTTGTCCTCTAATTC
PRNP fw	TGCTGGGAAGTGCCATGAG
PRNP rev	CGGTGCATGTTTTCACGATAGTA
TBP fw	TATAATCCCAAGCGGTTTGC
TBP rev	CTGTTCTTCACTCTTGGCTCCT

4.1.8 Software

Name	Supplier
Endnote X9	Microsoft
Graph Pad Prism 5.01	Graph Pad
ImageJ	NIH
LightCycler 480 Software 1.5.1.62	Roche
Fluoview FV10i	Olympus
Windows 7/8/10, MS Office	Microsoft

4.2 Methods

4.2.1 Cell culture

All cells were cultured under standard cell culture condition at 37 °C, 5 % CO_2 and 95 % humidity. For culturing, cells were washed 1x with PBS and incubated with 1x trypsin at 37 °C for five to ten minutes and split in a 1:8 ratio twice a week. HepG2 derived cell lines were kept on collagen (1:10) at all times.
HepaRG cells were kept two weeks in culture media and differentiated for subsequent two weeks in differentiation media (Gripon et al., 2002). Fully differentiated HepaRG were used for all experiments.

4.2.2 HBV infection

HBV stocks were kindly provided by Jochen M. Wettengel. HBV purified from HepAD38 producer cell supernatants using heparin affinity chromatography with subsequent sucrose gradient ultracentrifugation. Unless stated otherwise, cells were pre-differentiated two days prior and inoculated in the presence of 4 % polyethylene glycol (PEG) 6000 and 2.5 % DMSO for approximately 24 hours. The inoculum was removed and cells were washed once with PBS and kept on 2.5 % DMSO containing media.

4.2.3 HBV uptake assay

Human cells were seeded and differentiated for two days with 2.5 % DMSO. Cells were pre-chilled on ice for 15 min and cold HBV containing inoculum was added to cells on ice for 1 hour enabling the virus to bind to the cell surface. Medium was changed and cells were subsequently shifted to 37 °C for 1 to 72 hours. Cells were washed with PBS two times, shortly trypsinised for 3 minutes, and either kept for cccDNA or HBeAg measurements or collected for total intracellular HBV DNA.

4.2.4 DNA extraction

Total cellular DNA was extracted according to the standard manufactures protocol of the NucleoSpin Tissue Kit.

4.2.5 Quantification of HBV markers

Total intracellular HBV DNA, cccDNA and the reference gene PRNP were detected by the LightCycler 480 Real-time PCR system. Advanced relative quantification allowed normalisation to the reference gene considering the primer efficiency. One qPCR reaction consisted of 4 µl of total extracted DNA, 0.5 µl of each primer (20 µM) and 5 µl LightCycler 480 SYBR Green I Master mix. For a selective cccDNA qPCR isolated DNA was subjected to T5 endonuclease treatment in order to remove rcDNA or nicked DNA. One reaction consisted of 8.5 µl extracted DNA were mixed with 1 µl NEB buffer 4 and 0.5 µl T5 exonuclease that was incubated at 37 °C for 30 minutes with subsequent heat inactivation at 99 °C for 5 minutes and diluted 1:4 with water. HBeAg levels were analysed using the qualitative measurement on automated BEP III system (Siemens Healthcare).

Total intracellular HBV DNA and PRNP were with following qPCR adjustments:

	T [°C]	t [sec]	Ramp [°C/sec]	Acquisition mode	Cycles
Denaturation	95	300	4.4		1
Amplification	95	25	4.4	Single	40
	60	10	2.2		
	72	30	4.4		
Melting	95	1	4.4	5/°C	1
	65	60	2.2		
	95		0.11		
Cooling	40	30	2.2		1

qPCR program for cccDNA amplification:

	T [°C]	t [sec]	Ramp [°C/sec]	Acquisition mode	Cycles
Denaturation	95	600	4.4		1
Amplification	95	25	4.4	Single	50
	60	10	2.2		
	72	30	4.4		
	88	2	4.4		
Melting	95	1	4.4	5/°C	1
	65	15	2.2		
	95		0.11		
Cooling	40	30	2.2		1

4.2.6 Sodium dodecyl sulphate-polyacrylamide gel electrophoresis (SDS-PAGE) and Western blot

Cells were lysed for 10 minutes on ice with Pierce RIPA buffer that contain 1x protease inhibitor cocktail. Protein lysate were centrifuged (12,000 g, 10 minutes, 4 °C) to get rid of cell debris. Supernatant were mixed with Laemmli buffer and heated (99 °C, 5 min, 800 rpm). For NTCP detection cells were lysed in RIPA buffer containing 1M DTT and 4x Laemmli buffer without heating. NTCP deglycosylation was obtained through PNGase F treatment according to manufacturer's protocol (New England BioLabs). The lysates were subjected to 12 % SDS-PAGE and samples were separated together with a pre-stained protein ladder (Pager Ruler Plus) at 100V for 2 hours. In a wet blot, proteins were transferred onto a methanol-activated PVDF membrane at 300 mA for 1.5 hours. The membrane was blocked in 3 % milk in TBS-T and kept in primary antibody in 1 % milk overnight at 4 °C. After washing three times with TBS-T the blot was incubated with the secondary antibody in 1 % milk for one hour at room temperature. The Western Blot was developed after three times washing with TBS-T using the Amersham ECL Prime Western Blotting Detection Reagent.

4.2.7 Native Agarose Gel for HBV capsid analysis

Cells were washed twice with ice-cold PBS and lysed with core-lysis buffer and centrifuged at 12 000 g. 2 – 5 µl of the supernatant was mixed with 6x core loading dye and run on a 1.2 % agarose gel in Tri-borate EDTA buffer at 30 V for 10 – 15 minutes following increasing voltage up to 90 V for another 1 – 1.5 hours. Capsids on the agarose gel are directly transferred to a methanol-activated PVDF membrane through capillary transfer in 10x SSC buffer overnight. The membrane is washed in TBS-T and blocked in 3 % milk in TBS-T for one hour at room temperature. Incubation of primary antibody in 1 % milk at 4 °C overnight. After washing three times with TBS-T secondary antibody in 1 % milk in TBS-T was incubated for one hour at room temperature. After washing three times with TBS-T protein was detected using the Amersham ECL Prime Western Blotting Detection Reagent.

4.2.8 NTCP staining using labelled Myrcludex B

Cells on coverslips were washed with PBS and 200 nM Atto488 labelled Myrcludex B was added per well and incubated for 30 minutes at 37 °C. Cells were washed with PBS and fixed with 4 % PFA for 10 minutes at room temperature and mounted with Fluoromount G on slides.

4.2.9 Confocal Microscopy

Cells on coverslips were washed with PBS and fixed with 4 % PFA for 10 minutes at room temperature. After washing once with PBS cells were permeabilised with 0.5 % saponin in PBS for 10 minutes. Blocking was done in 0.1 % saponin and 10 % goat serum at 4 °C overnight. Primary antibody was added into blocking solution kept on cells at 4 °C overnight. Cells were washed three times with 0.1% Saponin in PBS and kept in secondary antibody with 0.1 % Saponin and 2 % goat serum for two hours at room temperature. Subsequently cells were washed three times with 0.1% Saponin in PBS with an extra wash in PBS and mounted on slides using Fluoromount G.

4.2.10 Cell viability assay

Cell viability was tested using CellTiter-Blue reagent (Promega) and performed according to manufacturer's instructions.

4.2.11 Generation and detection of EDC-HBV

HepG2.2.15 cells were grown in T175 flask until they reached a confluency of 100 %. 5-EDC (50 nM) was supplemented every day into the production media. Supernatant was taken every day for 5 days with the first supernatant being discarded. Collected media was pooled and run through a 0.45 µm filter and concentrated using Vivaspin 15. Concentrated virus was additionally washed with PBS in the filtration tube. Concentration (Geq/ml) was determined by qPCR. Upon HBV binding or uptake assay cells on slides were washed with PBS and fixed 4 % PFA for 10 minutes at room temperature. Cells were permeabilised with 0.5 % saponin in PBS for 10 minutes at room temperature. To enable click reaction the click reaction buffer was added for 30 minutes at room temperature. After washing twice with 0.5 % TBS-T Cy5 labelled streptavidin

(1/20) in 0.1 % saponin and 2 % goat serum in PBS for two hours protected from light. After washing twice with 0.1 % saponin in PBS and one wash with PBS cells were mounted with Fluoromount G.

4.2.12 Adenovirus transduction

Ad-HBV1.3L$^-$ was produced as reported before (Sprinzl et al., 2001) and cells were transduced for 2 hours at 37 °C with subsequent replacement of the media.

4.2.13 Cytoplasmic and nucleus Fractionation separation

Samples were separated using NE-PER™ Nuclear and Cytoplasmic Extraction Reagents according to manufacturer's protocol. Intracellular DNA from cytoplasm or nucleus was extracted using NucleoSpin Tissue kit (Macherey Nagel) and qPCR for HBV DNA and cccDNA was performed.

4.2.14 Statistical analysis

Single values are represented with means and standard deviation; *p*-values were calculated with Student's unpaired two-tailed *t*-test applying Prism 8 software.

5 Figures

6 References

Albecka, A., Montserret, R., Krey, T., Tarr, A. W., Diesis, E., Ball, J. K., Descamps, V., Duverlie, G., Rey, F., Penin, F. & Dubuisson, J. 2011. Identification of new functional regions in hepatitis C virus envelope glycoprotein E2. *J Virol,* 85**,** 1777-92.

Allweiss, L. & Dandri, M. 2017. The Role of cccDNA in HBV Maintenance. *Viruses,* 9.

Allweiss, L., Volz, T., Giersch, K., Kah, J., Raffa, G., Petersen, J., Lohse, A. W., Beninati, C., Pollicino, T., Urban, S., Lutgehetmann, M. & Dandri, M. 2018. Proliferation of primary human hepatocytes and prevention of hepatitis B virus reinfection efficiently deplete nuclear cccDNA in vivo. *Gut,* 67**,** 542-552.

Altan-Bonnet, N. & Altan-Bonnet, G. 2009. Fluorescence correlation spectroscopy in living cells: a practical approach. *Curr Protoc Cell Biol,* Chapter 4**,** Unit 4 24.

Andersson, T. B., Kanebratt, K. P. & Kenna, J. G. 2012. The HepaRG cell line: a unique in vitro tool for understanding drug metabolism and toxicology in human. *Expert Opin Drug Metab Toxicol,* 8**,** 909-20.

Anwer, M. S. & Stieger, B. 2014. Sodium-dependent bile salt transporters of the SLC10A transporter family: more than solute transporters. *Pflugers Arch,* 466**,** 77-89.

Appelman, M. D., Chakraborty, A., Protzer, U., Mckeating, J. A. & Van De Graaf, S. F. 2017. N-Glycosylation of the Na+-Taurocholate Cotransporting Polypeptide (NTCP) Determines Its Trafficking and Stability and Is Required for Hepatitis B Virus Infection. *PLoS One,* 12**,** e0170419.

Araki, K., Miyazaki, J., Hino, O., Tomita, N., Chisaka, O., Matsubara, K. & Yamamura, K. 1989. Expression and replication of hepatitis B virus genome in transgenic mice. *Proc Natl Acad Sci U S A,* 86**,** 207-11.

Atalay, G., Cardoso, F., Awada, A. & Piccart, M. J. 2003. Novel therapeutic strategies targeting the epidermal growth factor receptor (EGFR) family and its downstream effectors in breast cancer. *Ann Oncol,* 14**,** 1346-63.

Bayer, N., Schober, D., Prchla, E., Murphy, R. F., Blaas, D. & Fuchs, R. 1998. Effect of bafilomycin A1 and nocodazole on endocytic transport in HeLa cells: implications for viral uncoating and infection. *J Virol,* 72**,** 9645-55.

Beckebaum, S., Herzer, K., Bauhofer, A., Gelson, W., De Simone, P., De Man, R., Engelmann, C., Mullhaupt, B., Vionnet, J., Salizzoni, M., Volpes, R., Ercolani, G., De Carlis, L., Angeli, P., Burra, P., Dufour, J. F., Rossi, M., Cillo, U., Neumann, U., Fischer, L., Niemann, G., Toti, L. & Tisone, G. 2018. Recurrence of Hepatitis B Infection in Liver Transplant Patients Receiving Long-Term Hepatitis B Immunoglobulin Prophylaxis. *Ann Transplant,* 23**,** 789-801.

Bijsmans, I. T., Bouwmeester, R. A., Geyer, J., Faber, K. N. & Van De Graaf, S. F. 2012. Homo- and hetero-dimeric architecture of the human liver Na(+)-dependent taurocholate co-transporting protein. *Biochem J,* 441**,** 1007-15.

Bill, C. A. & Summers, J. 2004. Genomic DNA double-strand breaks are targets for hepadnaviral DNA integration. *Proc Natl Acad Sci U S A,* 101**,** 11135-40.

Birkmann, A., Mahr, K., Ensser, A., Yaguboglu, S., Titgemeyer, F., Fleckenstein, B. & Neipel, F. 2001. Cell surface heparan sulfate is a receptor for human herpesvirus 8 and interacts with envelope glycoprotein K8.1. *J Virol,* 75**,** 11583-93.

Bock, C. T., Schranz, P., Schroder, C. H. & Zentgraf, H. 1994. Hepatitis B virus genome is organized into nucleosomes in the nucleus of the infected cell. *Virus Genes,* 8**,** 215-29.

Boettiger, D. C., Kerr, S., Ditangco, R., Chaiwarith, R., Li, P. C., Merati, T. P., Pham, T. T., Kiertiburanakul, S., Kumarasamy, N., Vonthanak, S., Lee, C. K., Van Kinh, N., Pujari, S., Wong, W. W., Kamarulzaman, A., Zhang, F., Yunihastuti, E., Choi, J. Y., Oka, S., Ng, O. T., Kantipong, P., Mustafa, M., Ratanasuwan, W., Durier,

N., Law, M. & Database, T. a. H. O. 2016. Tenofovir-based antiretroviral therapy in HBV-HIV coinfection: results from the TREAT Asia HIV Observational Database. *Antivir Ther,* 21**,** 27-35.

Bogomolov, P., Alexandrov, A., Voronkova, N., Macievich, M., Kokina, K., Petrachenkova, M., Lehr, T., Lempp, F. A., Wedemeyer, H., Haag, M., Schwab, M., Haefeli, W. E., Blank, A. & Urban, S. 2016. Treatment of chronic hepatitis D with the entry inhibitor myrcludex B: First results of a phase Ib/IIa study. *J Hepatol,* 65**,** 490-8.

Bruns, M., Miska, S., Chassot, S. & Will, H. 1998. Enhancement of hepatitis B virus infection by noninfectious subviral particles. *J Virol,* 72**,** 1462-8.

Bruss, V. 2004. Envelopment of the hepatitis B virus nucleocapsid. *Virus Res,* 106**,** 199-209.

Burwitz, B. J., Wettengel, J. M., Muck-Hausl, M. A., Ringelhan, M., Ko, C., Festag, M. M., Hammond, K. B., Northrup, M., Bimber, B. N., Jacob, T., Reed, J. S., Norris, R., Park, B., Moller-Tank, S., Esser, K., Greene, J. M., Wu, H. L., Abdulhaqq, S., Webb, G., Sutton, W. F., Klug, A., Swanson, T., Legasse, A. W., Vu, T. Q., Asokan, A., Haigwood, N. L., Protzer, U. & Sacha, J. B. 2017. Hepatocytic expression of human sodium-taurocholate cotransporting polypeptide enables hepatitis B virus infection of macaques. *Nat Commun,* 8**,** 2146.

Cagno, V., Tseligka, E. D., Jones, S. T. & Tapparel, C. 2019. Heparan Sulfate Proteoglycans and Viral Attachment: True Receptors or Adaptation Bias? *Viruses,* 11.

Cai, D., Mills, C., Yu, W., Yan, R., Aldrich, C. E., Saputelli, J. R., Mason, W. S., Xu, X., Guo, J. T., Block, T. M., Cuconati, A. & Guo, H. 2012. Identification of disubstituted sulfonamide compounds as specific inhibitors of hepatitis B virus covalently closed circular DNA formation. *Antimicrob Agents Chemother,* 56**,** 4277-88.

Chang, M. P., Mallet, W. G., Mostov, K. E. & Brodsky, F. M. 1993. Adaptor self-aggregation, adaptor-receptor recognition and binding of alpha-adaptin subunits to the plasma membrane contribute to recruitment of adaptor (AP2) components of clathrin-coated pits. *EMBO J,* 12**,** 2169-80.

Chiang, J. Y. 2009. Bile acids: regulation of synthesis. *J Lipid Res,* 50**,** 1955-66.

Chin, R., Earnest-Silveira, L., Koeberlein, B., Franz, S., Zentgraf, H., Dong, X., Gowans, E., Bock, C. T. & Torresi, J. 2007. Modulation of MAPK pathways and cell cycle by replicating hepatitis B virus: factors contributing to hepatocarcinogenesis. *J Hepatol,* 47**,** 325-37.

Chu, C. J. & Lok, A. S. 2002. Clinical significance of hepatitis B virus genotypes. *Hepatology,* 35**,** 1274-6.

Cooper, J. A. 1987. Effects of cytochalasin and phalloidin on actin. *J Cell Biol,* 105**,** 1473-8.

Crowther, R. A., Kiselev, N. A., Bottcher, B., Berriman, J. A., Borisova, G. P., Ose, V. & Pumpens, P. 1994. Three-dimensional structure of hepatitis B virus core particles determined by electron cryomicroscopy. *Cell,* 77**,** 943-50.

Cui, X., Mcallister, R., Boregowda, R., Sohn, J. A., Cortes Ledesma, F., Caldecott, K. W., Seeger, C. & Hu, J. 2015. Does Tyrosyl DNA Phosphodiesterase-2 Play a Role in Hepatitis B Virus Genome Repair? *PLoS One,* 10**,** e0128401.

Dane, D. S., Cameron, C. H. & Briggs, M. 1970. Virus-like particles in serum of patients with Australia-antigen-associated hepatitis. *Lancet,* 1**,** 695-8.

Datta, S., Chatterjee, S., Veer, V. & Chakravarty, R. 2012. Molecular biology of the hepatitis B virus for clinicians. *J Clin Exp Hepatol,* 2**,** 353-65.

De Lima, M. C., Ramalho-Santos, J., Flasher, D., Slepushkin, V. A., Nir, S. & Duzgunes, N. 1995. Target cell membrane sialic acid modulates both binding and fusion activity of influenza virus. *Biochim Biophys Acta,* 1236**,** 323-30.

Devadas, D., Koithan, T., Diestel, R., Prank, U., Sodeik, B. & Dohner, K. 2014. Herpes simplex virus internalization into epithelial cells requires Na+/H+ exchangers and p21-activated kinases but neither clathrin- nor caveolin-mediated endocytosis. *J Virol,* 88**,** 13378-95.

Diao, J., Pantua, H., Ngu, H., Komuves, L., Diehl, L., Schaefer, G. & Kapadia, S. B. 2012. Hepatitis C virus induces epidermal growth factor receptor activation via CD81 binding for viral internalization and entry. *J Virol,* 86**,** 10935-49.

Dilley, R. L., Verma, P., Cho, N. W., Winters, H. D., Wondisford, A. R. & Greenberg, R. A. 2016. Break-induced telomere synthesis underlies alternative telomere maintenance. *Nature,* 539**,** 54-58.

Doherty, G. J. & Mcmahon, H. T. 2009. Mechanisms of endocytosis. *Annu Rev Biochem,* 78**,** 857-902.

Dohner, K. & Sodeik, B. 2005. The role of the cytoskeleton during viral infection. *Curr Top Microbiol Immunol,* 285**,** 67-108.

Dong, Z., Ekins, S. & Polli, J. E. 2013. Structure-activity relationship for FDA approved drugs as inhibitors of the human sodium taurocholate cotransporting polypeptide (NTCP). *Mol Pharm,* 10**,** 1008-19.

Donkers, J. M., Roscam Abbing, R. L. P. & Van De Graaf, S. F. J. 2019. Developments in bile salt based therapies: A critical overview. *Biochem Pharmacol,* 161**,** 1-13.

Donkers, J. M., Zehnder, B., Van Westen, G. J. P., Kwakkenbos, M. J., Ap, I. J., Oude Elferink, R. P. J., Beuers, U., Urban, S. & Van De Graaf, S. F. J. 2017. Reduced hepatitis B and D viral entry using clinically applied drugs as novel inhibitors of the bile acid transporter NTCP. *Sci Rep,* 7**,** 15307.

Dowrick, P., Kenworthy, P., Mccann, B. & Warn, R. 1993. Circular ruffle formation and closure lead to macropinocytosis in hepatocyte growth factor/scatter factor-treated cells. *Eur J Cell Biol,* 61**,** 44-53.

Dranoff, J. A., Mcclure, M., Burgstahler, A. D., Denson, L. A., Crawford, A. R., Crawford, J. M., Karpen, S. J. & Nathanson, M. H. 1999. Short-term regulation of bile acid uptake by microfilament-dependent translocation of rat ntcp to the plasma membrane. *Hepatology,* 30**,** 223-9.

Drose, S. & Altendorf, K. 1997. Bafilomycins and concanamycins as inhibitors of V-ATPases and P-ATPases. *J Exp Biol,* 200**,** 1-8.

Edeling, M. A., Smith, C. & Owen, D. 2006. Life of a clathrin coat: insights from clathrin and AP structures. *Nat Rev Mol Cell Biol,* 7**,** 32-44.

Esser, K., Lucifora, J., Wettengel, J., Singethan, K., Glinzer, A., Zernecke, A. & Protzer, U. 2018. Lipase inhibitor orlistat prevents hepatitis B virus infection by targeting an early step in the virus life cycle. *Antiviral Res,* 151**,** 4-7.

Forgac, M. 2007. Vacuolar ATPases: rotary proton pumps in physiology and pathophysiology. *Nat Rev Mol Cell Biol,* 8**,** 917-29.

Fouillot, N., Tlouzeau, S., Rossignol, J. M. & Jean-Jean, O. 1993. Translation of the hepatitis B virus P gene by ribosomal scanning as an alternative to internal initiation. *J Virol,* 67**,** 4886-95.

Friedrich, B., Wollersheim, M., Brandenburg, B., Foerste, R., Will, H. & Hildt, E. 2005. Induction of anti-proliferative mechanisms in hepatitis B virus producing cells. *J Hepatol,* 43**,** 696-703.

Fukano, K., Tsukuda, S., Oshima, M., Suzuki, R., Aizaki, H., Ohki, M., Park, S. Y., Muramatsu, M., Wakita, T., Sureau, C., Ogasawara, Y. & Watashi, K. 2018. Troglitazone Impedes the Oligomerization of Sodium Taurocholate Cotransporting Polypeptide and Entry of Hepatitis B Virus Into Hepatocytes. *Front Microbiol,* 9**,** 3257.

Funk, A., Mhamdi, M., Lin, L., Will, H. & Sirma, H. 2004. Itinerary of hepatitis B viruses: delineation of restriction points critical for infectious entry. *J Virol,* 78**,** 8289-300.

Gallucci, L. & Kann, M. 2017. Nuclear Import of Hepatitis B Virus Capsids and Genome. *Viruses,* 9.

Gao, W. & Hu, J. 2007. Formation of hepatitis B virus covalently closed circular DNA: removal of genome-linked protein. *J Virol,* 81**,** 6164-74.

Gerlich, W. H., Bremer, C., Saniewski, M., Schuttler, C. G., Wend, U. C., Willems, W. R. & Glebe, D. 2010. Occult hepatitis B virus infection: detection and significance. *Dig Dis,* 28**,** 116-25.

Gerlich, W. H. & Robinson, W. S. 1980. Hepatitis B virus contains protein attached to the 5' terminus of its complete DNA strand. *Cell,* 21**,** 801-9.

Glebe, D. 2006. Attachment sites and neutralising epitopes of hepatitis B virus. *Minerva Gastroenterol Dietol,* 52**,** 3-21.

Glebe, D. & Urban, S. 2007. Viral and cellular determinants involved in hepadnaviral entry. *World J Gastroenterol,* 13**,** 22-38.

Gripon, P., Cannie, I. & Urban, S. 2005. Efficient inhibition of hepatitis B virus infection by acylated peptides derived from the large viral surface protein. *J Virol,* 79**,** 1613-22.

Gripon, P., Diot, C., Theze, N., Fourel, I., Loreal, O., Brechot, C. & Guguen-Guillouzo, C. 1988. Hepatitis B virus infection of adult human hepatocytes cultured in the presence of dimethyl sulfoxide. *J Virol,* 62**,** 4136-43.

Gripon, P., Rumin, S., Urban, S., Le Seyec, J., Glaise, D., Cannie, I., Guyomard, C., Lucas, J., Trepo, C. & Guguen-Guillouzo, C. 2002. Infection of a human hepatoma cell line by hepatitis B virus. *Proc Natl Acad Sci U S A,* 99**,** 15655-60.

Grove, J., Huby, T., Stamataki, Z., Vanwolleghem, T., Meuleman, P., Farquhar, M., Schwarz, A., Moreau, M., Owen, J. S., Leroux-Roels, G., Balfe, P. & Mckeating, J. A. 2007. Scavenger receptor BI and BII expression levels modulate hepatitis C virus infectivity. *J Virol,* 81**,** 3162-9.

Gruenberg, J. & Van Der Goot, F. G. 2006. Mechanisms of pathogen entry through the endosomal compartments. *Nat Rev Mol Cell Biol,* 7**,** 495-504.

Guettouche, T. & Hnatyszyn, H. J. 2005. Chronic hepatitis B and viral genotype: the clinical significance of determining HBV genotypes. *Antivir Ther,* 10**,** 593-604.

Guo, H., Jiang, D., Zhou, T., Cuconati, A., Block, T. M. & Guo, J. T. 2007. Characterization of the intracellular deproteinized relaxed circular DNA of hepatitis B virus: an intermediate of covalently closed circular DNA formation. *J Virol,* 81**,** 12472-84.

Guo, H., Xu, C., Zhou, T., Block, T. M. & Guo, J. T. 2012. Characterization of the host factors required for hepadnavirus covalently closed circular (ccc) DNA formation. *PLoS One,* 7**,** e43270.

Guo, J. T. & Guo, H. 2015. Metabolism and function of hepatitis B virus cccDNA: Implications for the development of cccDNA-targeting antiviral therapeutics. *Antiviral Res,* 122**,** 91-100.

Gust, I. D., Burrell, C. J., Coulepis, A. G., Robinson, W. S. & Zuckerman, A. J. 1986. Taxonomic classification of human hepatitis B virus. *Intervirology,* 25**,** 14-29.

Hagenbuch, B. & Meier, P. J. 1994. Molecular cloning, chromosomal localization, and functional characterization of a human liver Na+/bile acid cotransporter. *J Clin Invest,* 93**,** 1326-31.

Hallen, S., Mareninova, O., Branden, M. & Sachs, G. 2002. Organization of the membrane domain of the human liver sodium/bile acid cotransporter. *Biochemistry,* 41**,** 7253-66.

Hayes, C. N., Zhang, Y., Makokha, G. N., Hasan, M. Z., Omokoko, M. D. & Chayama, K. 2016. Early events in hepatitis B virus infection: From the cell surface to the nucleus. *J Gastroenterol Hepatol,* 31**,** 302-9.

Heermann, K. H., Goldmann, U., Schwartz, W., Seyffarth, T., Baumgarten, H. & Gerlich, W. H. 1984. Large surface proteins of hepatitis B virus containing the pre-s sequence. *J Virol,* 52**,** 396-402.

Herbst, J. J., Opresko, L. K., Walsh, B. J., Lauffenburger, D. A. & Wiley, H. S. 1994. Regulation of postendocytic trafficking of the epidermal growth factor receptor through endosomal retention. *J Biol Chem,* 269**,** 12865-73.

Hewlett, L. J., Prescott, A. R. & Watts, C. 1994. The coated pit and macropinocytic pathways serve distinct endosome populations. *J Cell Biol,* 124**,** 689-703.

Hollinger, F. B. & Lau, D. T. 2006. Hepatitis B: the pathway to recovery through treatment. *Gastroenterol Clin North Am,* 35**,** 425-61, x.

Hruska, J. F., Clayton, D. A., Rubenstein, J. L. & Robinson, W. S. 1977. Structure of hepatitis B Dane particle DNA before and after the Dane particle DNA polymerase reaction. *J Virol,* 21**,** 666-72.

Hu, J., Lin, Y. Y., Chen, P. J., Watashi, K. & Wakita, T. 2019a. Cell and Animal Models for Studying Hepatitis B Virus Infection and Drug Development. *Gastroenterology,* 156**,** 338-354.

Hu, J., Protzer, U. & Siddiqui, A. 2019b. Revisiting Hepatitis B Virus: Challenges of Curative Therapies. *J Virol,* 93.

Huang, H. C., Chen, C. C., Chang, W. C., Tao, M. H. & Huang, C. 2012. Entry of hepatitis B virus into immortalized human primary hepatocytes by clathrin-dependent endocytosis. *J Virol,* 86**,** 9443-53.

Huang, Z. M. & Yen, T. S. 1995. Role of the hepatitis B virus posttranscriptional regulatory element in export of intronless transcripts. *Mol Cell Biol,* 15**,** 3864-9.

Ikonen, E. 2018. Mechanisms of cellular cholesterol compartmentalization: recent insights. *Curr Opin Cell Biol,* 53**,** 77-83.

Ikonen, E., Heino, S. & Lusa, S. 2004. Caveolins and membrane cholesterol. *Biochem Soc Trans,* 32**,** 121-3.

Iwamoto, M., Saso, W., Sugiyama, R., Ishii, K., Ohki, M., Nagamori, S., Suzuki, R., Aizaki, H., Ryo, A., Yun, J. H., Park, S. Y., Ohtani, N., Muramatsu, M., Iwami, S., Tanaka, Y., Sureau, C., Wakita, T. & Watashi, K. 2019. Epidermal growth factor receptor is a host-entry cofactor triggering hepatitis B virus internalization. *Proc Natl Acad Sci U S A,* 116**,** 8487-8492.

Jang, J. W., Kwon, J. H., You, C. R., Kim, J. D., Woo, H. Y., Bae, S. H., Choi, J. Y., Yoon, S. K. & Chung, K. W. 2011. Risk of HBV reactivation according to viral status and treatment intensity in patients with hepatocellular carcinoma. *Antivir Ther,* 16**,** 969-77.

Jilbert, A. R., Miller, D. S., Scougall, C. A., Turnbull, H. & Burrell, C. J. 1996. Kinetics of duck hepatitis B virus infection following low dose virus inoculation: one virus DNA genome is infectious in neonatal ducks. *Virology,* 226**,** 338-45.

Jordan, M. A. & Wilson, L. 1999. The use and action of drugs in analyzing mitosis. *Methods Cell Biol,* 61**,** 267-95.

Kann, M., Bischof, A. & Gerlich, W. H. 1997. In vitro model for the nuclear transport of the hepadnavirus genome. *J Virol,* 71**,** 1310-6.

Kann, M., Sodeik, B., Vlachou, A., Gerlich, W. H. & Helenius, A. 1999. Phosphorylation-dependent binding of hepatitis B virus core particles to the nuclear pore complex. *J Cell Biol,* 145**,** 45-55.

Kapadia, S. B., Barth, H., Baumert, T., Mckeating, J. A. & Chisari, F. V. 2007. Initiation of hepatitis C virus infection is dependent on cholesterol and cooperativity between CD81 and scavenger receptor B type I. *J Virol,* 81**,** 374-83.

Kenney, J. M., Von Bonsdorff, C. H., Nassal, M. & Fuller, S. D. 1995. Evolutionary conservation in the hepatitis B virus core structure: comparison of human and duck cores. *Structure,* 3**,** 1009-19.

Kirkham, M. & Parton, R. G. 2005. Clathrin-independent endocytosis: new insights into caveolae and non-caveolar lipid raft carriers. *Biochim Biophys Acta,* 1745**,** 273-86.

Kitamura, K., Que, L., Shimadu, M., Koura, M., Ishihara, Y., Wakae, K., Nakamura, T., Watashi, K., Wakita, T. & Muramatsu, M. 2018. Flap endonuclease 1 is involved in cccDNA formation in the hepatitis B virus. *PLoS Pathog,* 14**,** e1007124.

Kivipold, P., Vosa, L., Ustav, M. & Kurg, R. 2015. DAXX modulates human papillomavirus early gene expression and genome replication in U2OS cells. *Virol J,* 12**,** 104.

Ko, C., Bester, R., Zhou, X., Xu, Z., Blossey, C., Sacherl, J., Vondran, F. W. R., Gao, L. & Protzer, U. 2019. A New Role for Capsid Assembly Modulators To Target Mature Hepatitis B Virus Capsids and Prevent Virus Infection. *Antimicrob Agents Chemother,* 64.

Ko, C., Chakraborty, A., Chou, W. M., Hasreiter, J., Wettengel, J. M., Stadler, D., Bester, R., Asen, T., Zhang, K., Wisskirchen, K., Mckeating, J. A., Ryu, W. S. & Protzer, U. 2018. Hepatitis B virus genome recycling and de novo secondary infection events maintain stable cccDNA levels. *J Hepatol,* 69**,** 1231-1241.

Ko, C., Michler, T. & Protzer, U. 2017. Novel viral and host targets to cure hepatitis B. *Curr Opin Virol,* 24**,** 38-45.

Komiya, Y., Katayama, K., Yugi, H., Mizui, M., Matsukura, H., Tomoguri, T., Miyakawa, Y., Tabuchi, A., Tanaka, J. & Yoshizawa, H. 2008. Minimum infectious dose of hepatitis B virus in chimpanzees and difference in the dynamics of viremia between genotype A and genotype C. *Transfusion,* 48**,** 286-94.

Konig, A., Doring, B., Mohr, C., Geipel, A., Geyer, J. & Glebe, D. 2014. Kinetics of the bile acid transporter and hepatitis B virus receptor Na+/taurocholate cotransporting polypeptide (NTCP) in hepatocytes. *J Hepatol,* 61**,** 867-75.

Koniger, C., Wingert, I., Marsmann, M., Rosler, C., Beck, J. & Nassal, M. 2014. Involvement of the host DNA-repair enzyme TDP2 in formation of the covalently closed circular DNA persistence reservoir of hepatitis B viruses. *Proc Natl Acad Sci U S A,* 111**,** E4244-53.

Kostyusheva, A., Brezgin, S., Bayurova, E., Gordeychuk, I., Isaguliants, M., Goptar, I., Urusov, F., Nikiforova, A., Volchkova, E., Kostyushev, D. & Chulanov, V. 2019. ATM and ATR Expression Potentiates HBV Replication and Contributes to Reactivation of HBV Infection upon DNA Damage. *Viruses,* 11.

Kramvis, A. 2014. Genotypes and genetic variability of hepatitis B virus. *Intervirology,* 57**,** 141-50.

Kullak-Ublick, G. A., Glasa, J., Boker, C., Oswald, M., Grutzner, U., Hagenbuch, B., Stieger, B., Meier, P. J., Beuers, U., Kramer, W., Wess, G. & Paumgartner, G. 1997. Chlorambucil-taurocholate is transported by bile acid carriers expressed in human hepatocellular carcinomas. *Gastroenterology,* 113**,** 1295-305.

Lajoie, P. & Nabi, I. R. 2010. Lipid rafts, caveolae, and their endocytosis. *Int Rev Cell Mol Biol,* 282**,** 135-63.

Lambert, C., Thome, N., Kluck, C. J. & Prange, R. 2004. Functional incorporation of green fluorescent protein into hepatitis B virus envelope particles. *Virology,* 330**,** 158-67.

Lamontagne, R. J., Bagga, S. & Bouchard, M. J. 2016. Hepatitis B virus molecular biology and pathogenesis. *Hepatoma Res,* 2**,** 163-186.

Lavanchy, D. 2004. Hepatitis B virus epidemiology, disease burden, treatment, and current and emerging prevention and control measures. *J Viral Hepat,* 11**,** 97-107.

Le, P. U., Guay, G., Altschuler, Y. & Nabi, I. R. 2002. Caveolin-1 is a negative regulator of caveolae-mediated endocytosis to the endoplasmic reticulum. *J Biol Chem,* 277**,** 3371-9.

Lee, J., Zong, L., Krotow, A., Qin, Y., Jia, L., Zhang, J., Tong, S. & Li, J. 2018. N-Linked Glycosylation Is Not Essential for Sodium Taurocholate Cotransporting Polypeptide To Mediate Hepatitis B Virus Infection In Vitro. *J Virol,* 92.

Leistner, C. M., Gruen-Bernhard, S. & Glebe, D. 2008. Role of glycosaminoglycans for binding and infection of hepatitis B virus. *Cell Microbiol,* 10**,** 122-33.

Lempp, F. A. & Urban, S. 2014. Inhibitors of hepatitis B virus attachment and entry. *Intervirology,* 57**,** 151-7.

Lempp, F. A., Wiedtke, E., Qu, B., Roques, P., Chemin, I., Vondran, F. W. R., Le Grand, R., Grimm, D. & Urban, S. 2017. Sodium taurocholate cotransporting polypeptide is the limiting host factor of hepatitis B virus infection in macaque and pig hepatocytes. *Hepatology,* 66**,** 703-716.

Li, J. & Tong, S. 2015. From DCPD to NTCP: the long journey towards identifying a functional hepatitis B virus receptor. *Clin Mol Hepatol,* 21**,** 193-9.

Li, W. & Urban, S. 2016. Entry of hepatitis B and hepatitis D virus into hepatocytes: Basic insights and clinical implications. *J Hepatol,* 64**,** S32-S40.

Li, X., Xing, J., Qiu, Z., He, Q. & Lin, J. 2016. Quantification of Membrane Protein Dynamics and Interactions in Plant Cells by Fluorescence Correlation Spectroscopy. *Mol Plant,* 9**,** 1229-1239.

Liu, C., Cai, D., Zhang, L., Tang, W., Yan, R., Guo, H. & Chen, X. 2016. Identification of hydrolyzable tannins (punicalagin, punicalin and geraniin) as novel inhibitors of hepatitis B virus covalently closed circular DNA. *Antiviral Res,* 134**,** 97-107.

Long, Q., Yan, R., Hu, J., Cai, D., Mitra, B., Kim, E. S., Marchetti, A., Zhang, H., Wang, S., Liu, Y., Huang, A. & Guo, H. 2017. The role of host DNA ligases in hepadnavirus covalently closed circular DNA formation. *PLoS Pathog,* 13**,** e1006784.

Lu, X. & Block, T. M. 2004. Enhancement of infection of HepG2 cells in culture by predigestion of hepadnavirus with V8 protease. *Methods Mol Med,* 96**,** 199-208.

Luangsay, S., Gruffaz, M., Isorce, N., Testoni, B., Michelet, M., Faure-Dupuy, S., Maadadi, S., Ait-Goughoulte, M., Parent, R., Rivoire, M., Javanbakht, H., Lucifora, J., Durantel, D. & Zoulim, F. 2015. Early inhibition of hepatocyte innate responses by hepatitis B virus. *J Hepatol,* 63**,** 1314-22.

Lucifora, J., Arzberger, S., Durantel, D., Belloni, L., Strubin, M., Levrero, M., Zoulim, F., Hantz, O. & Protzer, U. 2011. Hepatitis B virus X protein is essential to initiate and maintain virus replication after infection. *J Hepatol,* 55**,** 996-1003.

Lucifora, J., Esser, K. & Protzer, U. 2013. Ezetimibe blocks hepatitis B virus infection after virus uptake into hepatocytes. *Antiviral Res,* 97**,** 195-7.

Lucifora, J. & Protzer, U. 2016. Attacking hepatitis B virus cccDNA--The holy grail to hepatitis B cure. *J Hepatol,* 64**,** S41-S48.

Luo, J., Cui, X., Gao, L. & Hu, J. 2017. Identification of an Intermediate in Hepatitis B Virus Covalently Closed Circular (CCC) DNA Formation and Sensitive and Selective CCC DNA Detection. *J Virol,* 91.

Mabit, H., Nakano, M. Y., Prank, U., Saam, B., Dohner, K., Sodeik, B. & Greber, U. F. 2002. Intact microtubules support adenovirus and herpes simplex virus infections. *J Virol,* 76**,** 9962-71.

Macovei, A., Petrareanu, C., Lazar, C., Florian, P. & Branza-Nichita, N. 2013. Regulation of hepatitis B virus infection by Rab5, Rab7, and the endolysosomal compartment. *J Virol,* 87**,** 6415-27.

Macovei, A., Radulescu, C., Lazar, C., Petrescu, S., Durantel, D., Dwek, R. A., Zitzmann, N. & Nichita, N. B. 2010. Hepatitis B virus requires intact caveolin-1 function for productive infection in HepaRG cells. *J Virol,* 84**,** 243-53.

Marion, M. J., Hantz, O. & Durantel, D. 2010. The HepaRG cell line: biological properties and relevance as a tool for cell biology, drug metabolism, and virology studies. *Methods Mol Biol,* 640**,** 261-72.

Marsh, M. & Helenius, A. 1989. Virus entry into animal cells. *Adv Virus Res,* 36**,** 107-51.

Marsh, M. & Helenius, A. 2006. Virus entry: open sesame. *Cell,* 124**,** 729-40.

Mason, W. S., Seal, G. & Summers, J. 1980. Virus of Pekin ducks with structural and biological relatedness to human hepatitis B virus. *J Virol,* 36**,** 829-36.

Mcconkey, M., Gillin, H., Webster, C. R. & Anwer, M. S. 2004. Cross-talk between protein kinases Czeta and B in cyclic AMP-mediated sodium taurocholate co-transporting polypeptide translocation in hepatocytes. *J Biol Chem,* 279**,** 20882-8.

Mehdi, H., Kaplan, M. J., Anlar, F. Y., Yang, X., Bayer, R., Sutherland, K. & Peeples, M. E. 1994. Hepatitis B virus surface antigen binds to apolipoprotein H. *J Virol,* 68**,** 2415-24.

Meier, O., Boucke, K., Hammer, S. V., Keller, S., Stidwill, R. P., Hemmi, S. & Greber, U. F. 2002. Adenovirus triggers macropinocytosis and endosomal leakage together with its clathrin-mediated uptake. *J Cell Biol,* 158**,** 1119-31.

Mercer, J. & Helenius, A. 2009. Virus entry by macropinocytosis. *Nat Cell Biol,* 11**,** 510-20.

Mercer, J., Schelhaas, M. & Helenius, A. 2010. Virus entry by endocytosis. *Annu Rev Biochem,* 79**,** 803-33.

Meredith, L. W., Hu, K., Cheng, X., Howard, C. R., Baumert, T. F., Balfe, P., Van De Graaf, K. F., Protzer, U. & Mckeating, J. A. 2016. Lentiviral hepatitis B pseudotype entry requires sodium taurocholate co-transporting polypeptide and additional hepatocyte-specific factors. *J Gen Virol,* 97**,** 121-127.

Mettlen, M., Pucadyil, T., Ramachandran, R. & Schmid, S. L. 2009. Dissecting dynamin's role in clathrin-mediated endocytosis. *Biochem Soc Trans,* 37**,** 1022-6.

Michailidis, E., Pabon, J., Xiang, K., Park, P., Ramanan, V., Hoffmann, H. H., Schneider, W. M., Bhatia, S. N., De Jong, Y. P., Shlomai, A. & Rice, C. M. 2017. A robust cell culture system supporting the complete life cycle of hepatitis B virus. *Sci Rep,* 7**,** 16616.

Mitra, B., Thapa, R. J., Guo, H. & Block, T. M. 2018. Host functions used by hepatitis B virus to complete its life cycle: Implications for developing host-targeting agents to treat chronic hepatitis B. *Antiviral Res,* 158**,** 185-198.

Modrow, S., Wenzel, J. J., Schimanski, S., Schwarzbeck, J., Rothe, U., Oldenburg, J., Jilg, W. & Eis-Hubinger, A. M. 2011. Prevalence of nucleic acid sequences specific for human parvoviruses, hepatitis A and hepatitis E viruses in coagulation factor concentrates. *Vox Sang,* 100**,** 351-8.

Molina, S., Castet, V., Fournier-Wirth, C., Pichard-Garcia, L., Avner, R., Harats, D., Roitelman, J., Barbaras, R., Graber, P., Ghersa, P., Smolarsky, M., Funaro, A., Malavasi, F., Larrey, D., Coste, J., Fabre, J. M., Sa-Cunha, A. & Maurel, P. 2007. The low-density lipoprotein receptor plays a role in the infection of primary human hepatocytes by hepatitis C virus. *J Hepatol,* 46**,** 411-9.

Nassal, M. 2015. HBV cccDNA: viral persistence reservoir and key obstacle for a cure of chronic hepatitis B. *Gut,* 64**,** 1972-84.

Nassal, M. & Rieger, A. 1996. A bulged region of the hepatitis B virus RNA encapsidation signal contains the replication origin for discontinuous first-strand DNA synthesis. *J Virol,* 70**,** 2764-73.

Ni, Y., Lempp, F. A., Mehrle, S., Nkongolo, S., Kaufman, C., Falth, M., Stindt, J., Koniger, C., Nassal, M., Kubitz, R., Sultmann, H. & Urban, S. 2014. Hepatitis B and D viruses exploit sodium taurocholate co-transporting polypeptide for species-specific entry into hepatocytes. *Gastroenterology,* 146**,** 1070-83.

Nunes-Correia, I., Eulalio, A., Nir, S., Duzgunes, N., Ramalho-Santos, J. & Pedroso De Lima, M. C. 2002. Fluorescent probes for monitoring virus fusion kinetics: comparative evaluation of reliability. *Biochim Biophys Acta,* 1561**,** 65-75.

Nyati, M. K., Morgan, M. A., Feng, F. Y. & Lawrence, T. S. 2006. Integration of EGFR inhibitors with radiochemotherapy. *Nat Rev Cancer,* 6**,** 876-85.

Oh, P., Mcintosh, D. P. & Schnitzer, J. E. 1998. Dynamin at the neck of caveolae mediates their budding to form transport vesicles by GTP-driven fission from the plasma membrane of endothelium. *J Cell Biol,* 141**,** 101-14.

Orlichenko, L., Huang, B., Krueger, E. & Mcniven, M. A. 2006. Epithelial growth factor-induced phosphorylation of caveolin 1 at tyrosine 14 stimulates caveolae formation in epithelial cells. *J Biol Chem,* 281**,** 4570-9.

Ozaki, T., Neumann, T., Wai, D., Schafer, K. L., Van Valen, F., Lindner, N., Scheel, C., Bocker, W., Winkelmann, W., Dockhorn-Dworniczak, B., Horst, J. & Poremba, C. 2003. Chromosomal alterations in osteosarcoma cell lines revealed by comparative genomic hybridization and multicolor karyotyping. *Cancer Genet Cytogenet,* 140**,** 145-52.

Parton, R. G. & Richards, A. A. 2003. Lipid rafts and caveolae as portals for endocytosis: new insights and common mechanisms. *Traffic,* 4**,** 724-38.

Parton, R. G. & Simons, K. 2007. The multiple faces of caveolae. *Nat Rev Mol Cell Biol,* 8**,** 185-94.

Pelkmans, L. & Helenius, A. 2002. Endocytosis via caveolae. *Traffic,* 3**,** 311-20.

Peng, M., Li, Y., Zhang, M., Jiang, Y., Xu, Y., Tian, Y., Peng, F. & Gong, G. 2014. Clinical features in different age groups of patients with autoimmune hepatitis. *Exp Ther Med,* 7**,** 145-148.

Podevin, P., Rosmorduc, O., Conti, F., Calmus, Y., Meier, P. J. & Poupon, R. 1999. Bile acids modulate the interferon signalling pathway. *Hepatology,* 29**,** 1840-7.

Pollard, T. D. & Cooper, J. A. 2009. Actin, a central player in cell shape and movement. *Science,* 326**,** 1208-12.

Qi, Y., Gao, Z., Xu, G., Peng, B., Liu, C., Yan, H., Yao, Q., Sun, G., Liu, Y., Tang, D., Song, Z., He, W., Sun, Y., Guo, J. T. & Li, W. 2016. DNA Polymerase kappa Is a Key Cellular Factor for the Formation of Covalently Closed Circular DNA of Hepatitis B Virus. *PLoS Pathog,* 12**,** e1005893.

Qiao, L. & Luo, G. G. 2019. Human apolipoprotein E promotes hepatitis B virus infection and production. *PLoS Pathog,* 15**,** e1007874.

Qiao, M., Scougall, C. A., Duszynski, A. & Burrell, C. J. 1999. Kinetics of early molecular events in duck hepatitis B virus replication in primary duck hepatocytes. *J Gen Virol,* 80 (Pt 8)**,** 2127-35.

Quasdorff, M. & Protzer, U. 2010. Control of hepatitis B virus at the level of transcription. *J Viral Hepat,* 17**,** 527-36.

Rabe, B., Glebe, D. & Kann, M. 2006. Lipid-mediated introduction of hepatitis B virus capsids into nonsusceptible cells allows highly efficient replication and facilitates the study of early infection events. *J Virol,* 80**,** 5465-73.

Rabe, B., Vlachou, A., Pante, N., Helenius, A. & Kann, M. 2003. Nuclear import of hepatitis B virus capsids and release of the viral genome. *Proc Natl Acad Sci U S A,* 100**,** 9849-54.

Racoosin, E. L. & Swanson, J. A. 1993. Macropinosome maturation and fusion with tubular lysosomes in macrophages. *J Cell Biol,* 121**,** 1011-20.

Rall, L. B., Standring, D. N., Laub, O. & Rutter, W. J. 1983. Transcription of hepatitis B virus by RNA polymerase II. *Mol Cell Biol,* 3**,** 1766-73.

Rippin, S. J., Hagenbuch, B., Meier, P. J. & Stieger, B. 2001. Cholestatic expression pattern of sinusoidal and canalicular organic anion transport systems in primary cultured rat hepatocytes. *Hepatology,* 33**,** 776-82.

Robinson, W. S. & Greenman, R. L. 1974. DNA polymerase in the core of the human hepatitis B virus candidate. *J Virol,* 13**,** 1231-6.

Roepstorff, K., Grandal, M. V., Henriksen, L., Knudsen, S. L., Lerdrup, M., Grovdal, L., Willumsen, B. M. & Van Deurs, B. 2009. Differential effects of EGFR ligands on endocytic sorting of the receptor. *Traffic,* 10**,** 1115-27.

Ruan, L., Hadden, J. A. & Zlotnick, A. 2018. Assembly Properties of Hepatitis B Virus Core Protein Mutants Correlate with Their Resistance to Assembly-Directed Antivirals. *J Virol,* 92.

Rusnati, M. & Urbinati, C. 2009. Polysulfated/sulfonated compounds for the development of drugs at the crossroad of viral infection and oncogenesis. *Curr Pharm Des,* 15**,** 2946-57.

Sainz, B., Jr. & Chisari, F. V. 2006. Production of infectious hepatitis C virus by well-differentiated, growth-arrested human hepatoma-derived cells. *J Virol,* 80**,** 10253-7.

Sarkar, S., Bananis, E., Nath, S., Anwer, M. S., Wolkoff, A. W. & Murray, J. W. 2006. PKCzeta is required for microtubule-based motility of vesicles containing the ntcp transporter. *Traffic,* 7**,** 1078-91.

Schaefer, S. 2007. Hepatitis B virus taxonomy and hepatitis B virus genotypes. *World J Gastroenterol,* 13**,** 14-21.

Schelhaas, M. 2010. Come in and take your coat off - how host cells provide endocytosis for virus entry. *Cell Microbiol,* 12**,** 1378-88.

Schreiner, S., Burck, C., Glass, M., Groitl, P., Wimmer, P., Kinkley, S., Mund, A., Everett, R. D. & Dobner, T. 2013. Control of human adenovirus type 5 gene expression by cellular Daxx/ATRX chromatin-associated complexes. *Nucleic Acids Res,* 41**,** 3532-50.

Schulze, A., Gripon, P. & Urban, S. 2007. Hepatitis B virus infection initiates with a large surface protein-dependent binding to heparan sulfate proteoglycans. *Hepatology,* 46**,** 1759-68.

Schulze, A., Mills, K., Weiss, T. S. & Urban, S. 2012. Hepatocyte polarization is essential for the productive entry of the hepatitis B virus. *Hepatology,* 55**,** 373-83.

Schulze, A., Schieck, A., Ni, Y., Mier, W. & Urban, S. 2010. Fine mapping of pre-S sequence requirements for hepatitis B virus large envelope protein-mediated receptor interaction. *J Virol,* 84**,** 1989-2000.

Seeger, C., Ganem, D. & Varmus, H. E. 1986. Biochemical and genetic evidence for the hepatitis B virus replication strategy. *Science,* 232**,** 477-84.

Seeger, C. & Mason, W. S. 2000. Hepatitis B virus biology. *Microbiol Mol Biol Rev,* 64**,** 51-68.

Seeger, C. & Mason, W. S. 2013. Sodium-dependent taurocholic cotransporting polypeptide: a candidate receptor for human hepatitis B virus. *Gut,* 62**,** 1093-5.

Seeger, C. & Mason, W. S. 2015. Molecular biology of hepatitis B virus infection. *Virology,* 479-480**,** 672-86.

Seitz, S., Iancu, C., Volz, T., Mier, W., Dandri, M., Urban, S. & Bartenschlager, R. 2016. A Slow Maturation Process Renders Hepatitis B Virus Infectious. *Cell Host Microbe,* 20**,** 25-35.

Shen, F., Li, Y., Wang, Y., Sozzi, V., Revill, P. A., Liu, J., Gao, L., Yang, G., Lu, M., Sutter, K., Dittmer, U., Chen, J. & Yuan, Z. 2018. Hepatitis B virus sensitivity to interferon-alpha in hepatocytes is more associated with cellular interferon response than with viral genotype. *Hepatology,* 67**,** 1237-1252.

Shouval, D., Ilan, Y., Adler, R., Deepen, R., Panet, A., Even-Chen, Z., Gorecki, M. & Gerlich, W. H. 1994. Improved immunogenicity in mice of a mammalian cell-derived recombinant hepatitis B vaccine containing pre-S1 and pre-S2 antigens as compared with conventional yeast-derived vaccines. *Vaccine,* 12**,** 1453-9.

Shukla, D., Liu, J., Blaiklock, P., Shworak, N. W., Bai, X., Esko, J. D., Cohen, G. H., Eisenberg, R. J., Rosenberg, R. D. & Spear, P. G. 1999. A novel role for 3-O-sulfated heparan sulfate in herpes simplex virus 1 entry. *Cell,* 99**,** 13-22.

Siddiqui, A., Sattler, F. & Robinson, W. S. 1979. Restriction endonuclease cleavage map and location of unique features of the DNA of hepatitis B virus, subtype adw2. *Proc Natl Acad Sci U S A,* 76**,** 4664-8.

Sieczkarski, S. B. & Whittaker, G. R. 2002. Dissecting virus entry via endocytosis. *J Gen Virol,* 83**,** 1535-45.

Smith, A. E. & Helenius, A. 2004. How viruses enter animal cells. *Science,* 304**,** 237-42.

Smythe, E. & Ayscough, K. R. 2006. Actin regulation in endocytosis. *J Cell Sci,* 119**,** 4589-98.

Smythe, E., Carter, L. L. & Schmid, S. L. 1992. Cytosol- and clathrin-dependent stimulation of endocytosis in vitro by purified adaptors. *J Cell Biol,* 119**,** 1163-71.

Somiya, M., Liu, Q., Yoshimoto, N., Iijima, M., Tatematsu, K., Nakai, T., Okajima, T., Kuroki, K., Ueda, K. & Kuroda, S. 2016. Cellular uptake of hepatitis B virus envelope L particles is independent of sodium taurocholate cotransporting polypeptide, but dependent on heparan sulfate proteoglycan. *Virology,* 497**,** 23-32.

Sorkin, A. 2004. Cargo recognition during clathrin-mediated endocytosis: a team effort. *Curr Opin Cell Biol,* 16**,** 392-9.

Sprinzl, M. F., Oberwinkler, H., Schaller, H. & Protzer, U. 2001. Transfer of hepatitis B virus genome by adenovirus vectors into cultured cells and mice: crossing the species barrier. *J Virol,* 75**,** 5108-18.

Stenmark, H. & Olkkonen, V. M. 2001. The Rab GTPase family. *Genome Biol,* 2**,** REVIEWS3007.

Stieger, B., Heger, M., De Graaf, W., Paumgartner, G. & Van Gulik, T. 2012. The emerging role of transport systems in liver function tests. *Eur J Pharmacol,* 675**,** 1-5.

Stross, C., Helmer, A., Weissenberger, K., Gorg, B., Keitel, V., Haussinger, D. & Kubitz, R. 2010. Protein kinase C induces endocytosis of the sodium taurocholate cotransporting polypeptide. *Am J Physiol Gastrointest Liver Physiol,* 299**,** G320-8.

Stross, C., Kluge, S., Weissenberger, K., Winands, E., Haussinger, D. & Kubitz, R. 2013. A dileucine motif is involved in plasma membrane expression and endocytosis of rat sodium taurocholate cotransporting polypeptide (Ntcp). *Am J Physiol Gastrointest Liver Physiol,* 305**,** G722-30.

Su, J. J. 1987. [Experimental infection of human hepatitis B virus (HBV) in adult tree shrews]. *Zhonghua Bing Li Xue Za Zhi,* 16**,** 103-6, 22.

Summers, P. R., Biswas, M. K., Pastorek, J. G., 2nd, Pernoll, M. L., Smith, L. G. & Bean, B. E. 1987. The pregnant hepatitis B carrier: evidence favoring comprehensive antepartum screening. *Obstet Gynecol,* 69**,** 701-4.

Sun, S., Yan, J., Xia, C., Lin, Y., Jiang, X., Liu, H., Ren, H., Yan, J., Lin, J. & He, X. 2014. Visualizing hepatitis B virus with biarsenical labelling in living cells. *Liver Int,* 34**,** 1532-42.

Sureau, C. & Salisse, J. 2013. A conformational heparan sulfate binding site essential to infectivity overlaps with the conserved hepatitis B virus a-determinant. *Hepatology,* 57**,** 985-94.

Tillmann, H. L. 2007. Antiviral therapy and resistance with hepatitis B virus infection. *World J Gastroenterol,* 13**,** 125-40.

Trepo, C. 2014. A brief history of hepatitis milestones. *Liver Int,* 34 Suppl 1**,** 29-37.

Untergasser, A. & Protzer, U. 2004. Hepatitis B virus-based vectors allow the elimination of viral gene expression and the insertion of foreign promoters. *Hum Gene Ther,* 15**,** 203-10.

Urban, J. A., Doherty, C. A., Jordan, W. T., 3rd, Bliss, J. E., Feng, J., Soruco, M. M., Rieder, L. E., Tsiarli, M. A. & Larschan, E. N. 2017. The essential Drosophila CLAMP protein differentially regulates non-coding roX RNAs in male and females. *Chromosome Res,* 25**,** 101-113.

Urban, S., Bartenschlager, R., Kubitz, R. & Zoulim, F. 2014. Strategies to inhibit entry of HBV and HDV into hepatocytes. *Gastroenterology,* 147**,** 48-64.

Velkov, S., Ott, J. J., Protzer, U. & Michler, T. 2018. The Global Hepatitis B Virus Genotype Distribution Approximated from Available Genotyping Data. *Genes (Basel),* 9.

Verrier, E. R., Colpitts, C. C., Schuster, C., Zeisel, M. B. & Baumert, T. F. 2016. Cell Culture Models for the Investigation of Hepatitis B and D Virus Infection. *Viruses,* 8.

Von Kleist, L., Stahlschmidt, W., Bulut, H., Gromova, K., Puchkov, D., Robertson, M. J., Macgregor, K. A., Tomilin, N., Pechstein, A., Chau, N., Chircop, M., Sakoff, J., Von Kries, J. P., Saenger, W., Krausslich, H. G., Shupliakov, O., Robinson, P. J., Mccluskey, A. & Haucke, V. 2011. Role of the clathrin terminal domain in regulating coated pit dynamics revealed by small molecule inhibition. *Cell,* 146**,** 471-84.

Walter, E., Keist, R., Niederost, B., Pult, I. & Blum, H. E. 1996. Hepatitis B virus infection of tupaia hepatocytes in vitro and in vivo. *Hepatology,* 24**,** 1-5.

Wang, C. M., Wang, Y., Fan, C. G., Xu, F. F., Sun, W. S., Liu, Y. G. & Jia, J. H. 2011. miR-29c targets TNFAIP3, inhibits cell proliferation and induces apoptosis in hepatitis B virus-related hepatocellular carcinoma. *Biochem Biophys Res Commun,* 411**,** 586-92.

Wang, X., Wang, P., Wang, W., Murray, J. W. & Wolkoff, A. W. 2016. The Na(+)-Taurocholate Cotransporting Polypeptide Traffics with the Epidermal Growth Factor Receptor. *Traffic,* 17**,** 230-44.

Watashi, K., Sluder, A., Daito, T., Matsunaga, S., Ryo, A., Nagamori, S., Iwamoto, M., Nakajima, S., Tsukuda, S., Borroto-Esoda, K., Sugiyama, M., Tanaka, Y., Kanai, Y., Kusuhara, H., Mizokami, M. & Wakita, T. 2014. Cyclosporin A and its analogs inhibit hepatitis B virus entry into cultured hepatocytes through targeting a membrane transporter, sodium taurocholate cotransporting polypeptide (NTCP). *Hepatology,* 59**,** 1726-37.

Watts, C. & Marsh, M. 1992. Endocytosis: what goes in and how? *J Cell Sci,* 103 (Pt 1)**,** 1-8.

Welch, M. D. & Mullins, R. D. 2002. Cellular control of actin nucleation. *Annu Rev Cell Dev Biol,* 18**,** 247-88.

White, J. & Helenius, A. 1980. pH-dependent fusion between the Semliki Forest virus membrane and liposomes. *Proc Natl Acad Sci U S A,* 77**,** 3273-7.

Wieduwilt, M. J. & Moasser, M. M. 2008. The epidermal growth factor receptor family: biology driving targeted therapeutics. *Cell Mol Life Sci,* 65**,** 1566-84.

Winer, B. Y., Shirvani-Dastgerdi, E., Bram, Y., Sellau, J., Low, B. E., Johnson, H., Huang, T., Hrebikova, G., Heller, B., Sharon, Y., Giersch, K., Gerges, S., Seneca, K., Pais, M. A., Frankel, A. S., Chiriboga, L., Cullen, J., Nahass, R. G., Lutgehetmann, M., Toettcher, J. E., Wiles, M. V., Schwartz, R. E. & Ploss, A. 2018. Preclinical assessment of antiviral combination therapy in a genetically humanized mouse model for hepatitis delta virus infection. *Sci Transl Med,* 10.

Xia, Y., Cheng, X., Li, Y., Valdez, K., Chen, W. & Liang, T. J. 2018. Hepatitis B Virus Deregulates the Cell Cycle To Promote Viral Replication and a Premalignant Phenotype. *J Virol,* 92.

Yan, H., Liu, Y., Sui, J. & Li, W. 2015. NTCP opens the door for hepatitis B virus infection. *Antiviral Res,* 121**,** 24-30.

Yan, H., Peng, B., Liu, Y., Xu, G., He, W., Ren, B., Jing, Z., Sui, J. & Li, W. 2014. Viral entry of hepatitis B and D viruses and bile salts transportation share common molecular determinants on sodium taurocholate cotransporting polypeptide. *J Virol,* 88**,** 3273-84.

Yan, H., Zhong, G., Xu, G., He, W., Jing, Z., Gao, Z., Huang, Y., Qi, Y., Peng, B., Wang, H., Fu, L., Song, M., Chen, P., Gao, W., Ren, B., Sun, Y., Cai, T., Feng, X., Sui, J. & Li, W. 2012. Sodium taurocholate cotransporting polypeptide is a functional receptor for human hepatitis B and D virus. *Elife,* 1**,** e00049.

Yang, J. & Shen, M. H. 2006. Polyethylene glycol-mediated cell fusion. *Methods Mol Biol,* 325**,** 59-66.

Zhang, Z., Zehnder, B., Damrau, C. & Urban, S. 2016. Visualization of hepatitis B virus entry - novel tools and approaches to directly follow virus entry into hepatocytes. *FEBS Lett,* 590**,** 1915-26.

Zhao, K., Liu, S., Chen, Y., Yao, Y., Zhou, M., Yuan, Y., Wang, Y., Pei, R., Chen, J., Hu, X., Zhou, Y., Zhao, H., Lu, M., Wu, C. & Chen, X. 2018. Upregulation of HBV transcription by sodium taurocholate cotransporting polypeptide at the postentry step is inhibited by the entry inhibitor Myrcludex B. *Emerg Microbes Infect,* 7**,** 186.

Acknowledgement

First, I want to thank my supervisor Prof. Ulrike Protzer for giving me the opportunity to work in her group on an interesting yet very challenging project. I am grateful for her support and scientific advice.

My sincerest thanks go to my second supervisor Prof. Jane A. McKeating for her professional guidance throughout my project. I am grateful for her endless support and want to thank her for hosting me in her lab in Birmingham and Oxford.

Further, I want thank Prof. Percy Knolle as a member of my thesis committee for valuable suggestions on my project.

A special thanks to Dr. Chunkyu Ko for constant support, patience and kindness throughout my PhD. “Ko-quality” helped me advance and grow during my PhD towards a more professional level.

Next, I want to thank my colleagues Stoyan Velkov, Andreas Oswald, Till Bunse and Samuel Jeske who I can call my dearest friends. Thanks not only for your scientific input but also for all the memorable and funny moments we had together!
Romina Bester, Julia Sacherl, Daniela Stadler, Martin Kächele, Fuwang Chen and Maarten van de Klundert thanks for creating a great and enjoyable working atmosphere in the 3. floor lab.
I would also like to thank the present and previous members of the group Theresa Asen, Philipp Hagen, Daniela Rizzi, Lisa Wolff, Anna Kosinska, Florian Wilsch, Jochen M. Wettengel, Doris Pelz, Wen-Min Chou, Marvin Festag and Julia Festag for experimental support and creating a friendly atmosphere.
Furthermore, I thank my intern and HiWi Christin Henning for contributing to my work.

A big thank you to everyone from the McKeating group for their help and expertise during my visits in Birmingham and Oxford.

An important thanks goes to all my friends in Germany and abroad for always believing in me.

I would like to express my deep and sincere gratitude to Niki who accompanied me through good but also rough moments during my studies. Thank you for your encouragements throughout this entire time.

Lastly, I want to thank my family. I am thankful to my brother for understanding and continuing support to remain sane and focused. I am extremely grateful to my mum for caring and sacrifices for educating me and endless support. I thank my father who is and always will be a role model in my life. For all the personal sacrifices he made to allow me and my brother to be successful in life. Thanks for always letting me know that there is no problem that cannot be solved and most obviously for your scientific advice when things got difficult.

Publications and meetings

Articles in peer-reviewed journals

Appelman, M.D., **Chakraborty, A.,** Protzer, U., McKeating, J.A. and van de Graaf, S.F., 2017. N-glycosylation of the Na+-taurocholate cotransporting polypeptide (NTCP) determines its trafficking and stability and is required for hepatitis B virus infection. *PloS one*, *12*(1).

Ko, C., **Chakraborty, A**., Chou, W.M., Hasreiter, J., Wettengel, J.M., Stadler, D., Bester, R., Asen, T., Zhang, K., Wisskirchen, K. and McKeating, J.A., 2018. Hepatitis B virus genome recycling and de novo secondary infection events maintain stable cccDNA levels. *Journal of hepatology*, *69*(6), pp.1231-1241.

Wing, P.A., Davenne, T., Wettengel, J., Lai, A.G., Zhuang, X., **Chakraborty, A**., D'Arienzo, V., Kramer, C., Ko, C., Harris, J.M. and Schreiner, S., 2019. A dual role for SAMHD1 in regulating HBV cccDNA and RT-dependent particle genesis. *Life science alliance*, *2(2.)*

Chakraborty, A, Ko, C, Henning, C, et al. Synchronised infection identifies early rate-limiting steps in the hepatitis B virus life cycle. *Cellular Microbiology*. 2020; 1– 13.

International conferences

2018 International HBV Meeting-The Molecular Biology of Hepatitis B Viruses
October 3-8, 2018, Taormina, Italy
Poster: Delineating early steps in the hepatitis B viral life cycle

2019 Joint annual meeting DGI-DZIF
November 21-23, 2019, Bad Nauheim, Germany
Poster: Delineating early hepatitis B viral infection events: particle entry to covalently closed circular DNA formation